Distribution Agreement

In presenting this thesis or dissertation as a partial fulfillment of the requirements for an advanced degree from Emory University, I hereby grant to Emory University and its agents the non-exclusive license to archive, make accessible, and display my thesis or dissertation in whole or in part in all forms of media, now or hereafter known, including display on the world wide web. I understand that I may select some access restrictions as part of the online submission of this thesis or dissertation. I retain all ownership rights to the copyright of the thesis or dissertation. I also retain the right to use in future works (such as articles or books) all or part of this thesis or dissertation.

Signature:

Claire E. Pillsbury
Name

6/30/2023
Date

Siglec-15 is required for evasion of immune response in acute lymphoblastic leukemia

By

Claire Evelyn Pillsbury
Doctor of Philosophy

Graduate Division of Biological and Biomedical Science
Cancer Biology

_____
Christopher C. Porter, MD
Advisor

_____
Curtis J. Henry, PhD
Committee Member

_____
Gregory Lesinski, PhD, MPH
Committee Member

_____
Renhao Li, PhD
Committee Member

_____
Chrystal Paulos, PhD
Committee Member

Accepted:

_____
Kimberly Jacob Arriola, Ph.D., MPH
Dean of the James T. Laney School of Graduate Studies

_____
Date

Siglec-15 is required for evasion of immune response in acute lymphoblastic leukemia

By

Claire Evelyn Pillsbury
BS, Pacific University, 2017

Advisor: Christopher C. Porter MD

An abstract of
A dissertation submitted to the Faculty of the
James T. Laney School of Graduate Studies of Emory University
in partial fulfillment of the requirements for the degree of
Doctor of Philosophy
in
Graduate Division of Biological and Biomedical Sciences
Cancer Biology
2023

Abstract

Siglec-15 is required for evasion of immune response in acute lymphoblastic leukemia

By Claire Evelyn Pillsbury

Relapsed/refractory pediatric B cell acute lymphoblastic leukemia (B-ALL) remains one of the leading causes of cancer-related death in children. Immunotherapies have shown promise in treatment of this disease, suggesting further study of the immune evasion mechanisms utilized by B-ALL can yield new therapeutic targets and improve patient outcomes. The sialic acid-binding molecule, Siglec-15 (Sig15), has recently emerged as a novel immunomodulatory molecule across a breadth of solid tumors, yet its role in blood cancers and its function in immunosuppression remains incomplete.

We began by characterizing the expression of Sig15 across blood cancers using *in silico* data, immortalized cell line models, and primary B-ALL patient samples, demonstrating pathological overexpression of Sig15 compared to healthy controls. This overexpression was found to be regulated by NF-κB, which also enhanced Sig15 localization to the cell surface and, notably, the release of a secreted/soluble form of Sig15 (sSig15) which circulates at elevated levels in the plasma of pediatric B-ALL patients. sSig15 was found to correlate with an overall more immunosuppressive circulating cytokine profile, and the protein in its recombinant form was successfully able to abrogate activation in a chimeric antigen receptor (CAR)-expressing Jurkat model. Sig15 ablation in a murine model of B-ALL significantly promoted leukemia clearance in immunocompetent recipients, accompanied by increases in $CD8^+$ T cell expansion, activation, and effector profiles as well as a decrease in leukemia-promoting bone marrow cytokines. Thus Sig15 targeting was able to successfully reverse the bone marrow tumor microenvironment (TME) and augment leukemia control.

Further study of Sig15 in B-ALL demonstrated the expression of multiple alternatively spliced isoforms, one of which (Sig15-204) was demonstrated to be expressed at significantly lower levels in B-ALL and lymphoma cells as compared to healthy peripheral blood mononuclear cells (PBMCs). Investigation into the regulation of canonical Sig15 demonstrated sensitivity of Sig15 expression to active cell cycling, wherein Sig15 expression was increased in both B-ALL and healthy PBMCs upon proliferation and was found to be highest in G2/M phase in B-ALL cells. The extracellular domain of Sig15 was also found to be present in the nucleus of both B-ALL and osteosarcoma cells, where in the case of the former, nuclear Sig15 was found to localize to perinucleolar compartments with implications towards regulating RNA metabolism.

This dissertation thus provides a complex profile of Siglec-15 as a potent immunosuppressive molecule with unique regulation and subcellular localization in B-ALL. It plays an active role in immune evasion in leukemia and may be targeted therapeutically to activate T lymphocytes against leukemia cells.

Siglec-15 is required for evasion of immune response in acute lymphoblastic leukemia

By

Claire Evelyn Pillsbury
BS, Pacific University, 2017

Advisor: Christopher C. Porter MD

A dissertation submitted to the Faculty of the
James T. Laney School of Graduate Studies of Emory University
in partial fulfillment of the requirements for the degree of
Doctor of Philosophy
in
Graduate Division of Biological and Biomedical Sciences
Cancer Biology
2023

Acknowledgements

There are a great number of people who helped, advised, and inspired my work through this Ph.D., and I cannot miss the opportunity to express even a modicum of my gratitude to them.

I want to thank first my PI and mentor, Dr. Chris Porter, who provided the guidance I needed to advance, the space I needed to grow, and the optimism I needed to push through the stalls of my project. Your confidence in my scientific ability from the very beginning taught me in turn to be confident in myself as an independent investigator, and I am unendingly grateful for the open, friendly, and encouraging atmosphere of the lab you have made. To my committee, Drs. Curtis Henry, Greg Lesinski, Renhao Li, and Chrystal Paulos, I would like to thank you for your encouragement and guidance on my project as well as the expertise you brought to the many puzzles I stumbled across. I am beyond grateful for the mentorship you each gave me, be it scientific, personal, professional, and beyond. To my former committee members, Drs. Andy Kowalczyk and Bob Schnepp, thank you also for the guidance you gave me while you were at Emory and your help in shaping the beginning of my Ph.D..

To the ladies of my lab, you are, have always been, and will continue to be an inspiration. Though I know we spent a lot of time commiserating over projects that never worked, silly lab blunders, and the general lows of life, I have always felt privileged be surrounded by your intelligence, strength, and kindness. The support and sass we gave equal and in turn made me happy to come into lab, even on days when I could not get a single experiment to work. I never once felt as if I was alone in my project with you all as my family. Thank you so incredibly much.

To my dad, no amount of words would be enough to convey just how much your love, support, and care drove me through this process. During my highest highs and lowest lows, you were the first person I would call, and I have never felt as happy with this accomplishment as when I got to tell you that I finally made it to end of the Ph.D.. To Michelle, Sarah, and Stone, thank you for supporting me through this process and always giving me a home to come back to no matter what. To Ellyson, though we were always such different people, I owe a lot of who I am today to you, and I know we both were so excited to see each other come into our own. Though I wish you could have been here to share the end of it with me, I know I will carry you with me on through the rest of my life.

To my cohort, I have always felt unfairly lucky to end up with such a fun, kind, and hilarious group. Thank you to Austin and Leon, who are exactly the kind of friends I needed to both support and goad me through some of the hardest moments. To Amanda (and Mini), you were the home and family I was always so relieved and grateful to come back to at the end of each day. Through the trials of quarantine and economic strain, the tribulations of our Ph.D.'s and everyday stress on top of it all, my cohort were my friends, family, and peers, and I would not be the scientist I am today without them.

To my friends at Emory, thank you for the fun conversation, for the opportunities to teach and learn, and for the comradery that made me drag myself to SCR events at the end of long workdays. The community I found within CB is one I have genuinely cherished, from hanging out after seminar to sinking gutter balls at bowling to the drive-by hallway conversations on the way to flow. I have watched the program grow and strengthen during my time here, even at times having the honor to contribute to that growth, and, for all its flaws and trials, it is something to which I am incredibly proud to belong.

Table of Contents

List of Figures

Chapter 1: Introduction

1.1 Introduction

Cancer is defined by the malignant expansion of abnormal cells in the body. This abnormal expansion can originate from virtually any of the more than 200 different cell types of the body, resulting in a highly heterogenous disease which can vary drastically in incidence, mortality, and cause. For this reason, our understanding of cancer and the optimal ways in which to treat it is equally varied despite the prevalence and aggressiveness of the disease. In the year of 2020, cancer accounted for nearly 10 million mortalities globally, making it one of the leading causes of death worldwide (1). Yet, to date, only 3 of 38 major types of cancer possess a 5-year survival rate above 95% (2), and incidence of cancer is still projected to increase by nearly 11 million cases globally by 2040 (3).

Cancer is often considered a disease of older adults, with a median age of incidence of 66 years and roughly 80% of new cases occurring in those above the age of 55 years (2). Yet childhood cancers remain the leading cause of non-accidental death in children below the age of 14 in the US, and roughly 1 in every 260 children will receive a cancer diagnosis by age 20 (4). Therapeutic optimization and rapid discovery have drastically improved the survival rates of childhood cancers from 58% to 85% over the last fifty years (5), yet there remains a number of pediatric cancers with dismal prognoses and stagnated therapeutic developments.

1.2 Leukemia

Leukemia is the most common of all childhood cancers, accounting for 28% of cases (4). It is defined as cancer which develops from immature blood cells, most often the precursors of white blood cells (leukocytes). These are the major effectors of the immune system responsible for identifying and clearing the body of foreign agents and disease. Leukemia originates in the bone marrow, the primary site for leukocyte development, where cancer cells can expand rapidly to occupy 20% or more of the total bone marrow content and further on into circulation in the blood (6). This is what separates leukemia from lymphoma, another “liquid” tumor which commonly commences in the lymph nodes, whereas

myeloma is a liquid tumor which also commences in the bone marrow but instead involves expansion of a subtype of fully matured leukocytes called plasma cells.

There are four major subtypes of leukemia, classified by cell of origin and the speed of disease progression. Leukemia is characterized by either slow progression ("chronic") or rapid progression ("acute"), the latter of which tends to be more aggressive and significantly more common in pediatric cases. As most leukocytes will differentiate into one of two major cell type lineages as they mature, leukemia can also be classified depending on whenever it develops from early progenitors of the myeloid lineage ("myeloblastic/myelogenous") or of the lymphocyte lineage ("lymphoblastic/lymphocytic").

1.2.1 ***Acute lymphoblastic leukemia (ALL)***

Our group's studies focus on acute lymphoblastic leukemia (ALL), which is characterized by the rapid expansion of immature lymphocyte-lineage immune cells called lymphoblasts. This expansion of malignant cells suppresses the growth and development of normal blood cells in the bone marrow, which can result in symptoms including repeated infections, abnormal bleeding, breathlessness, and fatigue. Patients presenting with these or additional symptoms will often have blood drawn for a complete blood count and undergo a bone marrow aspiration or biopsy to assess for the presence of these malignant lymphoblasts in circulation or within the marrow.

Following diagnosis, standard-of-care includes a chemotherapeutic induction utilizing drug combinations including vincristine, corticosteroids, and asparaginase, with or without doxorubicin or daunorubicin (7). Depending on the type of ALL, tyrosine kinase inhibitors may also be included in frontline treatment, which together is sufficient to induce complete remission in 98% of childhood cases (8). In the case of leukemia, remission is defined as having less than the normal 5% blast content in the bone marrow and normal blood counts at the end of chemotherapeutic induction. Those patients who meet these criteria yet still have detectable leukemia blasts in the bone marrow through high sensitivity assays such as flow cytometry and polymerase chain reaction (PCR) amplification are said to have minimal residual disease (MRD). The presence of MRD in an ALL patient is one of the most reliable risk factors

for relapse and patient outcome (9), though other factors, such as genetic alterations of the cancer, rate of response to induction therapy, and genetic syndromes or viral infections, may also contribute to risk.

ALL is the most common form of leukemia, with the highest risk for disease being in children below the age of 5 years old and adults over the age of 50 (10). ALL is also one of the most common forms of pediatric cancer, second only to brain cancer, which contributes to its status as one of the leading causes of disease-related death below the age of 15 in the US (11). As lymphoblasts have the capacity to differentiate into T or B cell lymphocytes during normal development, lymphoblastic leukemias can consequently be further subdivided into two major subtypes: T cell ALL (T-ALL), developing from early T cell lymphoblasts, and B cell ALL (B-ALL), developing from early B cell lymphoblasts (**Fig. 1.1**). Of these two subsets, B-ALL makes up the vast majority of pediatric ALL, accounting for approximately 85% of cases (12).

1.2.2 *B cell acute lymphoblastic leukemia (B-ALL)*

B cell acute lymphoblastic leukemia (B-ALL), also called B cell progenitor ALL (BCP-ALL), is an aggressive disease characterized by the unregulated proliferation of B-lineage precursor cells in the bone marrow. B cells are the antibody-producing immune cells which play a critical role in the humoral (macromolecule-mediated) response and function as antigen-presenting cells in the adaptive immune response. B cells thus have the capacity to produce and secrete antibodies highly specific for pathogens or antigens on diseased cells while also contributing to local cytokine signaling network and T cell priming through antigen presentation. The crosstalk between B cells and T cells is critical in the adaptive immune response, mediated by several concomitant interactive systems which B-ALL cells inherit from the normal B cell progenitors they developed from and may thus exploit in leukemia pathology.

There are a number of common genetic abnormalities which segregate B-ALL into subtypes with varied prognoses and therapeutic strategies. These include hyperdiploidy amplifications (including trisomies of chromosomes such as 5, 10, and 17) and the ETV6-RUNX1 translocation t(12;21), which both possess relatively more favorable prognoses and account for 25 and 30% of childhood B-ALL respectively, as well as the E2A-PBX1 translocation t(12;21) which occurs in roughly 5% of cases and

possessed a historically poorer prognosis until modern enhancement of chemotherapeutic induction with methotrexate (13). Another common genetic mutation is the t(9;22) chromosomal translocation known as the Philadelphia chromosome, which produces a constitutively activated version of the tyrosine kinase ABL1 through fusion to a component of the Breakpoint Cluser Region (BCR) gene. B-ALL which is positive for this translocation (Ph^+ B-ALL) can be highly susceptible to tyrosine kinase inhibitors such as dasatinib, which specifically target B-ALL cells with this mutation and have drastically improved patient outcomes in this genetic subgroup (14). The identification of these subtypes and optimization of their treatments has greatly improved the overall survival of childhood B-ALL, resulting in the encouraging 85% remission rate of today.

However, despite this increase in disease understanding and treatment, 15% of pediatric patients will eventually suffer relapse (15). Relapsed/refractory B-ALL is a highly aggressive disease, resistant to most salvage therapies with historic 5-year-survival rates of below 50% (16, 17). Enhanced chemotherapeutic regimens may be attempted to varied success, and patients with infiltration or primary relapse of leukemia in the central nervous system (CNS) may undergo intrathecal injection of chemotherapeutics or radiation therapy. For partial remission or high-risk cases which are initially ineligible for hematopoietic stem cell transplant (HSCT), immunotherapy has emerged as an effective treatment option and bridge to transplant.

Being of B cell lineage, B-ALL commonly expresses markers which are also found on the normal B cell progenitors from which they derive, such as CD19, CD20, and CD22. These markers can be targeted in immunotherapeutic treatment of refractory B-ALL (**Fig. 1.2**), using systems such as T cells genetically modified with chimeric antigen receptors (CAR T cells) specific for CD19. These T cells exhibit powerful and enduring activation in response to their CAR receptors binding CD19 on B-ALL cells, allowing them to effectively clear the leukemia cells and, incidentally, any normal $CD19^+$ B cells in patients. The combination of these CD19-CAR T cells with conditioning chemotherapy and HSCT was shown to induce a response in 94% of relapsed pediatric patients and improve overall survival to a remarkable 78% (18). Other immunotherapeutic agents include blinatumomab, a CD19-CD3 bispecific

antibody which binds $CD3^+$ T cells to $CD19^+$ B-ALL cells to promote activation, and Inotuzumab ozogamicin, a CD22 (Siglec-2) monoclonal antibody conjugated to the chemotherapeutic calicheamicin which specifically delivers the chemotherapeutic to $CD22^+$ B-ALL cells. These have both shown efficacy in treating relapsed B-ALL disease, demonstrating the susceptibility of B-ALL overall to immunotherapy (19, 20). Yet there is still much to understand about the mechanisms of immune evasion utilized by B-ALL, and further research is required to fully optimize therapeutic immunomodulation for this disease.

1.3 Immune evasion in B-ALL

The contributions of the immune system to the control and clearance of cancer have been a long-standing debate. The tumor microenvironment (TME), consisting of all non-cancerous cell types, such as stromal cells, endothelial cells, and tissue-resident or infiltrating immune cells, has historically been believed to be pro-tumorigenic and hostile to immune effectors (21). Better understanding of tumor-infiltrating immune cells has revealed that TME suppression of immune activity is vulnerable to therapeutic intervention (22-24), and utilization of immune-based therapies has shown great efficacy in treatment of aggressive cancers where few other therapies have (25-27). For this reason, extensive research on the mechanisms by which solid tumor cells evade the immune response has been documented, yet studies into these and other undiscovered mechanisms of immune escape in blood cancers are still emerging. As blood cancers derive from or share a common progenitor with those immune cells utilized in cancer immunotherapy, the potential for blood cancer cells to inherit and exploit the mechanisms by which immune cells communicate and cross-regulate one another is high. Should this be the case, the therapeutic potential and efficacy of immunotherapy in blood cancers should be equally high.

1.3.1 *Mechanisms of immune escape in B-ALL*

Downregulation or loss of MHC expression in cancer cells is a common intrinsic method of immune evasion which lowers the T cell capacity to detect and interact with tumor cells but increases the likelihood of clearance by KIR- and NKG2-expressing NK cells. In ALL, however, loss of MHC is only present in a rare subset of patients (28), and NK cells have been demonstrated to have little effectiveness in the clearance of ALL (29, 30). Despite this presence of stably expressed MHC, ALL is a cancer type

with relatively low mutational burden, which results in few neoantigens being presented on MHC complexes (31) and therefore reduces the targetability of the cancer cells by the adaptive immune response. Though a subset of B-ALL overexpresses the CD47 “don’t eat me” signal to avoid immune clearance through phagocytosis (32), B-ALL cells are known to express modest if negligible amounts of immune checkpoint ligands such as PD-L1 and Galectin-9 outside of unique circumstances (33, 34).

Thus, immune escape in B-ALL is primarily mediated through extrinsic means; remodeling and co-opting the cells of the TME to better suit leukemogenesis and disease progression. B-ALL has demonstrated resistance to NK cell cytotoxicity (29), mediated through secretion of factors such as TGF-β (30) which can effectively hold bone marrow NK cells inactive. The secretions of B-ALL cells, including such factors as BMP4, have also been shown to skew dendritic cells (DCs) to a more immunosuppressive profile and macrophages to the immunosuppressive M2 polarization state (35). Disruption of normal monocyte differentiation is an important component of B-ALL bone marrow remodeling, where higher proportions $CD16^+$ non-classical monocytes in the bone marrow at time of diagnosis correlate with poorer patient outcomes and contribute to therapeutic resistance in B-ALL models (36). This high myeloid cell infiltration of B-ALL bone marrow was utilized to generate $TIE2^+$ monocytes modified to deliver IFNα to the bone marrow in a manner which augmented CAR T therapy in a mouse model of B-ALL (37), suggesting this phenomenon may be further exploited to optimize B-ALL immunotherapies.

Considerable research has been done on the effects of B-ALL on T cells, where the disease appears to have a profound impact on T cell activation in the bone marrow. T regulatory cells (Tregs) are expanded in the marrow and blood of B-ALL patients (38), contributing to the local IL-10 and TGF-β immunosuppressive signaling pool and playing an emerging role in immunotherapeutic resistance in B-ALL (39, 40). Though B-ALL cells themselves do not typically express high amounts of immune checkpoint molecules, bone marrow resident $CD4^+$ and $CD8^+$ T cells have been demonstrated to express high levels of PD-1, TIM3, and TIGIT in B-ALL (41-43), which in some cases correlates with relapse and poorer patient outcomes (41). Treatment of B-ALL with immune checkpoint inhibitors has to-date showed underwhelming efficacy (44), likely due to the immune-ablative effects of chemotherapeutic

induction and the low mutational burden of B-ALL. Yet clinical trials combining immune checkpoint inhibitors with other therapies in B-ALL are still ongoing (NCT03512405, NCT05310591, and NCT02879695) and may yet prove effective. Our group and others have demonstrated B-ALL can induce exhausted T cell profiles within the bone marrow through disease progression and cellular secretions (45-47), yet the specific mechanisms by which B-ALL-mediated T cell suppression occurs is still in ongoing investigation, a few of which are discussed below.

1.3.2 *Calcineurin and IL-12 regulate B-ALL immune escape*

Our lab has performed extensive research detailing the changes of the bone marrow tumor microenvironment during B-ALL progression, primarily through study of immunomodulators calcineurin and IL-12. The serine/threonine phosphatase calcineurin upstream of the NFAT pathway has a well-demonstrated role in mediating "stemness" in T-ALL (48, 49), and, by our lab, in immune evasion of B-ALL (46). We have previously shown that knockdown of the critical calcineurin regulatory subunit (CnB) in BCR-ABL1^{+} murine B-ALL leukemia cells engrafted in immune competent mice leads to prolonged survival, an effect lost when engrafted into immunocompromised *Tcra*$^{-/-}$ mice, deficient in the alpha beta T cell receptor critical for differentiation of mature T lymphocytes (**Fig. 1.3A**). Further characterization of the immune populations in the bone marrow from immunocompetent mice engrafted with either control or calcineurin-deficient leukemia revealed an increase in CD8^{+} cytotoxic T cells in the latter (**Fig. 1.3B**), supporting calcineurin as a regulator of adaptive immune escape in B-ALL.

However, calcineurin is critical in physiological T cell development and activation (50, 51), and systemic inhibition for use as an anti-leukemia immunotherapy is not likely to be effective (46). Thus, to identify downstream mediators of calcineurin-dependent immune evasion, our lab performed experiments to characterize functional and phenotypic differences in calcineurin-deficient leukemia cells, including cytokine array analysis on the secretions of these murine leukemia cells. IL-12p40 was found to be secreted at significantly higher levels by the more immunogenic calcineurin knockdown cells (46). Further investigation demonstrated the therapeutic potential of recombinant IL-12 (rIL-12) in normalizing proportions of T cells and DCs as well as the cytokine milieu in the B-ALL-transformed bone marrow

niche. rIL-12 also demonstrated marked efficacy in reducing exhausted T cell profiles in B-ALL-suppressed T cells and augmenting blinatumomab therapy (47).

Aside from the cytokine array which identified IL-12 as a downstream effector of calcineurin-mediated immunosuppression, our group also performed RNA-sequencing of control or calcineurin knockdown leukemia cells sorted from the bone marrow of engrafted immunocompetent mice (**Fig. 1.3C**). Of the top three most significantly downregulated genes found in the more immunogenic calcineurin knockdown B-ALL, we were able to validate only the downregulation of the gene *Siglec15* using real time qPCR (RT-qPCR) (**Fig. 1.3D**), which became the foundation of the project described within this text. The mechanisms by which Siglec-15 (Sig15) alters the immune response to B-ALL is an ongoing area of interest for our lab; further identification of the impacted immune populations and consequent molecular mechanisms of leukemia-expressed Sig15 is one of the primary aims of this project.

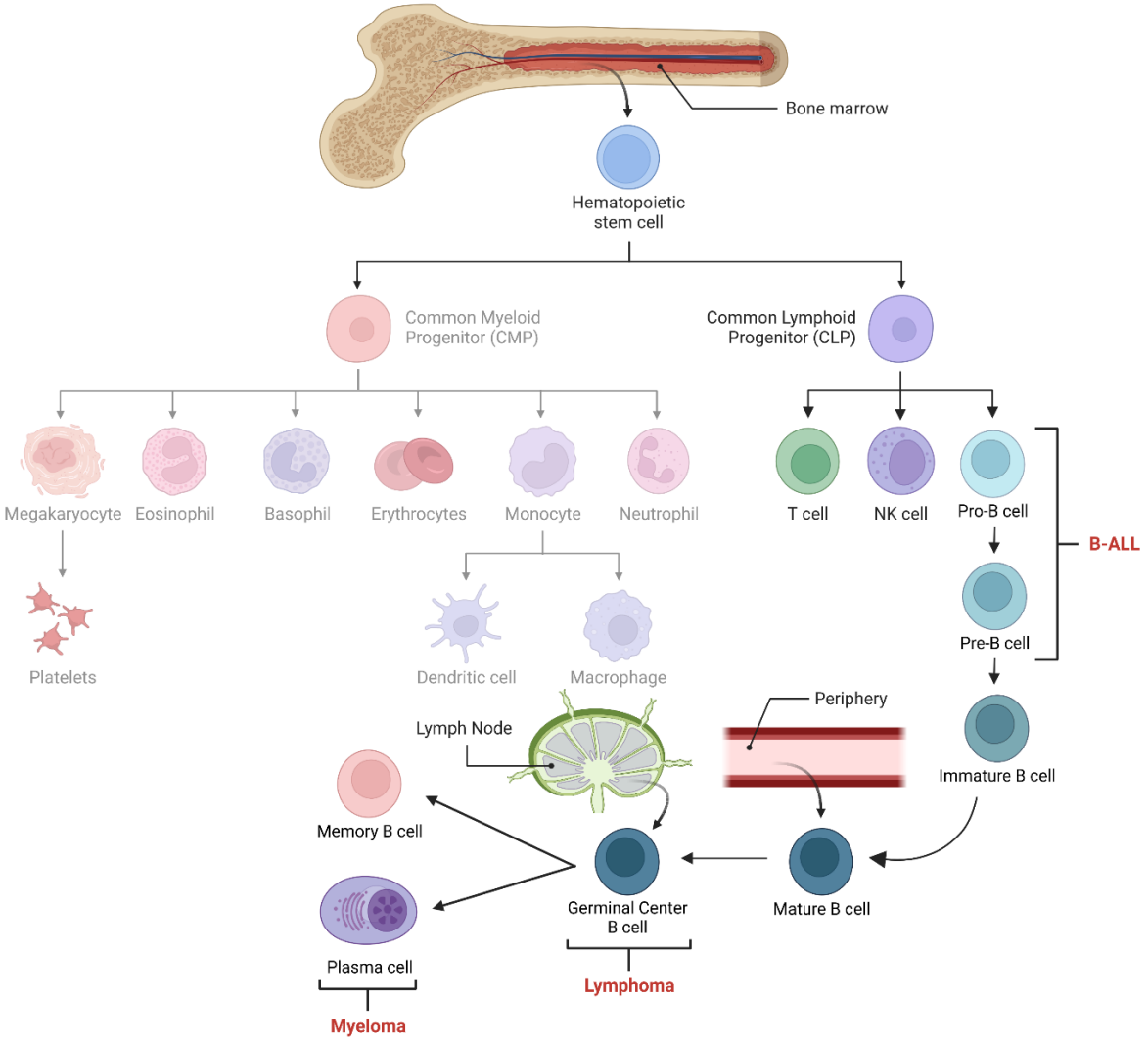

Figure 1.1 Normal hematopoiesis and lymphoblastic/lymphocytic cancer cells of origin. Schematic for hematopoietic cell differentiation, highlighting the maturation path of B cells in the human body. The cell types from which B-ALL, B cell lymphoma, and myeloma are believed to arise are indicated with brackets and red labels. Note that, while B cell lymphoma usually develops from germinal center B cells in the lymph nodes, it may also occur in other parts of the lymphatic system such as the thymus, spleen, or mucosa tissue. Adapted from “Stem Cell Differentiation from Bone Marrow”, created by "Dr. Akiko Iwasaki" using BioRender.com (2023). Retrieved from https://app.biorender.com/biorender-templates.

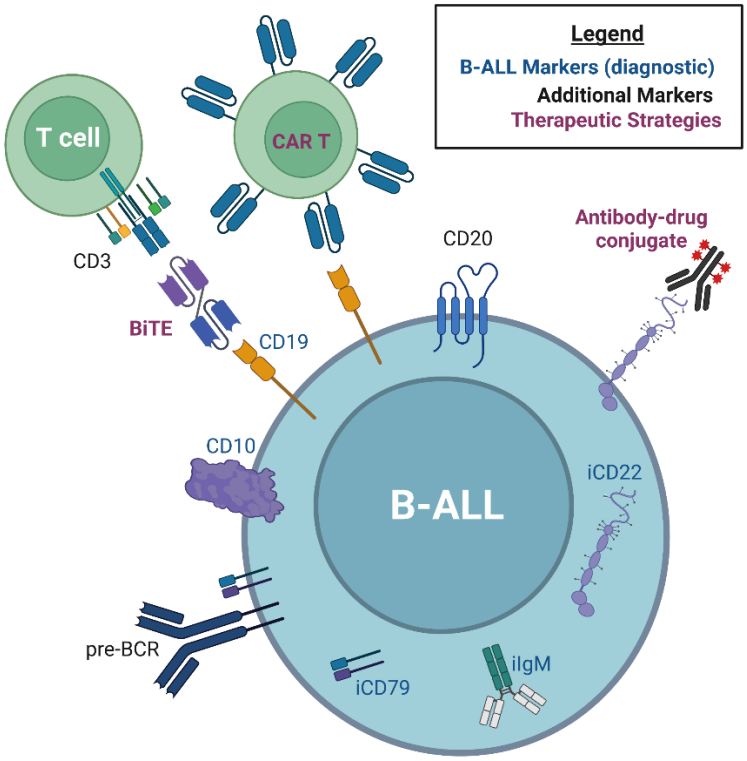

Figure 1.2 Proteins commonly expressed on B-ALL and their therapeutic targeting. Markers by which B-ALL cells are diagnosed through flow cytometric analysis are indicated **in blue**, including intracellular/cytoplasmic-detected proteins which are indicated with an "i-" preceding the protein name (e.g. "iCD79"). Other important markers are indicated **in black**, including markers such as CD20 and the pre-BCR which can be used for identification and characterization of B-ALL cells. A few therapeutic strategies for targeting markers on B-ALL cells are diagramed **in purple**: including bispecific T cell engagers (BiTE) such as blinatumomab which conjugates CD19-expressing B-ALL cells with CD3-expressing T cells, CD19-targeted CAR T cells, and antibody-drug conjugates such as the CD22-targeted Inotuzumab ozogamicin. Created with BioRender.com.

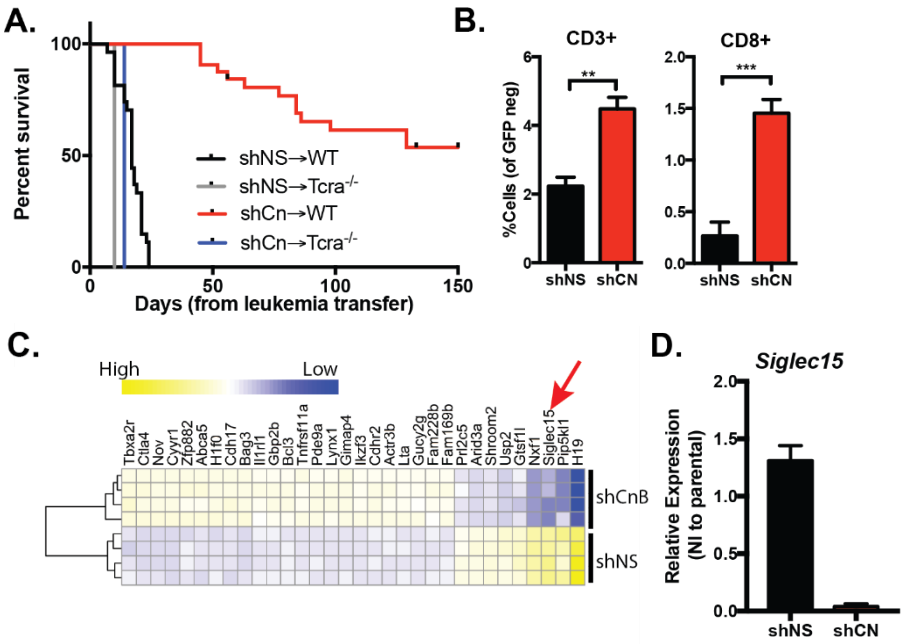

Figure 1.3 Calcineurin is a mediator adaptive immune evasion in B-ALL. **A.** Un-irradiated, WT or *Tcra*$^{-/-}$ C57Bl6 mice were injected with 5x10^5 non-silencing (shNS) or calcineurin knockdown (shCnB) leukemia cells. Kaplan Meier curve shows prolonged survival of WT recipients of shCnB leukemia. **B.** Bone marrow was harvested from WT recipients of GFP-tagged shNS and shCnB leukemia 7 days after transfer. GFP^{neg} cells were analyzed via flow cytometry for CD3 and CD8 proportions (**P<0.01, ***P<0.001). **C.** GFP$^+$ leukemia cells were harvested at day 7 and analyzed for gene expression analysis by RNA seq. The heatmap depicts the most highly differentially expressed genes, with stringent criteria of FDR<0.05 and >2-fold change. Red arrow identifies *Siglec15*. **D.** RT-qPCR was used to detect *Siglec15* from *ex vivo*-cultured shNS and shCnB leukemia cells. Data were normalized to expression levels in the parental cell line. All data taken from Rabe et al., 2019 (51). These data demonstrate calcineurin-dependent immune evasion by B-ALL cells and implicate Siglec-15 as one of its possible downstream effectors.

Chapter 2: Siglec-15 and immunosuppression

2.1 Siglec Family Proteins

Sig15 is a member of the Siglec (**s**ialic acid-binding **Ig**-like **lec**tin) family of proteins. These are I-type (or immunoglobin-like) lectins which can bind select sugar moieties called sialic acid on a variety of glycosylated proteins (52). As cell surface proteins, the Siglec family members (**Fig. 2.1**) are Type 1 transmembrane proteins which possess a single-pass transmembrane domain. Siglecs also possess an N-terminal V-set domain, which resembles the immunoglobin (Ig) variable region and has sialic-acid-binding capacity, and a variable number of C-set domains, which resemble the Ig constant region type 2 and are located between the V-set domain and the transmembrane domain (53). Siglec expression is both restricted to and highly heterogenous across all immune cell types with the exception of Siglec-4 (**m**yelin-**a**ssociated **g**lycoprotein, MAG) and Siglec-6 (CD327), which are expressed primarily on neuronal and placental cells respectively (53). While some lectins, such as Selectins and Lecticans, function primarily in cell adhesion and migration (54), Siglecs are of the class of lectins which modulate immune stimulatory or suppressive signaling effects. This is a function of the sialic acid-binding capacity of Siglecs, which allows for recognition and response to self-antigens in bodily tissues.

2.1.1 *Sialic acid and self-immunity*

Sialic acid is a form of sugar modification found on glycoproteins consisting of *N*- or *O*-linked derivates of the amino sugar called neuraminic acid. As an acid, this alpha-keto sugar modification carries a negative charge at normal pH and is typically the outermost component of the oligosaccharide sugar chains which modify cell surface or heavily glycosylated proteins such as mucins. In mammals, sialic acids are often found in one of three major types, including N-acetylneuraminic acid (Neu5Ac, NANA), deaminated neuraminic acid (KDN), and N-glycolylneuraminic acid (Neu5Gc). While humans are unable to naturally synthesize Neu5Gc and must therefore uptake it from dietary sources, Neu5Ac is highly and widely distributed across human tissues but notably not on most pathogens (55). Sialic acids therefore may act as self-associated molecular patterns (SAMPs), utilized by the immune system to discriminate and dampen immune response against self-tissue (56).

The natural co-evolution of immunity and pathogenesis has created over time two major mechanisms by which sialic acid-mediated immunosurveillance may be exploited: molecular mimicry and hypersialylation. In the case of molecular mimicry, pathogens have long evolved a variety of strategies in which to acquire and present "self" sialic acid moieties, primarily Neu5Ac, on their capsules to avoid immune clearance. Strains of *E. coli*, *N. meningitidis*, and *N. gonorrhoeae* have been demonstrated to attain sialic mimetics and sialic acids through unique *de novo* synthesis pathways or scavenging them from human secretions using sialyltransferases (57). This mimicry is believed to be the driving selective pressure behind modern sialic acid evolution, which has resulted in the development of over 50 different versions of sialic acids utilized in vertebrate tissues. In congruence with the rapid expansion of sialic acid evolution, Siglec evolution has equally expanded, giving rise to the highly specific immunostimulatory and immunosuppressive CD33-related Siglec family members in an evolutionary "arms race" (58), which is to be discussed later in this chapter.

Hypersialylation, defined as the increased presentation of sialic acid on surface proteins, is observed across a broad range of cancers. Mechanistically, this increased sialylation often occurs through increased expression of sialyltransferases and heightened metabolism of sialic acid precursors, which are commonly downstream of Ras or c-Myc activating mutations in cancer cells (59). Though largely considered a pathological phenomenon, high levels of sialic acid are in fact present on some normal cell types, including embryonic tissue, neuronal tissue, and, notably, red blood cells (RBCs) (60, 61). In the case of RBCs, the surface of these non-nucleated cells is concentrated with sialoglycans which protect RBCs from neutrophil activation and clearance in circulation, among other roles (62, 63). Hypersialylation is present across countless cancer types, including breast, colorectal, prostate, and pancreatic cancers, as well as leukemia (59). Tumor hypersialylation has been demonstrated to increase migration and invasion through promotion of extracellular matrix interactions, occlude antigen epitopes to block antibody binding in humoral immunity, and dampen immunoregulation by engaging with immunosuppressive Siglec family proteins. For these reasons, tumor hypersialylation is widely correlated with poor patient outcomes, and therapeutic strides are currently underway to target this phenomenon

using specific glycomimetics (64). While these emerging sialic acid-targeting therapies show promise in preclinical studies, an even greater amount of research and therapeutic development has occurred on the canonical sialic acid-binding proteins, the Siglecs.

2.1.2 *Siglecs in overview*

Siglec family proteins can be divided into two major subgroups by their conservation across vertebrate evolution. The first subgroup is the most evolutionarily conserved, present across all mammals with high homology, and includes Siglec-1 (sialoadhesin), Siglec-2 (CD22), Siglec-4 (MAG), and Siglec-15. The second group consists of the remaining Siglecs, which all bear structural similarities to Siglec-3 (CD33) but have relatively low homology across the different mammalian species and have been characterized through phylogenetics to have rapidly evolved in primates in recent evolution (65). As pathogens evolved molecular mimicry to present sialic acid derivatives, enabling pathogenic evasion of immune clearance and propagation in mammalian hosts, CD33-related Siglecs were selectively pressured to evolve higher specificity for their target sialoglycans, creating a co-evolutionary arms race between sialic acid-presenting pathogens and the mammalian immune cells they exploit (66). Thus, CD33-related Siglecs have demonstrated higher specificity for the sialic acid variants they will bind, mediated by the rapid genomic evolution of their sialic acid-binding V-set domains (67). Yet sialic acid specificity is not the only evolutionary change in CD33-related Siglecs which resulted from this arms race; some family members also developed alterations in their transmembrane and intracellular domains, which in turn altered their downstream signaling capacity.

In light of their similarity to Siglec-3, most CD33-related Siglecs possess immunosuppressive downstream signaling. These effects are mediated by the presence of ITIM (**i**mmunoreceptor **t**yrosine-based **i**nhibition **m**otif) and ITIM-like domains in their cytoplasmic tails (**Fig. 2.2A**), which, once phosphorylated by Src family kinases, can recruit immunosuppressive phosphatases such as SHP-1 and SHP-2 to the immune synapse and dampen upstream activity of pathways important to immune cell activation (68). Due to the exploitation of these immunosuppressive Siglecs by sialic acid-presenting pathogens, a new form of Siglec evolved over time which bound the same select sialic acid derivates as

its immunosuppressive counterparts and yet was immunostimulatory in nature, called activating Siglecs. The members of this new group, including Siglec-14 and Siglec-16, contain a positively-charged amino acid residue located within their transmembrane domains (**Fig. 2.2B**), which allows for coupling and stabilization of the ITAM (**i**mmunoreceptor **t**yrosine-based **a**ctivation **m**otif) domains of partner "adaptor" proteins such as DAP12 (TYROBP), DAP10 (HCST), and FcR gamma chain (FcRγ) (69). The ITAM domains of these adaptor proteins, when they are associated with sialic acid-bound activating Siglecs, are then phosphorylated by Src kinases and act as docking scaffolds for the SH2 domains of kinases such as SYK and ZAP-70, which activate downstream phosphorylation signaling cascades to activate immune cells. Notably, while Siglec-15 is not of the CD33-related Siglecs, its structure classifies it as an activating Siglec as well, the implications of which are to be discussed later in this chapter.

These activating Siglecs are often present as "paired receptors," wherein a single immunosuppressive and immunostimulatory Siglec both have specificity for the same sialic acid derivative but have opposing signaling capacity. Examples of this phenomenon include Siglec-5/Siglec-14 (70) and Siglec-11/Siglec-16 (71), but notably not Siglec-15. Such Siglec pairs are typically co-expressed, allowing for fine-tuning of the activation status of the immune cells which express them. Thus, a successful immune response may be mounted against sialylated pathogens while still identifying self-tissue through sialoglycans, modulated by the signaling cascades of the immunostimulatory and immunosuppressive Siglecs in tandem.

2.1.3 *Siglecs in cancer*

Given Siglecs are primarily expressed across a broad range of immune cells, their interaction with cancer cells can come in two main manners: Siglecs expressed on tumor-infiltrating immune cells and Siglecs expressed on immune cell-derived blood cancers. In this section, we will address the former. The structure of Siglec-1 (Sialoadhesin, CD169), lacking any intracellular signaling capacity but possessing a long extracellular chain of C2-set domains, makes it optimal for cell-cell interactions and migration. Siglec-1 is expressed on monocytes and macrophages, and Siglec-1-expressing macrophages play important roles in B cell priming in the lymph nodes for optimal humoral immune response (72). They

also facilitate priming and activation of $CD8^+$ cytotoxic T lymphocytes (CTL) in the lymph nodes, increasing CTL infiltration into the tumor, reducing lymph nodal metastasis, and overall correlating with improved patient survival in colorectal, gastric, and skin cancers (73-76). Siglec-4 (MAG), expressed on oligodendrocytes and Schwann cells in the central and peripheral nervous systems, similarly lacks intracellular signaling domains and plays a primary function in cell-cell adhesion in myelin-axon interactions. Limited research has demonstrated its contributions to neural invasion in pancreatic cancer through binding the highly glycosylated mucin MUC-1 (77). While the involvement of Siglec-2 (CD22) and Siglec-15 in cancer is to be discussed in the following sections, CD33-related Siglecs have well established roles in promotion of tumor-mediated immunosuppression.

Siglec-5, Siglec-7, Siglec-9, and Siglec-10, despite lacking expression in normal T cells, have all been demonstrated to be expressed on populations of tumor-infiltrating $CD8^+$ and $CD4^+$ T lymphocytes (TILs) in non-small cell lung cancer (NSCLC) (78). Siglec-5 is expressed on many leukocytes, including neutrophils, monocytes, B cells, and T cells; in the case of the latter, it has recently emerged as a novel marker of antigen-specific T cell activation. Containing both an ITIM and ITIM-like domain in its cytoplasmic tail, Siglec-5 has been demonstrated to attenuate NFAT and AP-1 signaling downstream of TCR engagement to suppress lymphocyte activation, an immunomodulatory axis that is exploited by some lymphoma cell lines which express ligands for Siglec-5^+ T cells (79). Siglec-5 also possesses an alternative spliceoform that is released as a soluble molecule (sSig5), which can bind to P-selectin ligand 1 (PSGL1) to inhibit leukocyte extravasation from the blood vessels at sites of inflammation (80).

Siglec-7 and Siglec-9 share considerable similarities in structure and sialic acid-binding preference, are expressed across a breadth of innate and adaptive immune cells, contain a single ITIM and ITIM-like domain in their cytoplasmic tails, and have well-established roles in suppressing immunity (81). Siglec-7 is ubiquitously expressed across NK cells and, when bound to sialoglycans expressed on tumor cells, plays a critical part in attenuation of NK cell activation and lysis (82). Despite this, NK cells lacking Siglec-7 which circulate in the blood of HIV and hepatocellular carcinoma patients have reduced activation and pro-inflammatory profiles (83, 84), suggesting Siglec-7 may play a more complex

modulatory role in NK cell function. Siglec-7 and Siglec-9 ligands expressed on pancreatic cancer cells were found to regulate the differentiation and co-option of tumor-associated macrophages (TAMs), promoting polarization of macrophages to their more tumor-supportive M2 state and the release of immunosuppressive factors such as IL-10 (85, 86). Siglec-9 is the highest Siglec expressed in NSCLC TILs and is also present in colorectal and ovarian cancer TILs, where it correlates with poor patient outcomes and is often co-expressed with immune checkpoint molecules such as PD-1, TIM-3, and LAG-3 in subsets of activated, tumor-specific PD-1^+ $CD8^+$ T cells (78). Indeed, Siglec-9 has an emerging role as an immune checkpoint molecule expressed on tumor-infiltrating $CD8^+$ T cells across many cancers, including melanoma, colon cancer, lung cancer, low grade glioma, and several others (87-89). This broad utilization across solid tumors has made it an attractive candidate for immune checkpoint therapy, where blocking antibodies against Siglec-9 have demonstrated the capacity to restore neutrophil-mediated tumor killing in mouse models of NSCLC and colorectal cancer (85) and to reduce metastasis and promote tumor clearance in a model of melanoma (87).

Siglec-10 is expressed widely across leukocytes, including monocyte/macrophages, dendritic cells, B cells, and eosinophils, and possesses 3 C2-set domains projecting extracellularly and a cytoplasmic tail consisting of one ITIM, one ITIM-like, and a Grb2-binding domain similar to that of CD22 near to its transmembrane domain (90). It has high binding affinity for heavily sialylated proteins such as CD24, contributing to the role of macrophage-expressed Siglec-10 in suppressing tissue damage-induced inflammation by inhibiting downstream NF-κB activation (91). Ovarian and triple-negative breast cancer cells are known to overexpress CD24 as a "don't eat me" signal in order to evade TAM-mediated phagocytosis, making it a potent target for inhibition in promoting tumor clearance (92). Yet another preferred binding partner of Siglec-10 is CD52, which can be released as a soluble molecule that binds Siglec-10 on subsets of $CD4^+$ T cells and monocytes to suppress TCR activity and pro-inflammatory cytokine secretion (93, 94). Soluble CD52 is known to be released by breast cancer and chronic lymphocytic leukemia (CLL) cells, promoting localized and systemic immunosuppression in the formation of the tumor microenvironment.

The contributions of the remaining Siglecs, including immune-activating Siglec-14 and Siglec-16, to tumor progression and immunoregulation remains emerging or otherwise unclear in the literature. Siglec-14 has been characterized as an important regulator in Group B streptococcal infection, where Siglec-14-deficient macrophages and fetal neutrophils have been demonstrated to be more susceptible to sialic acid-mediated infection, which, in the case of the former, was shown to be mediated through suppression of inflammasome activity downstream of NLRP3 signaling. When co-expressed with high levels of tissue sialoglycans, Siglec-16 has been shown to promote polarization of glioblastoma-infiltrating TAMS to a more pro-inflammatory M1 state and to positively correlate with patient survival (95). While data is still yet being gathered on these activation Siglecs, the emergence of their Siglec-15 counterpart as an apparent immunosuppressive checkpoint molecule in cancers (to be discussed later in this chapter) remains an incompletely understood phenomenon.

2.1.4 *Siglecs in leukemia*

As leukemias originate from the early predecessors of immune cells, many Siglecs are expressed on and functionally exploited by blood cancer cells, which supports Siglec targeting as a promising field for therapeutic research. Siglec-2 (CD22) is perhaps the best-known example of this, being exclusively expressed across B cells and B cell malignancies. With 3 ITIM, 1 ITIM-like, and 1 Grb2-binding domain on its cytoplasmic tail, sialic acid-bound CD22 can potently suppress B cell receptor (BCR) activation by recruiting immunosuppressive phosphatases to the immune synapse (96). Due to its widespread expression across precursor, mature, and malignant B cells, as well as its role in suppressing activation and antigen presentation in B cells (97), CD22 has emerged as a potent target for therapy in B cell leukemias and lymphomas, including B-ALL, DLBCL and other forms of non-Hodgkin's lymphoma (NHL) (98-100). This is often accomplished using blocking antibodies such as epratuzumab or drug-conjugated antibodies such as inotuzumab-ozogamicin, which is conjugated to the antibiotic calicheamicin that causes apoptosis-inducing DNA double strand breaks in tumor cells (101). Another role has recently emerged for CD22 as a target for CAR T therapy in B cell malignancies. With antigen escape being one of the most common causes for relapse in CD19-targeted CAR T therapy (102), CD22

expression has been demonstrated to be maintained in even CD19-negative relapsed leukemia cells (103), prompting design and utilization of CD22-targeted CAR T cells alone or in combination with CD19-targeted CAR T cells in the treatment of relapsed/refractory B-ALL (104, 105).

Siglec-3 (CD33) plays a similar role in AML, being expressed on most myeloid precursors, monocytes/macrophages, mast cells, and microglia. Its cytoplasmic tail consists of an ITIM and ITIM-like domain which can dock SHP-1/SHP-2 inhibitory phosphatases to attenuate activation in a mechanism which is not currently fully understood, though it is known that the SYK/ZAP-70 pathways are required (68, 106). As 85-90% of AML cases are CD33-expressing (107) and CD33 has been demonstrated to promote AML proliferation (106), it is yet another promising target in treatment of AML, though it maintains therapeutic challenges. Gentuzumab-ozogamicin, a CD33-antibody conjugated to calicheamicin, has demonstrated efficacy in combination with chemotherapy in $CD33^{hi}$ newly-diagnosed and relapsed AML patients of moderate-to-low risk groups (108). Attempts have also been made to engineer CD33-targeted CAR T cells, which have demonstrated limited efficacy thus far due to difficulties in efficient CAR manufacturing (109), and CD33 BiTE molecules which show promise in early phase clinical trials (110).

With the addition of Siglec-6, which has recently been demonstrated to be expressed on CLL cells and thus be an effective target for CAR T therapy (111), these Siglecs are aberrantly expressed on blood cancers and play important roles in mediating immunosuppression. Therapeutically targeting these molecules provides efficacy in a twofold manner: inhibiting the immunosuppressive activity of the molecule itself to restore the tumor-controlling bone marrow niche and allowing for effective identification/elimination of the Siglec-expressing leukemia cells with minimized off-target toxicity to any healthy precursor immune cells present. It is for this reason that the emergence of Siglec-15 as an immune checkpoint molecule and possible target for therapeutic intervention in leukemia provides an enticing area for new research.

2.2 Siglec-15 as a highly conserved immunomodulator

Siglec-15 (Sig15) is the smallest of the 17 (112) Siglec family members (**Fig. 2.3**), containing a single V-set and C2-set domain in its extracellular projection, a short cytoplasmic tail with no notable structural domains, and, as an activating Siglec, a lysine residue in its transmembrane domain which allows it to couple with and activate the ITAM domains of adapter proteins DAP12, DAP10, and FcRγ to activate downstream SYK and ERK/Akt in osteoclasts and myeloid cells (113). *SIGLEC15* is located on a different chromosome from the CD33-related Siglecs, and it maintains a striking homology through vertebrate evolutionary history which is not observed in the recently-evolved CD33-related Siglecs, suggesting it belongs in the group of conserved Siglecs instead. To the latter point, Sig15 is expressed across all major branches of vertebrates with considerably homology, making it one of the most highly conserved Siglecs aside from MAG and therefore likely an "ancestral" Siglec (113). Though bearing similar structural and functional properties as the other activating Siglecs, the conservation of Sig15 across phylogeny would suggest this resemblance to Siglec-14 and Siglec-16 is likely an instance of convergent evolution rather than any ancestral derivation. The selective pressure driving this conservation is an ongoing area of speculation, though it likely involves the critical roles that Sig15 plays in bone remodeling and immunoregulation, to be discussed in the next sections.

Murine Sig15 has been previously demonstrated to have high affinity for binding the Sialyl Tn (sTn) modification, an O-linked derivative of Neu5Ac which is widely overexpressed on cancer-associated mucins and solid tumor cells (114, 115). Human Sig15, however, has been shown to have lower binding affinity for sialic acid (113), and reports have varied regarding its preference for binding sTn over other derivatives (116, 117), possibly suggesting a higher promiscuity in protein-protein interaction. Sig15 is known to be expressed on mature dendritic cell (DC) and macrophage populations (113, 118) as well as mature osteoclasts (119). Interestingly, Sig15 was found to be intracellularly localized in some DCs and macrophages, a phenomenon which can be attributed to the rapid internalization motif in its cytoplasmic tail (113). This "YxxØ" motif promotes quick turnover of a protein at the membrane by the clathrin-associated AP-2 complex, facilitating recycling to the endosomal and, occasionally, lysosomal compartments (120). It has been previously demonstrated that expression of

adaptor proteins such as DAP12 can stabilize Siglecs at the cellular surface (71, 121), which could provide rationale for the variability in Sig15 surface localization amongst different cellular populations. To note, Sig15 is exclusively present at the membrane in mature osteoclasts, which express considerable amounts of DAP12 and other adaptor proteins and require the Sig15/adaptor intracellular signaling cascade to undergo physiological maturation.

2.2.1 *Siglec-15 in osteoclasts and osteoporosis*

Bone remodeling is mediated by two major cellular populations: osteoblasts, which synthesize the collagen and extracellular matrix that eventually becomes bone, and osteoclasts, which are multi-nucleated cells that secrete large amounts of hydrolytic enzymes that break down and digest the bone matrix (122). The latter cells are derived from myeloid precursor cells in the bone marrow that differentiate into immature osteoclasts when exposed to osteoclast-inducing factors secreted by osteoblasts. Sig15 has been demonstrated to play a crucial role in the maturation of osteoclasts. Sig15 is upregulated in osteoclast precursors when exposed to osteoclast-inducing factor RANKL, allowing sialic acid-bound Sig15 to couple with DAP12 and promote downstream PI3K/Akt and MAPK activation crucial to osteoclast development (123). Sig15 is so critical to this process, in fact, that mice completely deficient in *Siglec15* expression manifest no discernible phenotype aside from osteopetrosis, or hardening of the bone, in the trabecular and metaphyseal regions of the bone (123-125).

Antibodies targeting Sig15 have shown efficacy in inhibiting the function and development of osteoclasts (119, 126, 127), making it an attractive target for treatment of diseases which involve excessive breakdown of bone tissue, called “resorption.” Pathological bone resorption is one of the primary causes of osteoporosis, though it can commonly occur as a secondary symptom to other conditions including menopause, arthritis, malnutrition, and aging (128). Sig15-blocking antibodies have thus been developed and demonstrate efficacy in treating bone resorption in menopause, rheumatoid arthritis, and ovariectomy patients (125, 129, 130). Bone resorption is also a major concern of pediatric B-ALL, where both the therapeutic agents used to treat B-ALL (131, 132) and the disease progression itself (133) contribute to excessive bone loss. Thus the addition of a Sig15-blocking antibody to B-ALL

therapies could be beneficial in restoring the normal bone matrix niche as well as reversing immunosuppression.

2.2.2 *Siglec-15 and immunosuppression*

Though Sig15 is known to play a key role in the differentiation of osteoclasts, which have various characterized functions in immunosuppression (134-136), the role of Sig15 in immunomodulation is still emerging. As an activating Siglec, Sig15 has been demonstrated to be upregulated on barrier epithelial cells and PBMC-derived myeloid cells upon exposure to sialylated pathogens such as *C. albicans* (137, 138) and *A. fumigatus* (139), promoting immunity against vulvovaginal candidiasis and influenza-associated aspergillosis. Yet antibody-mediated blocking of Sig15 on macrophages in lung cancer has been shown to skew TAM polarization to the more pro-inflammatory M1 state (140). TAM-expressed Sig15 has the capacity to engage with tumor sialoglycans, promoting SYK and MAPK activation and, in some models, enhance TAM secretion of immunosuppressive factors such as TGF-β (116, 117). Sig15 expression has also been demonstrated to be negatively correlated with pro-inflammatory interferon signaling (118), which we have confirmed in our own models for Sig15 regulation in leukemia (to be discussed in **Chapters 3** and **4**). Given the extracellular structure of Sig15 bears striking resemblance to that of the B7 family of costimulatory and coinhibitory proteins (118), it is perhaps unsurprising that Sig15 may bear a complex role in regulating immunity, particularly in the context of cancer.

2.2.3 *Siglec-15 in cancer*

A seminal study by Dr. Lieping Chen's group into Sig15 in NSCLC and other solid tumors, primarily as expressed by tumor-infiltrating myeloid cells, demonstrated a role for Sig15 in suppressing antigen-specific T cell activation in cancer (118). Patient tissue from bladder, colon, endometrial, and several other solid tumors showed higher Sig15 staining than healthy tissue controls, and macrophage-limited knockout of *Siglec15* expression greatly enhanced the immune response to a NSCLC cell line model. In light of the homology between Sig15 and the B7 family proteins, and the inversely correlated expression of Sig15 with inflammation-induced checkpoints such as PD-L1, they thus proposed a role for

Sig15 as a new immune checkpoint which acts independently of the PD-1/PD-L1 axis to regulate immune activity of tumor-infiltrating myeloid cells.

Interest in Sig15 as a cancer immunomodulator has expanded rapidly in the last five years, with publications supporting its contributions across several cancers. Sig15 was found to correlate with metastasis and poor patient outcomes in osteosarcoma through upregulation of pro-invasion phosphatase DUSP1 and downstream MAPK activation (141). Studies into clear cell renal carcinoma demonstrate the upregulation of Sig15 through aberrant expression of long non-coding RNAs which promote tumor growth and attenuate T cell-mediated immunity in coculture and *in vivo* model assays (142, 143). High Sig15 expression in thyroid cancer correlated with a more immune-exhausted profile and increased lymph nodal invasion (144). The role of Sig15 in blood cancers is only recently emerging and remains unclear in the literature. Primary AML cells have been demonstrated to express excess Sig15, which is targetable through antibody-mediated blocking (145). Sig15 expression on macrophages was found to be a favorable prognostic indicator in DLBCL infiltration of the central nervous system (146), suggesting the contributions of macrophage-expressed Sig15 can be contextually dependent. Our group has sought to better elucidate the involvement of Sig15 as expressed on blood cancer cells, particularly B-ALL, in disease progression and immunosuppression.

2.3 Rationale and Research Goals

As discussed in this chapter, Sig15 is yet unstudied in the context of immune evasion in ALL and may be a potent immune-modulating therapeutic target for this disease. Thus the research objective of this dissertation is to characterize the role of Sig15 as a novel effector of immune evasion mechanisms in hematological malignancies. The central hypothesis of our studies is that Sig15 is aberrantly expressed in B-ALL and can be targeted to promote T cell-mediated immune clearance of leukemia cells. This hypothesis derives from our data to be discussed in **Chapter 3**, which demonstrates aberrant pathological expression of Sig15 in human B-ALL as compared to healthy controls with a unique mechanism for regulation of expression as well as surface localization and release of a secreted/soluble molecule. We also demonstrated the critical role of Sig15 in promoting clearance of leukemia when engrafted into

immunocompetent but not immunodeficient *Rag1*$^{-/-}$ mice, supported by an overall re-normalization of the bone marrow immune cell niche and cytokine milieu.

Yet this research lacks important context regarding the unique molecular biology, regulatory mechanisms, and multi-functionality which contribute to Sig15-driven B-ALL pathology, prompting further discussion of the molecule itself in **Chapter 4**. Our preliminary data support multiple isoforms of Sig15 which are differentially expressed across normal and pathological hematological samples, some of which appear to be regulated by independent signaling pathways and by active cell cycling. Particular domains of the Sig15 structure also appear to have capacity to localize to the nucleus in B-ALL and osteosarcoma cell lines, for which we have identified a unique importin β nuclear localization sequence that remains to be experimentally verified. There remains much to understand about the biology of Sig15 and how it may behave aberrantly in a malignant and/or lymphocytic context as compared its physiological myeloid context. Our long-term goal is thus to gain a greater understanding of the role of Sig15 in modulation of the adaptive immune response and its contributions to the B-ALL pathogenicity.

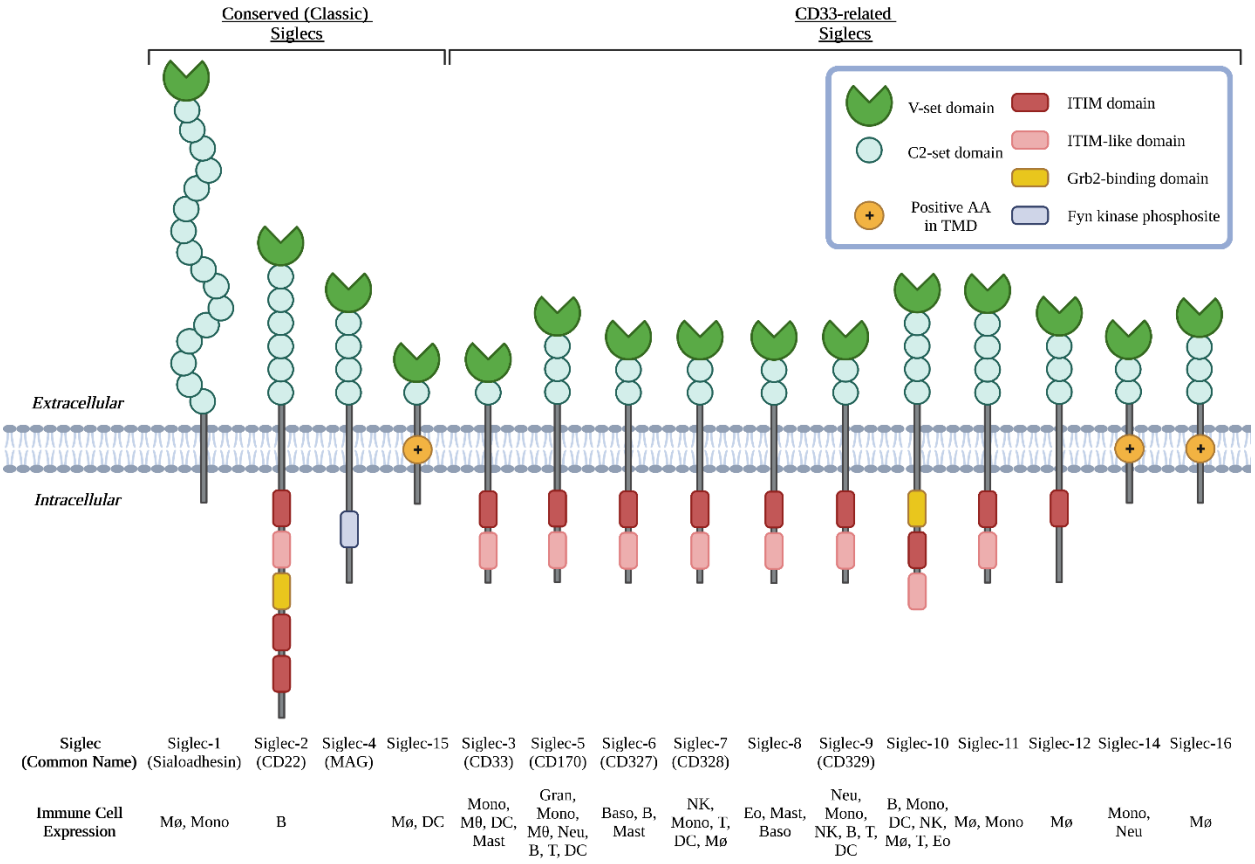

Siglec (Common Name)	Siglec-1 (Sialoadhesin)	Siglec-2 (CD22)	Siglec-4 (MAG)	Siglec-15	Siglec-3 (CD33)	Siglec-5 (CD170)	Siglec-6 (CD327)	Siglec-7 (CD328)	Siglec-8	Siglec-9 (CD329)	Siglec-10	Siglec-11	Siglec-12	Siglec-14	Siglec-16
Immune Cell Expression	Mø, Mono	B		Mø, DC	Mono, Mθ, DC, Mast	Gran, Mono, Mθ, Neu, B, T, DC	Baso, B, Mast	NK, Mono, T, DC, Mø	Eo, Mast, Baso	Neu, Mono, NK, B, T, DC	B, Mono, DC, NK, Mø, T, Eo	Mø, Mono	Mø	Mono, Neu	Mø

Figure 2.1 The name, structure, and common immune cell expression pattern of all human-expressed Siglec family proteins. Siglec proteins consist of an extracellular face (containing one sialic acid-binding V-set domain and a variable number of C2-set domains), a single pass transmembrane domain (TMD) which may contain a positively-charged amino acid (AA), and a cytoplasmic tail which may possess intracellular signaling capacity. Siglecs are divided into conserved/classical Siglecs and CD33-related Siglecs. To note, Siglec-13 and Siglec-17 are present only in an inactive, pseudogenic form in humans(112), while Siglec-12 (Siglec-XII) possess a point mutation in its V-set domain which renders it incapable of binding sialic acid moieties(147). Abbreviations for immune cell populations including the following: MΦ (macrophages), Mono (monocytes), B (B cells), DC (dendritic cells), Mast (mast cells), Gran (granulocytes), Neu (neutrophils), T (T cells), Baso (basophils), NK (NK cells), and Eo (eosinophils). Legend describing structural information in the upper right corner. Created with

BioRender.com, adapted from “Figure 1: Siglec-family proteins in humans and rodents” from Crocker, Paulson, and Varki, 2007 (53).

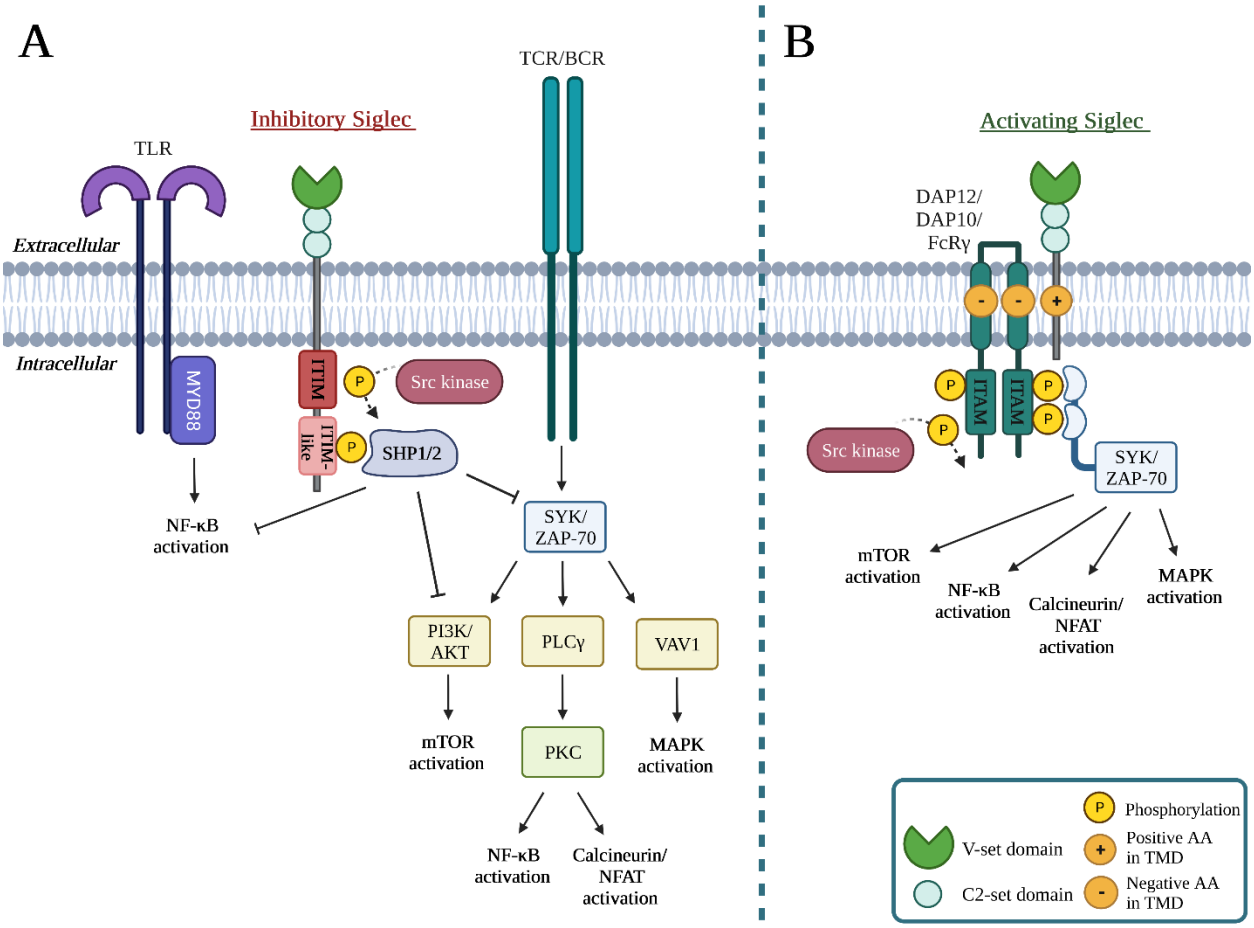

Figure 2.2 Siglecs may be further subdivided into inhibitory or activating Siglecs depending on their structure. (**A)** Binding of **inhibitory Siglecs** to their preferred sialoglycans results in a conformational change which allows the ITIM or ITIM-like domains in their cytoplasmic tails to be phosphorylated by Src family kinases. This in turn allows docking and recruitment of immunosuppressive phosphatases to the site of TCR/BCR or TLR signaling activation nearby. These phosphatases then attenuate phosphorylation cascades of factors such as SYK/ZAP-70, PI3K, and IKK, which consequently suppresses downstream immune activation. **(B)** Binding of **activating Siglecs** to their preferred sialoglycans results in a conformational change which allows interaction of a positively-charged amino acid (AA) in the transmembrane domain (TMD) to interact with a negatively-charged amino acid in the transmembrane domain of adaptor proteins such as DAP12, DAP10, and FcRγ. This interaction stabilizes the adaptor proteins, which allows for Src family kinases to dock and phosphorylate the ITAM domains

in the cytoplasmic tails of these adaptors, facilitating recruitment and activation of SYK/ZAP-70 kinases which activate multiple downstream immunostimulatory pathways. Created with BioRender.com.

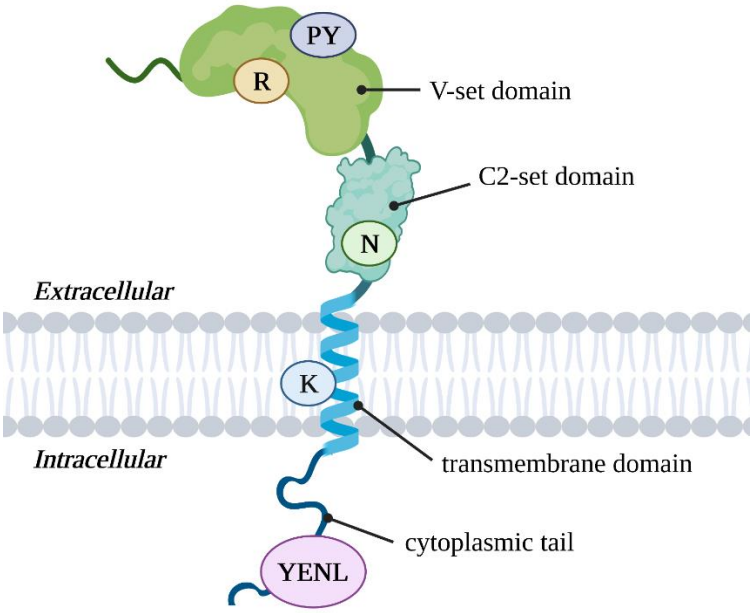

Figure 2.3 The structure and notable features of SIGLEC15. SIGLEC15 (Sig15) consists of an extracellular V-set domain, an extracellular C2-set domain, a helical transmembrane domain, and a cytoplasmic tail. Notable features also include a suspected PY-NLS motif (AA82-87; "PY")for importin β (to be discussed in **Chapter 4**) within the V-set domain, the positively-charged arginine (R143; "R") within the V-set domain that binds sialic acid moieties, an asparagine (N172; "N") predicted to be a site for N-linked glycosylation modifications (148), a positively-charged lysine (K274; "K") which allows for coupling and stabilization of adaptor proteins such as DAP12, and a YxxØ rapid internalization motif (AA310-313 ; "YENL") in the cytoplasmic tail which promotes rapid Sig15 internalization at the membrane. It should be noted that Sig15 contains a signal peptide sequence at its N-terminus upon translation (AA1-19) which is cleaved prior to translocation to the membrane. Created with BioRender.com.

Chapter 3: Siglec-15 promotes evasion of adaptive immunity in B-cell acute lymphoblastic leukemia

This chapter is adapted from a manuscript submitted by Pillsbury CE, Dougan J, Rabe JL et al. Siglec-15 promotes evasion of adaptive immunity in B-cell acute lymphoblastic leukemia. *Cancer Res. Comm.* 2023. (In press)

Claire E. Pillsbury,[1] Jodi Dougan,[2] Jennifer L. Rabe,[3] Jairo A. Fonseca,[2] Chengjing Zhou,[2] Alyssa N. Evans,[4] Hasan Abukharma,[5] Ona Ichoku,[5] Gloria Gonzalez-Flamenco,[6] Sunita Park,[6,7] Ahmed Aljudi,[6,7] Deborah DeRyckere,[2,4,8] Sharon M. Castellino,[2,4,8] Sarwish Rafiq,[4] Sol Langermann,[5] Linda N. Liu,[5] Curtis J. Henry,[2,4,8] Christopher C. Porter[2,4,8]

1. Cancer Biology Program, Laney Graduate School, Emory University, Atlanta, GA.
2. Department of Pediatrics, Emory University School of Medicine, Atlanta, GA.
3. Molecular Biology Program, University of Colorado Denver, Aurora, CO.
4. Winship Cancer Institute, Emory University, Atlanta, GA.
5. NextCure, Inc. Beltsville, MD
6. Clinical Laboratory, Children's Healthcare of Atlanta, GA
7. Department of Pathology, Emory University School of Medicine, Atlanta, GA.
8. Aflac Cancer & Blood Disorders Center, Children's Healthcare of Atlanta, GA.

3.1 Abstract

Siglec-15 (Sig15) has been implicated as an immune checkpoint expressed in solid tumor-infiltrating macrophages and is being targeted in clinical trials with mAbs to normalize the tumor immune microenvironment and stimulate antitumor immunity. However, the role of Sig15 in hematologic malignancies remains undefined. Sig15 mRNA and protein expression levels in hematologic malignancies were determined from publicly available databases, cell lines, and primary patient samples. Human B-cell acute lymphoblastic leukemia (B-ALL) cell lines were used to identify signaling pathways involved in the regulation of Sig15 expression. Secreted/soluble Sig15 and cytokine levels were measured from the plasma of children with leukemia and healthy controls. Knockdown and knockout of *Siglec15* in a murine model of B-ALL was used to evaluate the effect of leukemia-derived Sig15 on the immune response to leukemia. We observed pathologic overexpression of Sig15 in a variety of hematologic malignancies, including primary B-ALL samples. This overexpression was driven by NFκB activation, which also increased the surface localization of Sig15. Secreted/soluble Sig15 was found to circulate at elevated levels in the plasma of children with B-ALL and correlated with an immune-suppressive cytokine milieu. Genetic inhibition of Sig15 in murine B-ALL promoted clearance of the leukemia by the immune system and a marked reversal of the immuneprivileged leukemia bone marrow niche, including expanded early effector $CD8^+$ T cells and reduction of immunosuppressive cytokines. Thus, Sig15 is a novel, potent immunosuppressive molecule active in leukemia that may be targeted therapeutically to activate T lymphocytes against leukemia cells.

3.2 Introduction

B cell acute lymphoblastic leukemia (B-ALL) is the most frequent subtype of acute lymphoblastic leukemia and is the most common leukemia in children (149). Though standard-of-care treatment for ALL is sufficient to induce complete remission in up to 98% of cases (150), relapse occurs in approximately 15-20% of cases (151) and is characterized by highly aggressive disease, resistance to most salvage therapies, and historic 5-year-survival rates of below 50% (17). Treatment of refractory B cell malignancies using CD19-targeted chimeric antigen receptor expressing T cells (CAR T) and

blinatumomab, a CD19-CD3 bispecific antibody, have shown dramatic potential (18, 152), highlighting the potential of harnessing the immune system to treat these diseases. Nonetheless, responses are often incomplete or short-lived, and there remains much to understand about the mechanisms of immune evasion critical to disease progression and the best strategies to fully optimize therapeutic immunomodulation for B cell malignancies.

In previous work, we noted differential expression of *Siglec15* (Sig15) in an immunogenic mouse model of B-ALL as compared to the non-immunogenic control leukemia (46). Sig15 is a member of the sialic acid binding Ig-like lectin (Siglec) family of proteins, which are known to bind sialic acid sugar moieties on a variety of proteins and have immune stimulatory or suppressive signaling effects in select immune subsets (53). These effects are mediated by either the presence of immunoreceptor tyrosine-based inhibition motif (ITIM) domains or positively-charged amino acid residues located within their transmembrane domains; the latter allows for coupling and stabilization of the immunoreceptor tyrosine-based activation motif (ITAM) domains of partner adaptor proteins to enable downstream signaling activation (69).

Sig15 is known to be expressed in certain subsets of dendritic cells and macrophages (113, 118), as well as mature osteoclasts (123, 126), where it has been demonstrated to be critical for osteoclast differentiation and physiological bone growth/remodeling (119, 124). It possesses a lysine residue in its transmembrane domain which allows it to couple with the ITAM domains of adapter proteins DAP12 and FcRγ to activate downstream Syk and ERK/Akt in osteoclasts and myeloid cells (113), a pathway that can be exploited by tumor cells to promote TGFβ secretion in adjacent tumor-associated macrophages (116). A seminal study of Sig15 in non-small cell lung cancer, primarily as expressed by tumor-infiltrating myeloid cells, suggests a role for this molecule in suppressing antigen-specific T cell activation (118). Further studies in clear-cell renal cell carcinoma and osteosarcoma have implicated an immunosuppressive function for this molecule across solid tumor types (141, 143). However, the unique regulation and underlying mechanisms of immunomodulation by Sig15, particularly in leukemias and other hematological malignancies, remains to be defined.

Our investigations detected high Sig15 expression across hematological malignancies in both immortalized cell lines and primary patient samples. In the context of B-ALL, we have characterized a novel intracellular localization pattern and regulatory axis for Sig15. We have also demonstrated for the first time the release of a secreted or soluble form of Sig15 which circulates in the plasma of pediatric B-ALL patients and correlates with markers of systemic immunosuppression. Silencing of Sig15 expression in a murine model of B-ALL results in higher expansion and activation of select T cell populations and a decrease in immunosuppressive cytokines in the bone marrow, which suggests a niche for Sig15 as a target for therapeutic development in hematological malignancies.

3.3 Materials and Methods

Cell Lines and Tissue Culture

The human B-ALL cell lines REH (RRID:CVCL_1650), RCH-ACV (RRID: CVCL_1851), SEM RRID:CVCL_0095), Nalm6 (RRID:CVCL_0092), KOPN8 (RRID:CVCL_1866), RS411 (RRID:CVCL_0093), and 697 (RRID:CVCL_0079) were obtained from ATCC (Manassas, VA) and grown in RPMI 1640 or Iscove's Modified Dulbecco's Medium (IMDM) media supplemented with either 10% or 20% fetal bovine serum (FBS) and 1% penicillin/streptomycin. Human cell lines were not authenticated, but were periodically tested for Mycoplasma by RT-PCR (most recently in June, 2022). The luciferase-expressing, p185 *BCR-ABL1*$^{+}$ *Arf*$^{-/-}$ murine B-ALL cell line was generously provided by Dr. Richard Williams (St. Jude Children's Research Hospital, Memphis, TN) (153-155) and was periodically tested for Mycoplasma by RT-PCR (most recently in November, 2022). This cell line was cultured in RPMI 1640 supplemented with 20% FBS, 1% penicillin/streptomycin, and 0.1% β-Mercaptoethanol. All cell lines were cultured in a 37°C humidified incubator with 5% CO_2 for a maximum of 2 months before thawing a new vial of frozen stock.

To knockout *Siglec15*, the murine leukemia cells were transduced with a pCW-Cas9 construct (RRID:Addgene_50661) for doxycycline-inducible, FLAG-tagged Cas9 expression, as well as two guide RNA (gRNA) sequences cloned into the pLX-sgRNA (RRID:Addgene_50662) plasmid. Cas9 expression was induced with 10 ug/mL blasticidin for 3 days and cells were then seeded for single cell isolation.

Monoclonal colonies were harvested and assessed for genetic knockout using RT-qPCR. Short-hairpin RNA targeting *Siglec15* expressed from pLKO.1 (shSig15; Sigma-Aldrich; TRCN0000255303) was used to knock down expression with a non-silencing sequence as a control (shNS; Sigma-Aldrich; SHC002).

Chimeric Antigen Receptor (CAR) expressing Jurkat cells were generated by retrovirally transducing Jurkats (RRID:CVCL_0065) with a CAR containing a CD19-binding domain, the CD28 transmembrane and signaling domain and the CD3ζ signaling domain, as previously described (156). CAR-expressing Jurkats and $CD19^+$ REH cells were co-cultured at a 2:1 effector:target ratio, at which point 50 μg/mL of human IgG1 (Abcam) or His-tagged recombinant SIGLEC15 protein (ABclonal) was added to the co-culture and incubated for 4 hours prior to analysis.

Quantitative Gene and Protein Analysis

For gene expression analysis, human cell lines were harvested at a concentration of $8x10^5$ cells/mL, and RNA was isolated from these samples using the Quick-RNA Miniprep Kit (Zymo Research). RNA was reverse transcribed using the High-Capacity cDNA Reverse Transcription Kit (ThermoFisher) and run in technical triplicate for real-time, quantitative PCR (RT-qPCR) reactions utilizing the SYBR™ Green PCR Master Mix (ThermoFisher). Sig15 expression was normalized using reference genes GAPDH and 18srRNA. Publicly available data was queried from the Oncomine (https://www.oncomine.org; accessed online 5/2018), TARGET ALL Phase 2 (https://ocg.cancer.gov/programs/target; accessed online October 2020), and St. Jude PeCan (https://pecan.stjude.cloud/; accessed online 8/2020) databases. For survival analyses relative to mRNA expression, the median *SIGLEC15* level was used as a cutoff to define high versus low expression.

For protein expression analysis, human cell lines were harvested at a concentration of $8x10^5$ cells/mL and lysed on ice for 45 minutes in RIPA lysis buffer (ThermoFisher) containing protease inhibitors (Roche). Lysates were then clarified at 14,000 g for 10 minutes and quantified using the BCA protein assay kit (ThermoFisher). Western immunoblots were probed for Sig15 using a polyclonal antibody from Invitrogen (1:2000) and monoclonal antibodies from Creative Biolabs (Clone A9E8;

1:1000) and NextCure (Clone 1F7; 2 ug/mL). Additional probes included DAP12 (Sigma Aldrich; 1:250), FcRγ (Cell Signaling Technology; 1:1000), and B-actin (Sigma Aldrich; Clone AC-15; 1:2000).

Immunofluorescence

Human B-ALL cells were seeded at a concentration $5x10^5$ cells/mL to a poly-L-lysine (Sigma Aldrich) coated 8-well removable chamber microscope slide (ibidi) and allowed to adhere for 24 hours at 37°C prior to treatment. At harvest, the wells were washed twice with cold phosphate buffered saline (PBS), fixed with 4.2% paraformaldehyde (PMA) at 4°C for 10 minutes, permeabilized with 0.2% Triton X-100 (Sigma Aldrich) for 10 minutes at room temperature, and blocked for 30 minutes at room temperature. Wells were stained for Sig15 (Invitrogen; 1:400) and Golgin-97 (ThermoFisher; Clone CDF4; 1:200) for 20 minutes at room temperature, washed in triplicate with PBS, and stained with fluorescent secondary antibodies against either antigen. Slides were mounted using Prolong Gold Antifade with DAPI (Invitrogen) and imaged on an Olympus FV1000 confocal microscope. All co-localization analysis was performed using the Coloc2 plugin in Fiji (157).

Primary Human Samples

All research involving samples from human subjects was approved by the Institutional Review Board of Emory University (Atlanta, GA) and performed in accordance with recognized ethical guidelines (e.g., U.S. Common Rule). Plasma samples from pediatric leukemia patients were obtained from the Leukemia/Lymphoma Biorepository of the Aflac Cancer & Blood Disorders Center at Children's Healthcare of Atlanta (Atlanta, GA; IRB#34535). Peripheral blood and plasma from healthy individuals were obtained from the Clinical and Translational Discovery Core at Emory University (Atlanta, GA; IRB#89506). All samples were acquired after written informed consent was provided. Residual, fresh bone marrow aspirate and peripheral blood samples from pediatric B-ALL patients were analyzed for Sig15 expression by flow cytometry under protocol (IRB#96145). Bone marrow aspirate from healthy donors was purchased from AllCells (Alameda, CA).

Flow Cytometry

Human cell lines were harvested at a concentration of $8x10^5$ cells/mL and stained with LIVE/DEAD™ Fixable Aqua Stain (ThermoFisher) and Sig15 (NextCure; Clone NP159; 1:100), washed with PBS in triplicate, and stained with an Alexa Fluor 488 goat anti-mouse secondary antibody. Intracellular stains were performed using the BD Cytofix/Cytoperm™ (BD Biosciences) kit. Fresh pediatric B-ALL samples from bone marrow aspirate (BMA) and peripheral blood (PBL) were collected, counted, washed, and then stained with a pre-selected antibody cocktail. Samples were then RBC-lysed with Ammonium Chloride Lyse Reagent (Medialab), washed, decanted, and fixed with 1% buffered formalin (Medialab) prior to flow cytometric analysis. FlowJo Software (BD Biosciences; RRID:SCR_008520) was used for all flow cytometry data analyses.

Secreted/Soluble Sig15 (sSig15) and Cytokine/Chemokine Detection

Aliquots from plasma samples and human B-ALL cell line supernatants were analyzed for Sig15 using electrochemiluminescence on a Meso QuickPlex reader (Meso Scale Diagnostics, Rockville, MD). Patient plasma was also analyzed for cytokines and chemokines using the Cytokine 35-plex Human Panel (ThermoFisher) for the Luminex 200 System, which has been previously reported (47). Secreted or soluble Sig15 (sSig15) was captured using the 5G12 monoclonal antibody (NextCure) and detected via the NP159 antibody (NextCure) for analysis. A subset of reliably detected cytokines was selected for correlation with sSig15 levels. Data were log2 transformed prior to analyses using Pearson's correlation test. Pearson r values are depicted in the heatmap that was generated using Morpheus (www.software.broadinstitute.org/Morpheus).

In vivo *Experiments*

C57BL/6 mice of either wildtype (WT; RRID:MGI:2159769) or *Rag1*$^{-/-}$ (B6.129S7-Rag1^{tm1Mom}/J; RRID:IMSR_JAX:002216) background were obtained from the Jackson Laboratory. Female mice used in this study were 4-8 weeks of age. Mice were housed in pathogen free conditions in the Division of Animal Resources Facility in the Health Sciences Research Building on Emory University campus (Atlanta, GA). All animal studies in this investigation were approved by the Emory University Institutional Animal Care and Use Committee (Atlanta, GA).

For survival experiments, unirradiated wildtype (WT) or *Rag1*$^{-/-}$ mice were injected with $2x10^5$ murine B-ALL cells via tail vein injection. Isoflurane-anesthetized mice were intraperitoneally injected with luciferin and imaged on the *In Vivo* Image System (IVIS) Spectrum (Perkin Elmer) to measure leukemia progression. Recipient mice were removed from the study upon either manifesting an ill appearance or when their luciferase signal exceeded 10^8 photons/second based on previous experience (46).

For short-term immunophenotyping experiments, wildtype mice were injected with $2x10^5$ leukemia cells and monitored for seven days, at which point all recipients were euthanized. Bone marrow supernatant was harvested and analyzed using the Mouse Cytokine 44-plex Array (Eve Technologies; Calgary, AB, Canada). Bone marrow cells were harvested and analyzed via flow cytometry using a multi-parameter panel on a Cytek Aurora (RRID:SCR_019826).

Statistical Analyses

Statistical analyses were performed using GraphPad Prism software (RRID:SCR_002798). Statistical significance between groups was determined using ANOVA with Tukey's multiple comparisons test, unless otherwise specified. Error bars in figures represent the standard deviation and may be obscured when narrow. Animal experiments included at least 3 mice per group and were repeated at least once. Data from all mice are included in the results.

Data Availability Statement

The results published here include data generated by the Therapeutically Applicable Research to Generate Effective Treatments (https://ocg.cancer.gov/ programs/target) initiative, phs000218. The data used for this analysis are available at https://portal.gdc.cancer.gov/projects.

3.4 Results

Sig15 is widely expressed across hematological malignancies.

Sig15 expression has been documented in subsets of dendritic cells, macrophages, and mature osteoclasts, and there exists some evidence that it is also expressed in some acute myeloid leukemias (AML) (158, 159). The extent of Sig15 expression in hematological malignancies, specifically of lymphoid origin, remains undefined. We queried the Oncomine cancer microarray database, finding

higher *SIGLEC15* expression in both B-ALL and AML patient samples compared to healthy donor peripheral blood mononuclear cells (PBMCs) (**Fig. 3.1A**). From the St. Jude PeCan database, among common pediatric cancers, we found higher *SIGLEC15* expression in B-ALL, AML, mixed lineage leukemia (MLL), and osteosarcoma (OS) relative to the median expression across all tumors (**Fig. 3.1B**). Among pediatric B-ALL subtypes, *SIGLEC15* expression was highest in patients with the ETV6-RUNX1 translocation, the most common fusion gene in childhood ALL. Notably, higher expression of *SIGLEC15* mRNA in the bone marrow was associated with longer event-free survival in a cohort of 98 children with B-ALL enriched for those with early relapse.

Across a panel of eight immortalized human B-ALL cell lines, we observed higher SIGLEC15 expression compared to healthy donor PBMCs (**Fig. 3.1C**) by Western blot. This was consistent across AML, and diffuse large B cell lymphoma (DLBCL) (**Fig. 3.1D**). We also performed flow cytometry for Sig15 on primary B-ALL cells gated from fresh bone marrow aspirate (BMA) and peripheral blood (PBL) samples from pediatric B-ALL patients. Three of seven pediatric B-ALL BMA and one of eight PBL samples stained positive/dim-positive for Sig15 on their surface, while all normal bone marrow hematogones and circulating B cells from non-leukemia donors (n=8) were Sig15-negative (**Fig. 3.1E**).

The expression and localization of Sig15 are regulated by NF-κB.

Immunosuppressive cytokines, such as M-CSF and IL-10, have previously been demonstrated to induce Sig15 expression in macrophages (116, 118). Although we tested these and several other candidate cytokines for their effects on Sig15 expression after 24 hours of treatment in an immortalized B-ALL cell line, REH, only chemical stimulation with PMA strongly induced Sig15 expression (**Fig. 3.2A**). This PMA-mediated induction was dependent upon PKC activation, as *SIGLEC15* upregulation was abrogated when cells were stimulated for 24 hours with a combination of PMA and a pan-PKC inhibitor, Gö6983 (**Fig. 3.2B**). As PKC activation is upstream of both calcineurin/NFAT and NF-κB activation, we used an IKK-2 inhibitor (BOT64) and a calcineurin inhibitor (Cyclosporin A; CSA) in combination with 24-hour PMA stimulation to demonstrate that PMA-induced upregulation of Sig15 expression is dependent upon NF-κB activation (**Fig. 3.2C-D**). Analyses of gene expression from the ALL project of the TARGET

Program demonstrated strong positive correlations of *SIG15* expression with markers of PKC, calcineurin, and NF-κB activity in pediatric B-ALL samples (**Fig. 3.2E**). As CD40L is a major immunoregulatory molecule upstream of NF-κB activation in mature B cells, we tested its role in stimulating Sig15 expression in B-ALL cells. We found that stimulation for 24 hours with CD40L increased levels of SIG15 (**Fig. 3.2F**), suggesting that this inducer of the B cell NF-κB signaling axis are involved in regulation of SIG15 in B-ALL. Due to its critical role in lymphocyte development and survival, constitutive or overactivation of the NF-κB pathway is common in subsets of B cell malignancies (160, 161), which may contribute to the pathological overexpression of Sig15.

Though we have demonstrated the high pathological expression of Sig15 in B-ALL, none of the B-ALL cell lines expressed the primary Sig15 binding partner DAP12 (**Fig. 3.1C**) or alternative binding partner FcRγ (data not shown), which are required for downstream activation of Syk kinase and PI3K in myeloid cells (123). Binding of Siglec family members to these adapter proteins has been demonstrated to anchor these molecules at the cell membrane when they would otherwise turnover in the endosomal complex (162). Indeed, flow cytometry demonstrated that Sig15 appeared to be primarily localized intracellularly in human B-ALL cell lines (**Fig. 3.3A**). Further, immunofluorescence revealed that intracellular Sig15 strongly co-localized with the Golgi apparatus and trans-Golgi network (TGN) marker, Golgin-97 (**Fig. 3.3B**), suggesting retention of Sig15 in the Golgi apparatus in B-ALL cells with limited trafficking to the membrane along the TGN. In accordance with other transmembrane proteins that possess regulated trafficking to the membrane, the intracellular domain of Sig15 contains a rapid internalization motif which can promote recycling of the protein back through the endosomal compartments (113), resulting in eventual localization in the lysosome (**Fig. S3.1A**) unless otherwise stabilized at the membrane. Interestingly, PMA-induced NF-κB activation for 24 hours reduced localization of Sig15 in the Golgi compartment and increased Sig15 at the surface of B-ALL cells (**Fig. 3.3C-D**). This increase in surface localization of Sig15 was mediated through NF-κB activation, with peak surface expression at approximately 8 hours post-stimulation (**Fig. S3.1B**).

Sig15 circulates in the plasma of B-ALL patients.

As the TGN along which Sig15 traffics is known to regulate vesicular secretion of proteins (163), and as other Siglec family member proteins have been demonstrated to exist in soluble form (164, 165), we hypothesized that B-ALL cells have the capacity to release a secreted or soluble form of Sig15 (sSig15). We detected sSig15 in the supernatant of REH cells in culture using MSD, which was increased with PMA stimulation (**Fig. 3.4A**). Combination treatment with the calcineurin inhibitor, cyclosporine A, demonstrated that calcineurin activation, downstream of PKC, regulates sSig15 release into the supernatant but not its mRNA expression level. We then assayed cryopreserved plasma from healthy subjects and pediatric leukemia patients collected at the time of diagnosis for sSig15 levels, finding significantly higher sSig15 in the plasma of pediatric B-ALL patients relative to healthy donors (**Fig. 3.4B**).

Though some members of the Siglec family proteins are known to circulate in plasma (164, 165), to our knowledge, this is the first demonstration of a circulating, secreted/soluble form of Sig15. Further analyses of circulating cytokine levels in these leukemia patient plasma samples via Luminex multiplex assay found a correlation between sSig15 and the cytokines MCP-1/CCL2 and IL-6 (**Fig. 3.4C**), which have been demonstrated to support the formation of the pro-leukemic bone marrow microenvironment (166, 167). Notably, sSig15 strongly negatively correlated with IL-12 levels, a pro-inflammatory cytokine with potent anti-leukemia activity (46, 47). To address the functional capacity of sSig15 to suppress immune activity, we treated CD19-CAR expressing Jurkat cells with recombinant human Sig15 in co-culture with a $CD19^+$ B-ALL cell line. Recombinant Sig15 significantly suppressed the early activation of the CAR^+ Jurkat cells (**Fig. 3.4D-E**), suggesting that sSig15 may directly suppress T cell activation and function.

Sig15 is required for immune evasion by B-ALL cells.

With data supporting the pathological expression and immunosuppressive effects of Sig15 in B-ALL, we next sought to characterize the effects of Sig15 ablation in a murine model of B-ALL. We performed shRNA knockdown and CRISPR-mediated deletion of Sig15 in a well-characterized *BCR-ABL1*$^+$ *Arf*$^{-/-}$ murine B-ALL cell line (**Fig. 3.5A-B**)(153). In immune-competent wild-type (WT) and

immune-deficient *Rag1*$^{-/-}$ recipients, the control leukemias progressed rapidly, necessitating euthanasia of all recipients within 2-3 weeks of leukemia transfer (**Fig. 3.5C-D**). In stark contrast, after 7-10 days, the leukemia burden in WT recipients of Sig15-deficient leukemia dramatically declined to below the limit of detection, and the WT recipients of Sig15-deficient leukemia survived significantly longer than recipients of the control leukemias (**Fig. 3.5E-F**). Sig15 ablation did not alter basal apoptosis levels nor proliferation rates of these cells (**Fig. S3.2A-B)**. The initial increase in leukemia burden in immunocompetent recipients of Sig15-deficient leukemia, followed by regression around day 7, is consistent with well-described kinetics of T cell responses *in vivo*(168).

To better understand the effects of Sig15 on immune response to B-ALL, we engrafted immunocompetent recipients with control or Sig15 knockout (Sig15 KO) leukemia and harvested bone marrow at Day 7 post-engraftment for immunophenotyping by flow cytometry. The numbers of bone marrow CD3^{+} T cells, NK cells, and neutrophils were all significantly higher in Sig15 KO leukemia recipients compared to control leukemia (**Fig. 3.6A-D**), characterizing a more robust anti-leukemia immune response. Among T cell subsets (**Fig. 3.6E**), CD8^{+} cytotoxic T cells (CTLs) were significantly expanded in Sig15 KO recipients, making the proportion of CD8:CD4 T cells comparable to levels in mice without leukemia (**Fig. 3.6F-H**). In addition, markers of T cell activation and degranulation were significantly increased in CD8^{+} T cells in Sig15 KO recipients (**Fig. 3.6I; S3.3A-B**), while activation markers were more variably elevated in NK cells, classical dendritic cells, and neutrophils (**Fig. S3.3E-J**). Those CD8^{+} T cell populations expected to be critical in the early stages of immunologic control, such as short-lived effector cell (SLEC) and memory precursor effector CD8^{+} cells (MPEC) populations, were significantly higher (**Fig. 3.6J-K**) along with precursors to central and effector memory T cells (**Fig. 3.6L-M**), suggesting both heightened early response and long-term immunologic benefit. Lastly, we observed a significant decrease in IL-6, LIF, and IL-5 in the bone marrow of Sig15 KO recipients (**Fig. 3.6N-P**). LIF and IL-5 have been demonstrated to mediate antigen-specific immune tolerance through induction and modulation of regulatory T cells (169, 170), while IL-6 is known to suppress CD8^{+} T cell-mediated clearance of B-ALL in response to chemotherapy (171). Thus, Sig15 expressed by B-ALL cells

may contribute to the formation of a more immunologically favorable leukemia bone marrow niche via these factors.

3.5 Discussion

The results of our investigation support Sig15 as a critical immunomodulator in suppression of T cell-mediated response to leukemia and disease clearance in B-ALL. Sig15 is widely expressed across hematological malignancies at consistently higher levels compared to healthy controls in primary samples and in B-ALL, T-ALL, and DLBCL cell lines. This overexpression of Sig15 compared to paired healthy tissue has been demonstrated in several solid tumors, including non-small cell lung cancer (NSCLC) (118) and clear cell renal cell carcinoma (143), but has yet to be described in ALL. Our findings in primary pediatric populations also corroborate the published overexpression of Sig15 in other diseases such as osteosarcoma (141) and AML (158). The scope of malignancies which overexpress this molecule provide support for a selective advantage to pathological upregulation of Sig15 by cancer cells and tumor-associated immune cells.

To date, most publications on Sig15 have characterized its role in the context of mature osteoclasts, which have shared precursors with myeloid cells (172), as well as tumor-infiltrating myeloid cells and myeloid blood cancers. These myeloid-derived cells often express abundant amounts of the adaptor proteins DAP12 and FcRy (173), which can couple with sialic acid-bound Sig15 to recruit Syk kinase and PI3K to their ITAM domains (116, 123), allowing for intracellular signal transduction. As we did not detect these adaptor molecules in lymphoid blood cancers, this intracellular signaling axis is likely not active, which could suggest that ALL-expressed Sig15 does not function primarily as a receptor in ALL. Rather, alongside data from others demonstrating inhibition of T cell activity with recombinant Sig15 (118), our observations of dynamic Sig15 surface localization and circulating sSig15 could suggest the possibility of a primary function as a ligand, locally and systemically. Indeed, recombinant Sig15 attenuated activation of CD19-CAR expressing Jurkat cells, when cultured with $CD19^{+}$ B-ALL cells. Though recent studies have demonstrated binding of recombinant Sig15 protein to partners such as CD44 (174), the canonical receptor for cancer-expressed Sig15, particularly as expressed on T cell populations,

remains to be defined. An important consideration of all of the data regarding extracellular Sig15 is that the studied recombinant forms are tagged with His or Fc sequences that may alter function. Characterization of the sequence and structure of sSig15 will be critical to fully understand its physiologic function.

Lack of expression of adaptor molecules DAP12 and FcRy in lymphoblastic leukemias could also contribute to the select trafficking and localization of Sig15 at the membrane in ALL. We observed that Sig15 localized primarily intracellularly in B-ALL cell lines unless stimulated with an inducer of NF-κB, which increased both total Sig15 and cell surface expression. As a cell surface molecule, Sig15 has been demonstrated to be localized on the surface of mature osteoclasts (123, 175) as well as subsets of macrophages (118). Some subsets of DC-SIGN-expressing macrophages and dendritic cells, however, have been shown to have intracellular Sig15 (113), which suggests dynamic regulation of the expression and localization of Sig15 in these cells and in B-ALL, the latter being mediated through NF-κB activation.

NF-κB has been demonstrated in some contexts to regulate membrane protein trafficking through activation of downstream mediator AKT (176) or through direct regulation of expression of intracellular trafficking proteins Rab10 and Acp5 (177). Though the mechanism by which NF-κB activation regulates Sig15 localization in ALL is still being explored, our analysis revealed Sig15 on the surface of many primary B-ALL leukemia samples from the bone marrow which was not seen in comparable healthy donor B cell progenitors. As the NF-κB pathway is often active in B-ALL cells and enhanced in the leukemia bone marrow niche (160, 161, 178), this could drive both the pathological expression and surface-localization of Sig15 in B-ALL. Our findings also suggest a role for the CD40L-CD40 signaling axis, upstream of NF-κB, in regulating Sig15 expression. CD40L is upregulated during T cell activation, and its binding with CD40 has been demonstrated to result in upregulation of PD-L1 in tumor-infiltrating macrophages (179). It is thus possible that CD40L in the B-ALL bone marrow niche may locally enhance Sig15 expression through NF-κB activation, which could further suggest a role for Sig15 in regulating inflammation and T cell activation alongside other immune checkpoint molecules.

Immunofluorescent imaging revealed that intracellular Sig15 strongly colocalized with Golgin-97 signal in human B-ALL cells. The protein sequence of Sig15 also contains a signal peptide motif often present in secreted proteins (180), which together suggests these cells have the capacity to release Sig15 through the secretory pathway. Other Siglec family member proteins are also known to be released as soluble proteins through expression of alternative isoforms lacking transmembrane domains or undergoing ectodomain shedding at the membrane (165, 181). Though the method by which sSig15 is released from B-ALL cells is still in ingoing investigation, sSig15 was in fact detectable both in the supernatant of human B-ALL cell lines and in the plasma of pediatric B-ALL patients. This is to our knowledge the first demonstration of a secreted/soluble form of Sig15 in humans. In contrast to the regulatory axis of Sig15 expression, the release of sSig15 appears to be regulated by calcineurin activation. Calcineurin has been demonstrated through activation of NFAT and other downstream targets to regulate vesicular trafficking and secretion of proteins (182) as well as the expression and activity of extracellular proteases such as cathepsins responsible for protein shedding (183). sSig15 in pediatric B-ALL patients was found to negatively correlate with anti-leukemia cytokines such as IL-12 and positively correlate with immunosuppressive factors such as MCP-1/CCL2 and IL-6, suggesting sSig15 is one component of a complex immunosuppressive local and systemic microenvironment in B-ALL. Our demonstrations of the capacity of recombinant Sig15 to suppress early activation in a CAR-T cell model further suggest its functionality in directly regulating immunosuppression. Nonetheless, whether cell surface or extracellular Sig15 is most functional in B-ALL remains to be demonstrated.

Although higher Sig15 mRNA levels are associated with prolonged event-free survival in the cohort that we analyzed, these data need to be interpreted cautiously, as the cohort is enriched in those with early relapse and is clinically and molecularly diverse. Moreover, the protein levels of Sig15, cell surface or circulating, are not known. Most importantly, Sig15 was found to be critical for the capacity of B-ALL cells to evade immune clearance in a murine model of B-ALL. Ablation of Sig15 expression in these leukemia cells resulted in increased expansion and activation of multiple immune populations in the bone marrow, including NK cells, classical dendritic cells, neutrophils, and $CD8^+$ T cells. For the former,

the $CD8^+/CD4^+$ T cell ratio was returned to basal levels observed in mice without leukemia, and early effector populations were highly expanded at the Day 7 timepoint in the bone marrow of Sig15 KO leukemia recipients. These SLEC and MPEC populations are predicted to be the primary effectors at the peak of acute inflammatory response (184), suggesting that their expansion in Sig15 KO leukemia recipients facilitates greater leukemia control. There were also notable reductions in the leukemia-induced immunosuppressive cytokine milieu of Sig15 KO leukemia recipients, marked by decreases in IL-6, LIF, and IL-5 that all contribute to a more immune-privileged bone marrow niche. These results, combined with our data in primary human samples, suggest Siglec-15 is a novel, potent immunosuppressive molecule active in leukemia that may be targeted therapeutically to activate cytotoxic T cells against leukemia.

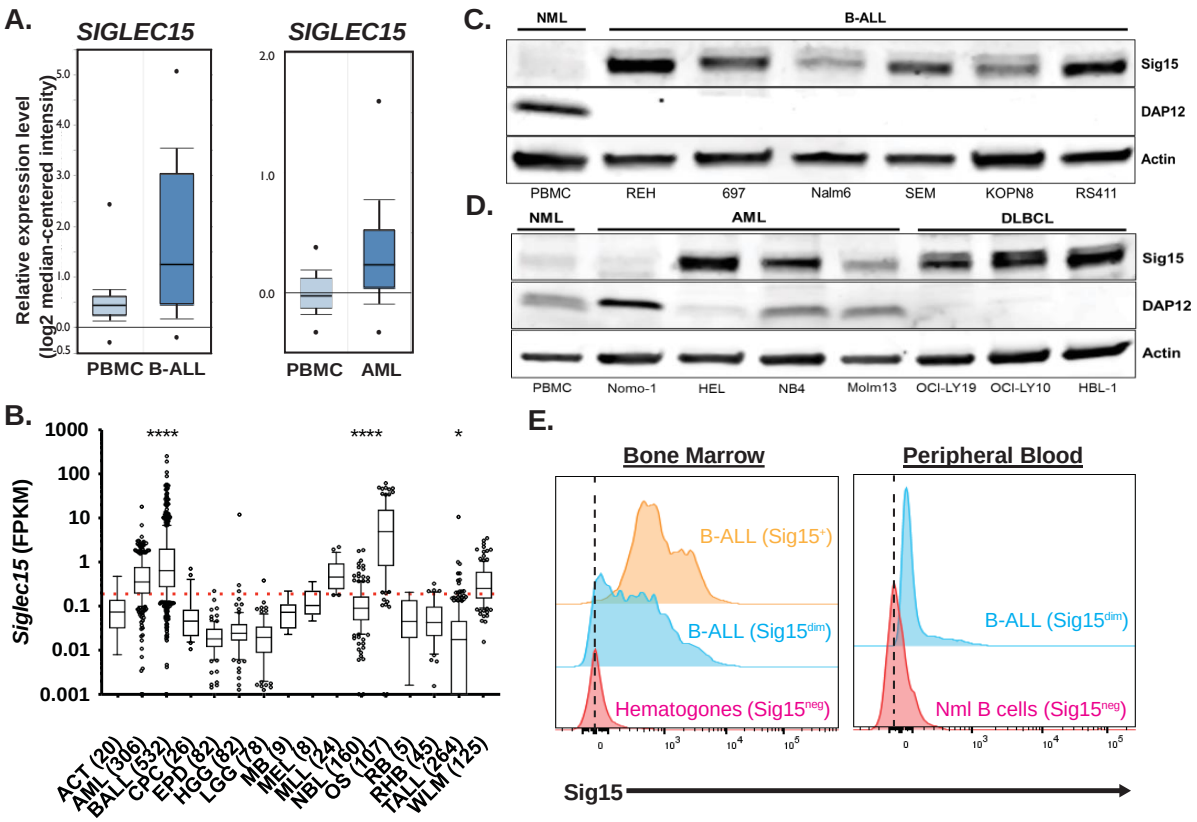

Figure 3.1. Sig15 is highly expressed in B-ALL and additional hematological malignancies. **A.** Relative *SIG15* expression. B cell acute leukemia (B-ALL; N=147; $P=3.6x10^{-19}$) and acute myelogenous leukemia (AML; N=542; $P=2.0x10^{-9}$) samples showed higher *SIG15* than normal peripheral blood mononuclear cell samples (PBMC; N=74). Data adapted from Haferlach *et al* through Oncomine.org (185) **B.** Relative *SIG15* expression across a panel of common childhood cancers from the St. Jude PeCan database. Dotted red line indicates median expression for all tumors in the graph (*P<0.05, ****P<0.0001, ANOVA). **C-D.** Western blot analysis shows higher SIG15 expression across a panel of (**C**) B-ALL, (**D**) AML, and diffuse large B cell lymphoma (DLBCL) human cell lines compared to normal healthy peripheral blood mononuclear cells (NML). No B-ALL or DLBCL cell lines show detectable levels of the Sig15 binding partner DAP12. SIG15 was probed using the Invitrogen polyclonal antibody. **E.** Representative flow cytometry of primary childhood B-ALL. 3 of 7 BMA samples had B-ALL cells which stained positive/dim-positive for Sig15 and 1 of 8 PBL samples had B-ALL cells which stained positive. 0 of 2 hematogones from non-leukemia donor BMA samples and 0 of 6 B cells from PBL samples from non-

leukemia donors were positive for Sig15. Dotted lines represent the mean fluorescence intensity from normal hematogones and B cells. SIG15 was probed using the NP159 monoclonal antibody (NextCure) conjugated to Alexa Fluor 647.

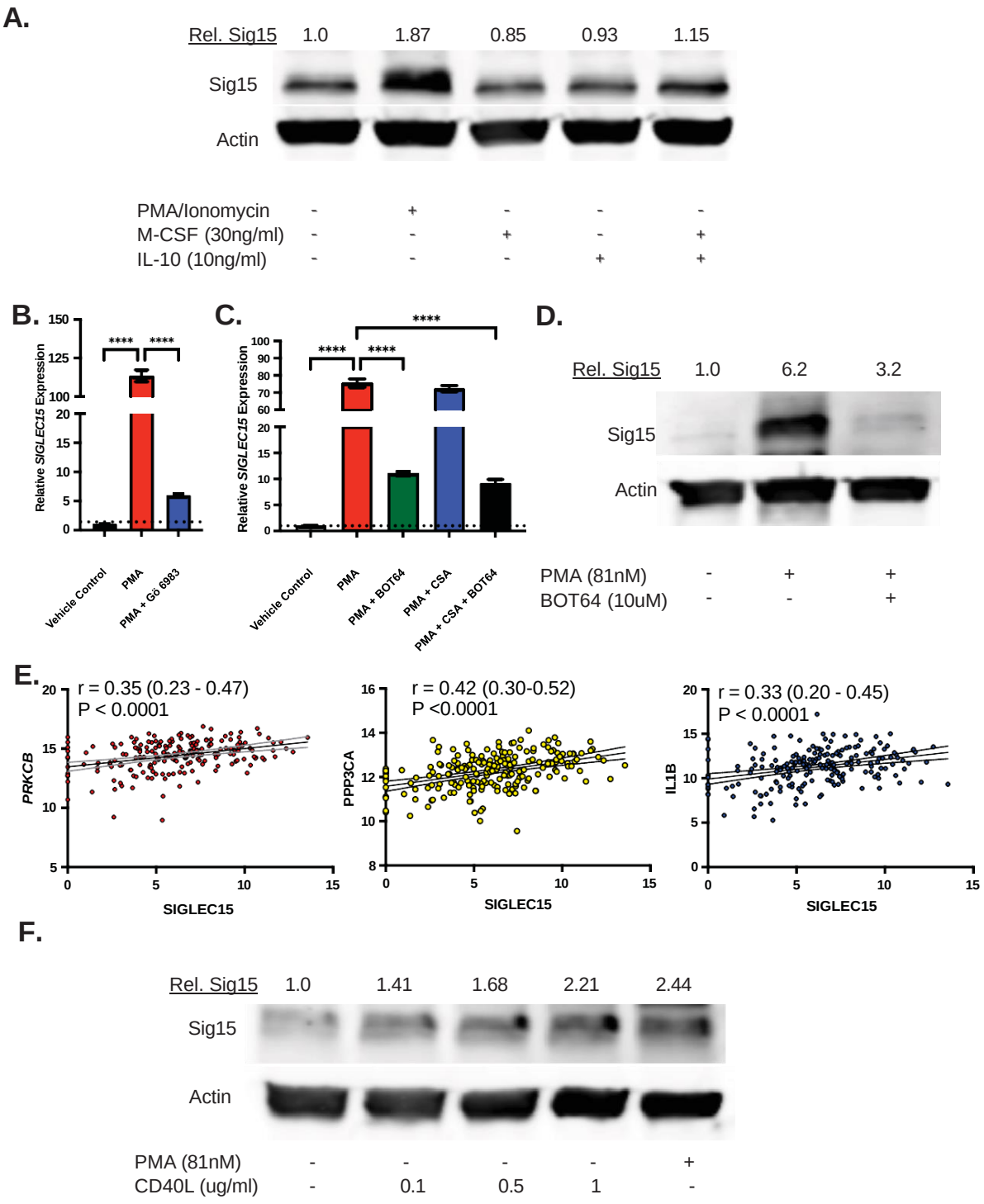

Figure 3.2. Sig15 expression is regulated by NF-κB activation in B-ALL. **A.** Western blot shows upregulated SIG15 expression in REH cells stimulated for 24 hours with a PMA/ionomycin stimulation (81 nM PMA and 1.3 uM ionomycin) but not with 30 ng/mL of recombinant human M-CSF and/or IL-10. Densitometric analysis of SIG15 is quantified above. SIG15 was probed using the Invitrogen polyclonal

antibody. **B.** RT-qPCR from REH cells treated with PMA (81 nM) with or without pan-PKC inhibitor Gö 6983 (5 μM) for 24 hours, showing that PKC inhibition abrogates *SIG15* induction by PMA. (****P<0.0001). **C.** RT-qPCR from REH cells stimulated with PMA (81 nM) and/or treated with calcineurin inhibitor CSA (1 μM) or IKK-2 inhibitor BOT64 (10 μM) for 24 hours, demonstrating that NF-κB inhibition but not calcineurin inhibition abrogates PMA-induced *SIG15* transcription (****P<0.0001). **D.** Western blot analysis shows SIG15 expression in REH cells following 24 hours of stimulation with 81 nM PMA alone or in combination with 10 uM of the IKK-2 inhibitor BOT64. NF-κB inhibition attenuates PMA-induced upregulation of SIG15. SIG15 was probed using the 1F7 monoclonal antibody (NextCure). **E.** *SIG15* expression from the B-ALL TARGET database correlated with protein kinase C β (*PRKCB*; r=0.35; p<0.0001, Pearson's correlation), calcineurin catalytic subunit alpha (*PPP3CA*; r=0.42; p<0.0001), and IL-1β (*IL1B*; r=0.33; p<0.0001, Pearson's correlation). **F.** Western blot shows increased SIG15 protein in REH cells stimulated for 24 hours with increasing doses of recombinant human CD40L. Densitometric analysis of SIG15 is quantified above. SIG15 was probed using the 1F7 monoclonal antibody (NextCure).

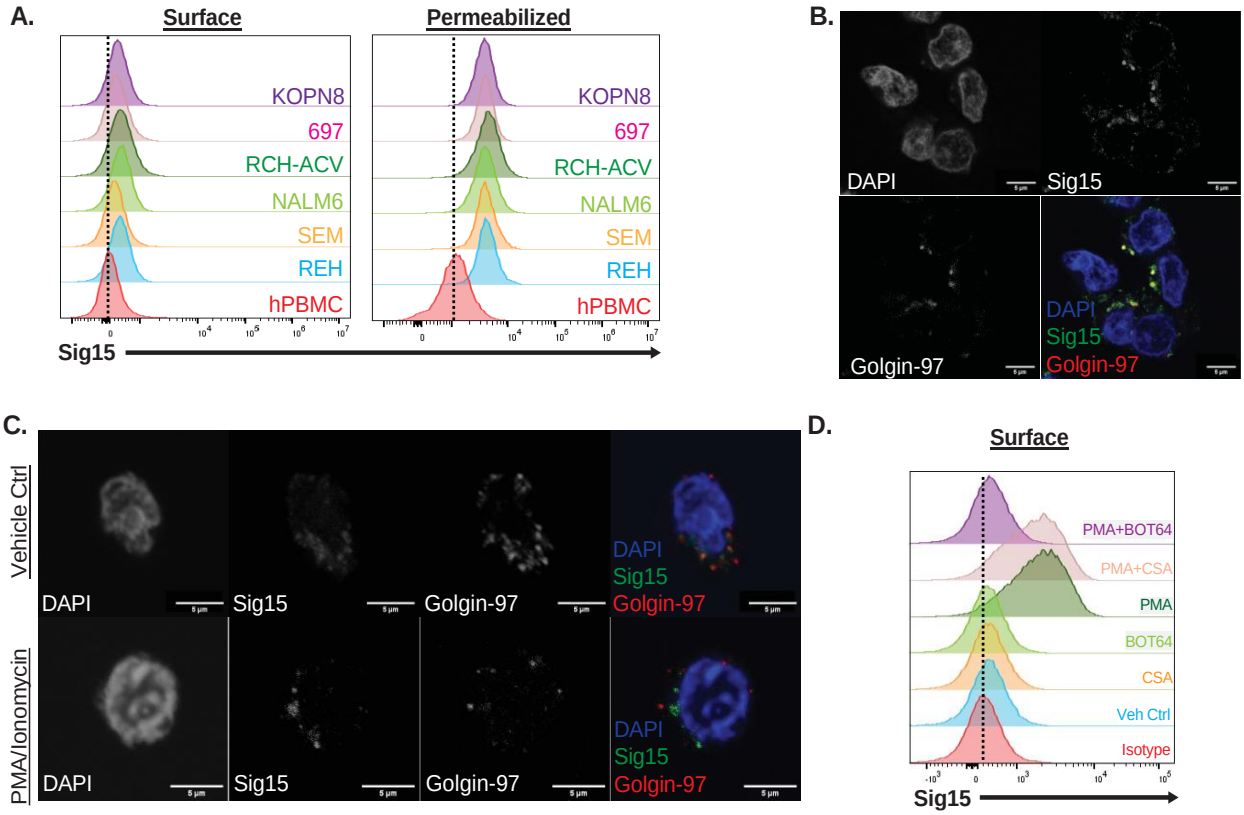

Figure 3.3. B-ALL-expressed Sig15 has dynamic sub-cellular localization. **A.** Flow cytometry of human B-ALL cell lines probed for SIG15 in both permeabilized and unpermeabilized (Surface) cells. Dotted line marks mean fluorescence intensity (MFI) of healthy PBMC (hPBMC) signal (data representative of 3 independent experiments). Leukemia and PBMCs had modest surface expression of SIG15, while leukemia cells expressed higher intracellular SIG15 compared to PBMCs. SIG15 was probed using the NP159 monoclonal antibody (NextCure). **B-C.** Immunofluorescence of REH cells staining for DAPI, Sig15, and Golgin-97. (**B)** Imaging depicts limited surface localization of Sig15 and strong co-localization with the Golgi apparatus and TGN in unstimulated REH cells. (**C)** Representative images depict REH cells treated for 24 hours with DMSO (vehicle control) or 81 nM PMA and 1.3 uM ionomycin. Stimulated REH cells show decreased colocalization of Sig15 signal with Golgin-97. SIG15 was probed using the Invitrogen polyclonal antibody. **D.** Flow cytometry of unpermeabilized REH cells treated with PMA with or without BOT64 for 6 hours, demonstrating that NF-kB activation stimulates Sig15 localization at the cell surface (data representative of 3 independent experiments; dotted line

represents MFI of isotype staining). SIG15 was probed using the NP159 monoclonal antibody (NextCure) conjugated to Alexa Fluor 647.

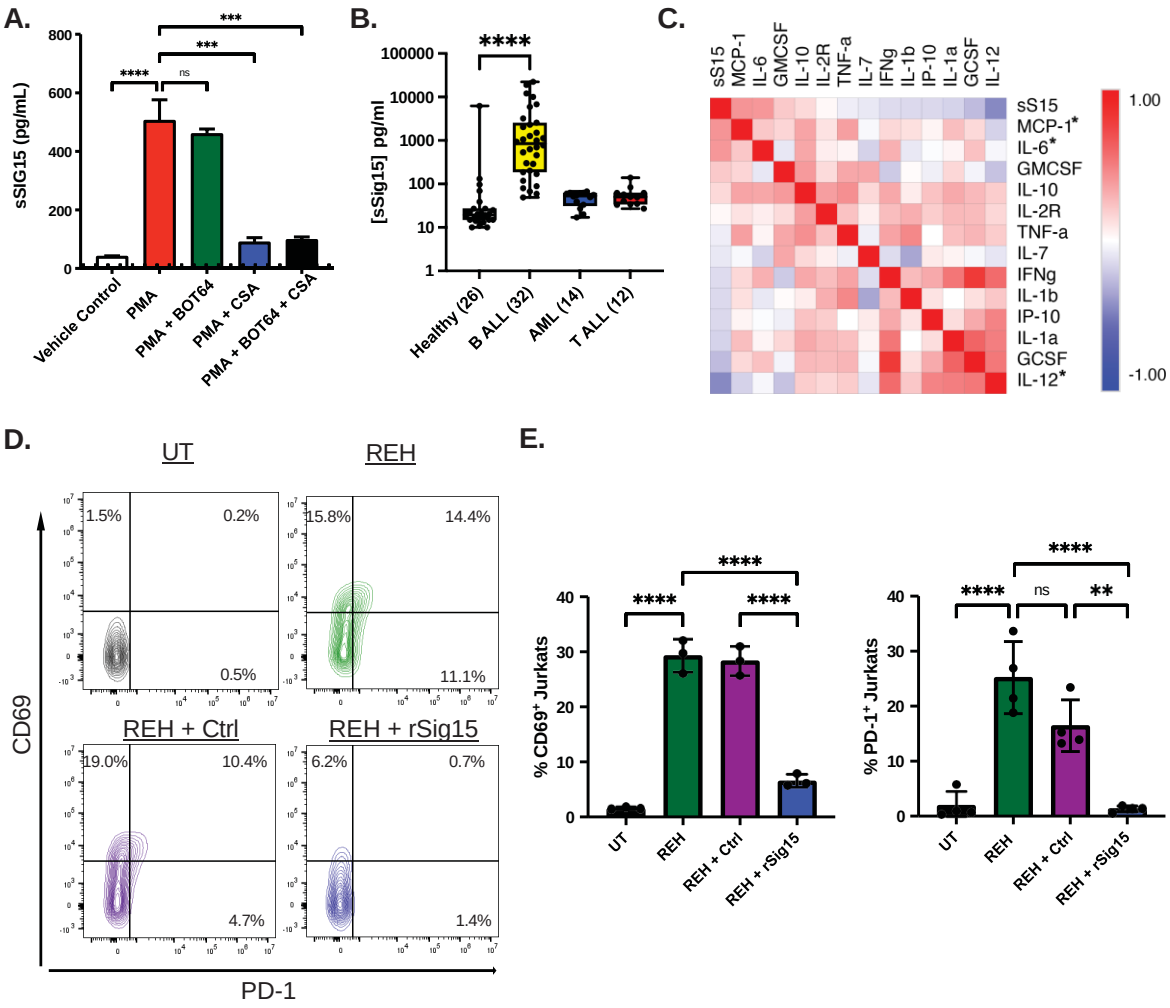

Figure 3.4. B-ALL cells release secreted/soluble Sig15 (sSig15) that circulates in plasma and inhibits activation of CAR-expressing Jurkat cells. **A.** sSIG15 detected via electrochemiluminescence (MSD) from the supernatant of REH cells treated for 24 hours with combinations of PMA (81 nM), BOT64 (10 uM), and CSA (1 uM). Dotted line represents the assay limit of detection (10 pg/mL). PMA induces a calcineurin-dependent increase in the release of sSig15. **B.** sSIG15 detected via MSD from the plasma of pediatric patients with B-ALL, AML or T-ALL and healthy controls (sample size in parentheses). Pediatric B-ALL patients showed higher plasma concentration of sSIG15 than healthy donors (****P<0.0001). **C.** Cytokines were measured in the plasma from children with leukemia using Luminex and compared to sSig15. Pearson's correlation of a subset is depicted graphically using the nearest neighbor algorithm (*P<0.05). **D-E.** Jurkat cells expressing CD19-CAR constructs cultured alone (UT = untreated) or co-cultured with $CD19^{+}$ REH B-ALL cells (REH) at an E:T of 2:1 with or without 50 ug/mL

protein control (Ctrl = human IgG) or recombinant Sig15 (rSig15) for 4 hours and stained for early activation markers CD69 and PD-1. (**D)** Representative contour plots of flow cytometry data. (**E)** Quantification of 4 independent experiments. Recombinant Sig15 inhibits early Jurkat activation when in co-culture with B-ALL cells.

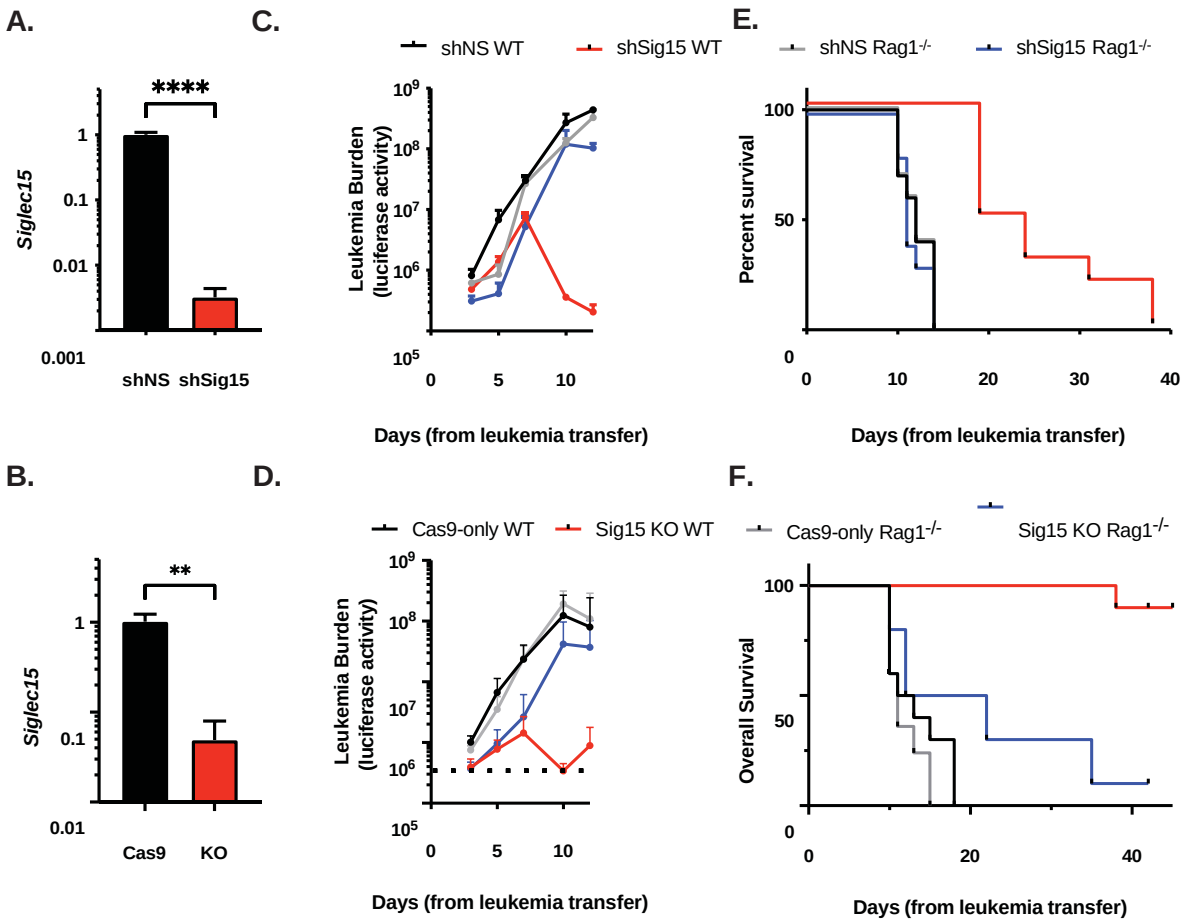

Figure 3.5. Sig15 is required for adaptive immune escape in murine B-ALL. **A-B.** RT-qPCR shows genetic knockdown of *Siglec15* expression in a murine model of B-ALL by (**A)** shRNA (shSig15) or knocked out using (**B)** CRISPR/Cas9 (Sig15 KO). Data are normalized to the expression levels of a non-silencing vector control (shNS) or Cas9 expressing cells without gRNA (Cas9). **C-D.** Un-irradiated wildtype (WT) or *Rag1*$^{-/-}$ C57BL6 mice were injected via tail-vein with $5x10^5$ control or Sig15 deficient leukemia cells. Luciferase signal over time represents disease burden as measured via IVIS imaging over 14 days. **E-F.** Kaplan Meier curve shows prolonged survival of WT recipients of Sig15-deficient leukemia. (**E)** P<0.0001; shNS WT v. shSig15 WT, Mantel-Cox log-rank test; n=10 per group from 2 independent experiments. (**F)** P<0.0001, Cas9-only WT v. Sig15 KO WT; n=10 per group from 2 independent experiments.

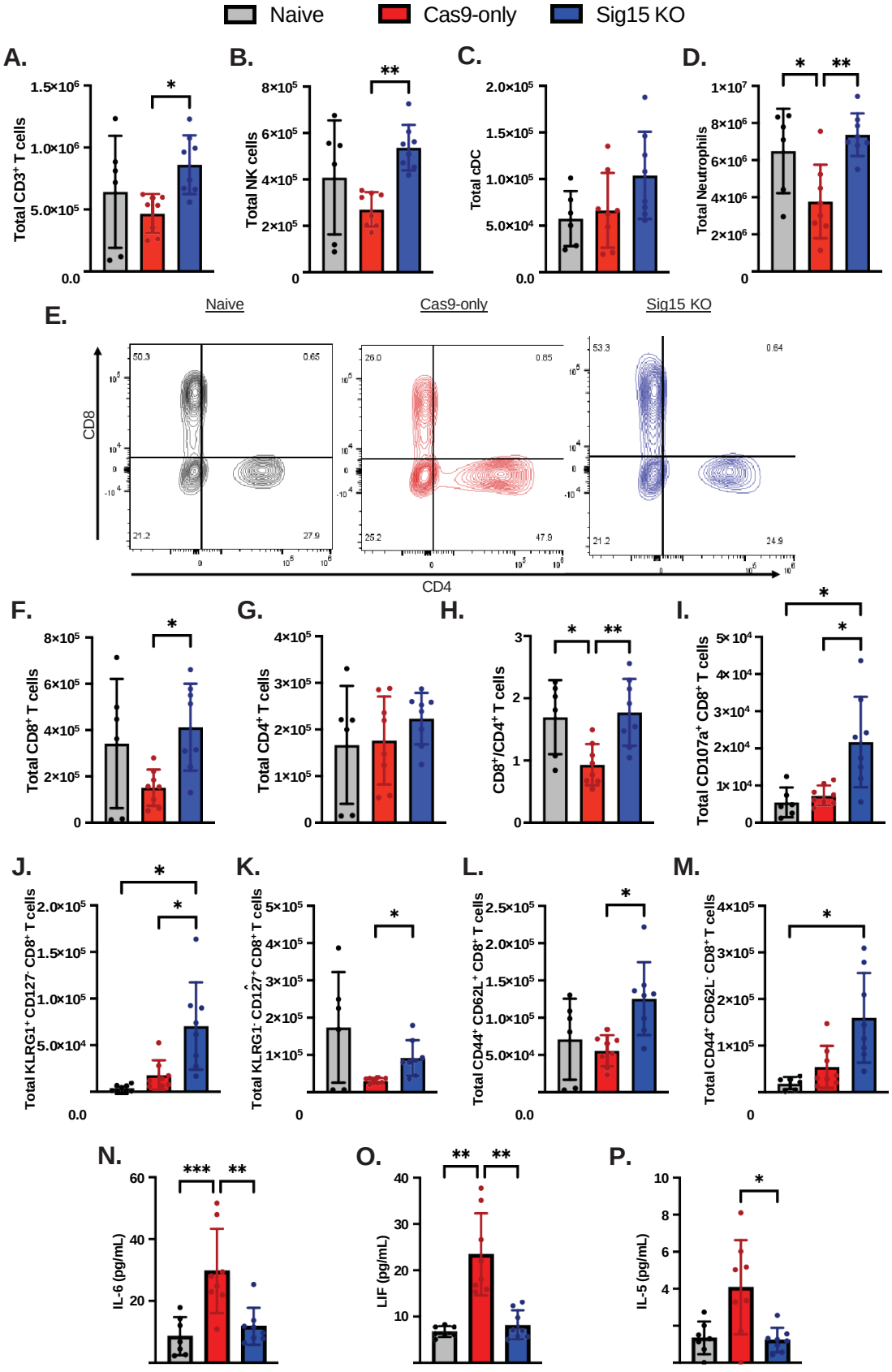
Naive
Cas9-only
Sig15 KO
A.
Total CD3+ T cells
B.
Total NK cells
C.
Total cDC
D.
Total Neutrophils
E.
Naive
Cas9-only
Sig15 KO
CD8
CD4
50.3
0.65
21.2
27.9
26.0
0.85
25.2
47.9
53.3
0.64
21.2
24.9
F.
Total CD8+ T cells
G.
Total CD4+ T cells
H.
CD8+/CD4+ T cells
I.
Total CD107a+ CD8+ T cells
J.
Total KLRG1+ CD127- CD8+ T cells
K.
Total KLRG1- CD127+ CD8+ T cells
L.
Total CD44+ CD62L+ CD8+ T cells
M.
Total CD44+ CD62L- CD8+ T cells
N.
IL-6 (pg/mL)
O.
LIF (pg/mL)
P.
IL-5 (pg/mL)

Figure 3.6. Sig15 promotes an immunosuppressive tumor microenvironment in B-ALL. **A-M**. Un-irradiated WT C57BL6 mice were injected via tail vein with $5x10^5$ Cas9-only (n=8 from 2 independent experiments) or Sig15 KO (n=8) leukemia. Bone marrow was harvested 7 days later for highly dimensional flow cytometry of non-leukemia bone marrow populations. Healthy, leukemia-naive mice (Naive) were included as controls (n=6). (**A**) $CD3^+$ T cells, (**B**) NK cells, (**C**) classical dendritic cells (cDC), and (**D**) neutrophils were variably present at higher totals in the bone marrow of Sig15 KO recipient mice compared to control leukemia. (**E)** Representative contour plots of T cell populations. Proportions of (**F**) $CD8^+$ but not (**G**) $CD4^+$ T cells were higher in Sig15 KO recipients than control leukemia, increasing the (**H**) $CD8^+/CD4^+$ T cell ratio to levels comparable to Naive mice. (**I**) Degranulated $CD8^+$ T cells were higher in Sig15 KO recipient mice, as were (**J**) SLEC and (**K**) MPEC $CD8^+$ T cell populations. Early memory-like populations consistent with (**L**) central and (**M**) effector memory $CD8^+$ T cell populations were also higher in Sig15 KO recipients. **N-P.** From the same experiments, bone marrow supernatant from control and Sig15 KO leukemia recipient mice was analyzed via 44-plex cytokine/chemokine assay. Levels of (**N**) IL-6, (**O**) LIF, and (**P**) IL-5 were all significantly lower in the bone marrow of Sig15 KO recipients as compared to control leukemia (*P<0.05, **P<0.01, ***P<0.001, ****P<0.0001). Sig15 expression on B-ALL cells suppresses $CD8^+$ T cell expansion and activation and contributes overall to formation of a more pro-leukemia bone marrow microenvironment.

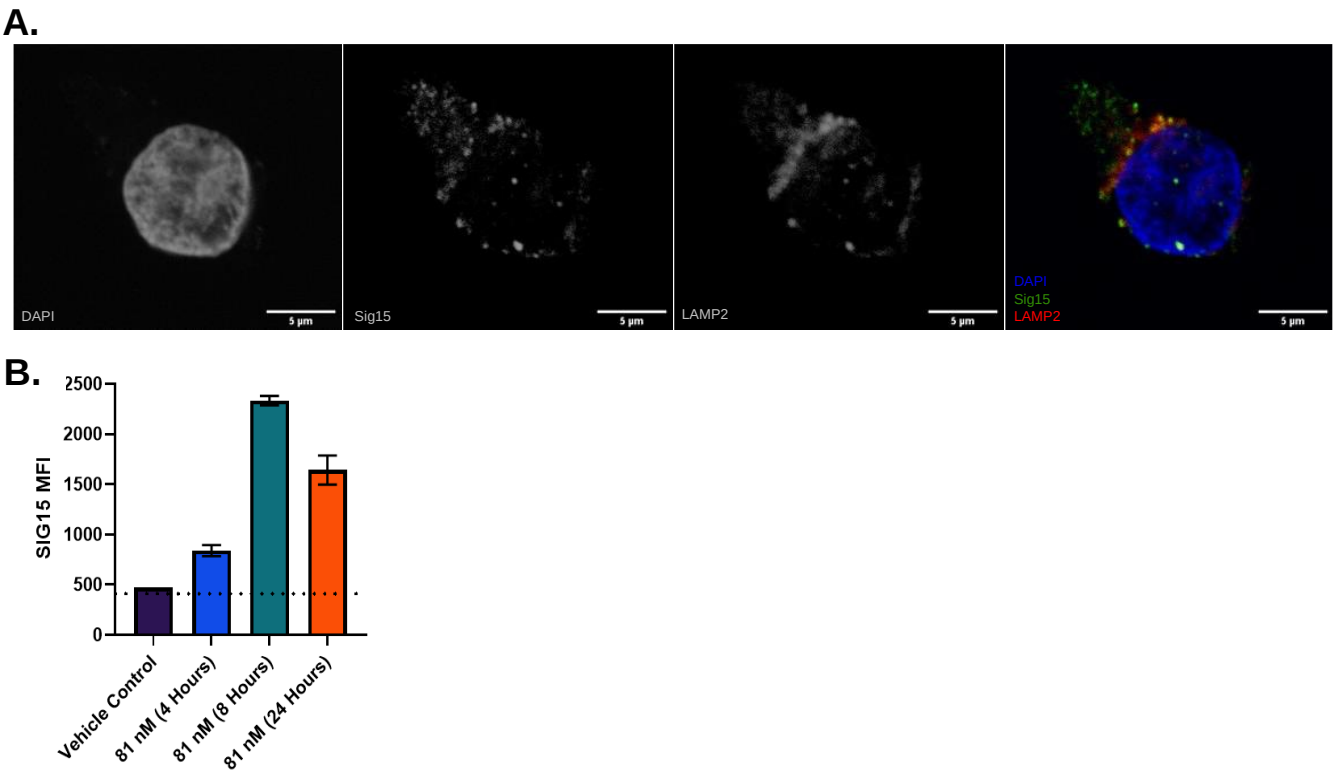

Supplementary Figure 3.1. Sig15 localizes to the Golgi apparatus and TGN in B-ALL.

(A) Immunofluorescence of REH cells staining for DAPI, Sig15, and LAMP2, a marker of the lysosomal compartment. Imaging depicts modest co-localization of Sig15 with LAMP2 in unstimulated REH cells. SIG15 was probed using the 1F7 monoclonal antibody (NextCure). **(B)** Flow cytometry of unpermeabilized REH cells dosed with 81 nM PMA at various timepoints, demonstrating that peak Sig15 localization at the cell surface occurs at approximately 8 hours post-stimulation with a modest, maintained increase at 24 hours (dotted line represents isotype MFI).

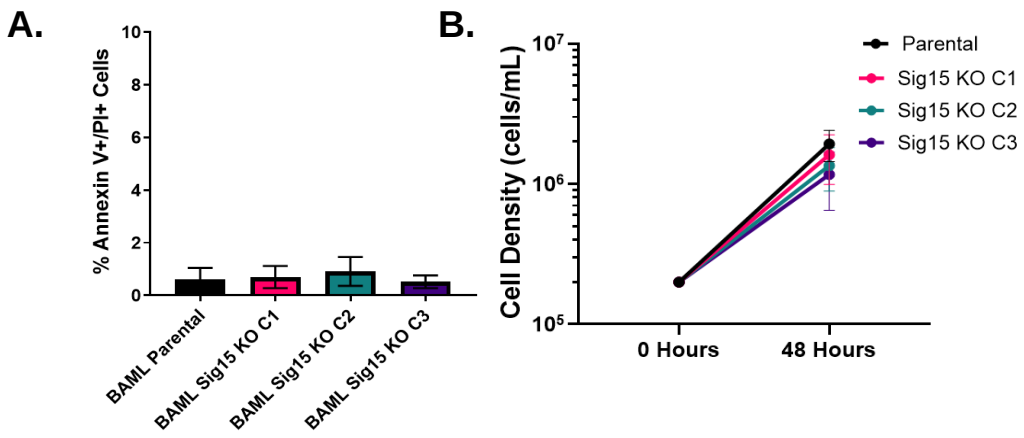

Supplementary Figure 3.2. Sig15 is not required for maintenance of proliferation or intrinsic survival in murine B-ALL. (**A)** Flow cytometry of three monoclonal knockouts of *Siglec15* in mB-ALL and the parental cell line to assess basal apoptosis levels as measured via Annexin V and Propidium iodide double-positive staining. *Siglec15* knockout did not alter basal apoptosis levels as compared to parental cells. Clone 3 was selected for further analysis in murine experiments. (**B)** Cell proliferation of three monoclonal knockouts of *Siglec15* in mB-ALL and the parental cell line as measured by cellometer at 48 hours. *Siglec15* knockout did not alter proliferation of the mB-ALL cells as compared to parental.

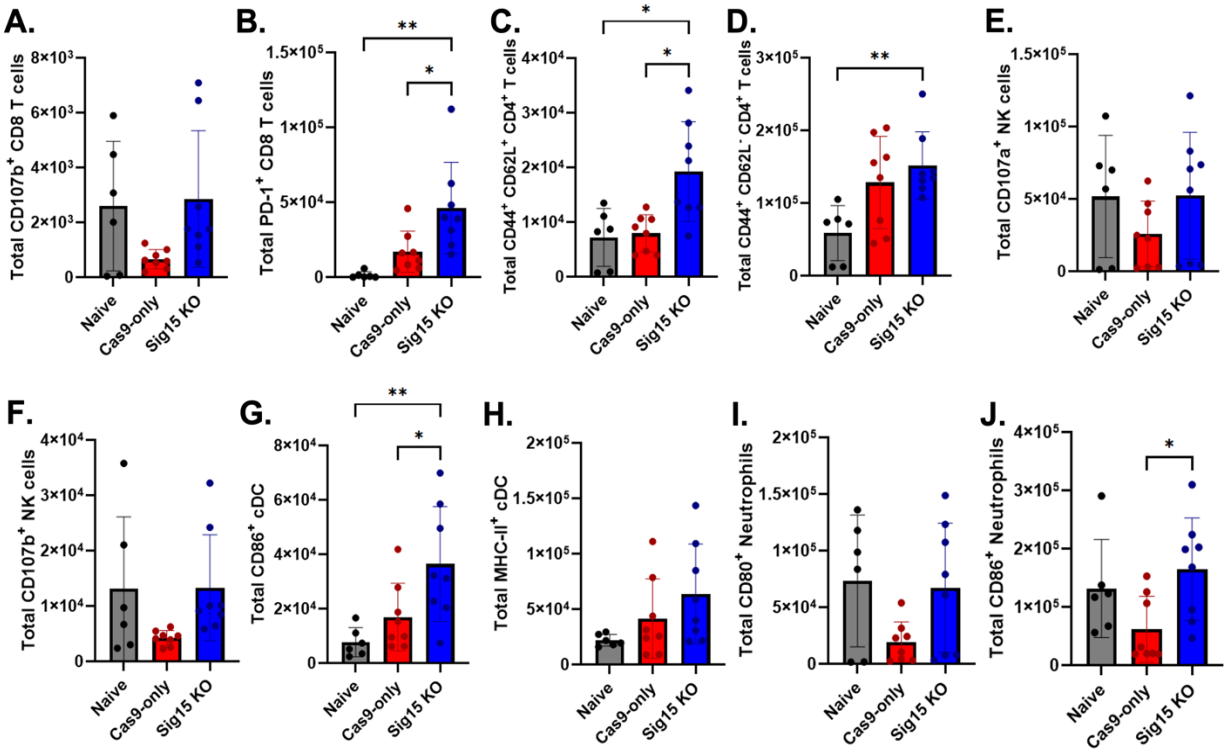

Supplementary Figure 3.3. Sig15 ablation in murine B-ALL promotes an adaptive immune response against leukemia. **A-J.** Un-irradiated WT C57BL6 mice were injected via tail vein with $5x10^5$ Cas9-only or Sig15 KO cells. Bone marrow was harvested 7 days later for highly dimensional flow cytometry of non-leukemia bone marrow populations. **A.** CD107b as a marker of degranulation was non-significantly higher in Sig15 KO recipients compared to Cas9-only control leukemia. **B.** PD-1 as a marker of $CD8^+$ T cell activation was significantly higher in Sig15 KO recipients. **C-D.** Memory-like early $CD4^+$ Tcm but not Tem populations were significantly higher in Sig15 KO recipients. **E-F.** Degranulation of NK cells in Sig15 KO recipients had a non-significant increase comparable to baseline levels. **G-H.** CD86 costimulatory expression but not MHC-II expression was significantly higher in Sig15 KO recipients. **I-J.** CD86 but not CD80 costimulatory expression on neutrophils was significantly higher in Sig15 KO recipients.

Chapter 4: Siglec-15 possesses unique localization and alternative isoform expression in lymphoblastic cancers

As discussed in the previous chapter, unique localization patterns and extracellular release of Sig15 are observed in B-ALL, some of which are suspected to occur due to lack of co-expression with DAP12 and related adaptor proteins. Sig15 appears to rapidly cycle back into the endosomal and lysosomal compartments in B-ALL unless otherwise stabilized at the membrane through a to-be-determined mechanism which is independent of adaptor protein expression and dependent upon NF-κB activation. Yet there remains much to be understood about Sig15, particularly in the context of B-ALL, where its NF-κB-driven expression and intracellular localization may drive a more aberrant expression pattern and pathogenic functionality than in other physiological contexts and myeloid-derived/associated diseases. The first of these pertinent investigations involves study of the splice variants expressed in normal leukocytes and hematological malignancies, which may dramatically alter Sig15 biology.

4.1 Siglec-15 isoform expression differs between normal and malignant leukocytes

RNA splicing is the process of cleaving out the intronic sequences of pre-mRNA and splicing the exonic regions together to form the matured mRNA sequence (186). Alternative splicing is an expansion on this, wherein different exons in the same gene may be alternatively spliced together, creating multiple different mRNAs from the same gene sequence which may or may not be protein-coding. Alternative splicing of these isoforms, also known as spliceoforms or splice variants, may result in the inclusion of parts of or different exons, shifts in or complete ablation of the open reading frame (ORF) required for protein translation, as well as inclusion of intronic sequence within the fully matured mRNA. Siglec family members have been demonstrated across diseases and normal physiology to undergo alternative splicing, though the regulation and consequence of these alternative isoforms is still emerging. Alternative isoforms across Siglecs often contain variable numbers of intracellular signaling domains, which may alter functional capacity (187, 188), or are deficient in their transmembrane domains, generating a soluble form of the Siglec protein which may be released into circulation (164, 165, 189).

Though we have demonstrated aberrant expression of the canonical sequence of Sig15 in B-ALL, the expression and pathogenicity of its alternative isoforms has yet to be explored.

The genomic sequence of Sig15 is approximately 65% GC content (113), an overall high score for GC enrichment which should contribute to consistent, stable expression of Sig15 in humans. Yet the GTEx data portal (dbGaP Accession phs000424.v8.p2) demonstrates highly variable expression of the different Sig15 exons according to tissue type (**Fig. 4.1A**), with Exon 8 being the most highly and consistently expressed, while Exon 1 is minimally expressed in nearly all tissue types aside, notably, from EBV-transformed lymphocytes. Aside from the canonical mRNA sequence of *SIGLEC15* (Sig15-201), shotgun sequencing data from the Human Genome Project has identified four predicted alternative isoforms of human Sig15 (**Fig. 4.1B**) which can account for the differential expression of exons across tissue types. Though lacking a putative translation start codon and thus not predicted to be protein coding, Sig15-204 is the most highly and widely expressed isoform of Sig15, commencing in the intronic region between Exons 4 and 5 and extending past an alternative polyadenylation site "AGTAAA" at the end of the canonical Sig15 3' UTR region. Expression of this isoform is enriched across a broad spectrum of tissue types, particularly compared to the canonical Sig15 isoform, which is most heavily enriched in EBV-transformed lymphocytes. Distribution of coding sequences for the different Sig15 protein domains ranges widely across exons (**Fig. 4.1C**), with only the canonical form containing the full sequence for the N-terminus signal peptide and Sig15-204 lacking the V-set domain coding sequence. As indicated, mRNA sequences can vary widely between these predicted Sig15 isoforms, which may consequently affect the protein structure for those isoforms which are protein coding.

Using the predicted RNA sequences of each Sig15 isoform, we designed primer sets (**Fig. 4.2A**) which allow for selective amplification of either the canonical Sig15-201 sequence (by amplifying across Exons 1, 3, and 4; "First 3 Exons"), Sig15-201 and Sig15-203 protein-coding isoforms (by placing both forward and reverse primers within Exon 4; "Exon 4"), Sig15-204 (by placing the forward primer in the retained intronic region preceding Exon 5; "Pre-Exon 5"), and Sig15-201, -202, and -205 using a primer set within the 3' UTR sequence. All qPCR reactions were performed on DNase-treated RNA samples so

as to eliminate the possibility of off-target amplification of genomic DNA. Fascinatingly, though canonical Sig15 mRNA expression is roughly equivalent to or higher across most human B-ALL cell lines as compared to healthy PBMCs, expression of the alternative isoforms in B-ALL is relatively less (**Fig. 4.2B**). When probing for SIGLEC15 expression in these cell lines, alternative bands to canonical Sig15 (at 36 kDa) are observable at approximately 25 and 55 kDa in healthy PBMCs which are largely missing from B-ALL cells (**Fig. 4.2C**). The predicted molecular weight of both protein-coding isoforms, Sig15-202 and Sig15-203, is approximately 18 kDa. While the signal at 25 kDa could be resultant from a glycosylated or otherwise post-translationally modified version of these isoforms, our preliminary data (not shown) suggest this signal is instead derived from a fully deglycosylated form of canonical Sig15. This is also further corroborated with data from GTEx, which identifies near exclusive expression of these alternative protein-coding isoforms in testis tissue (queried from dbGaP Accession phs000424.v8.p2). Thus further isolation and analysis of these alternative Sig15 protein signals is required. Interestingly, we found alternative isoform expression was not limited to leukemias compared to healthy PBMCs but rather within hematological malignancies as well. A small panel of DLBCL cell lines appeared to lack expression of Sig15-201 and Sig15-203 but expressed moderate amounts of Sig15-204 (**Fig. 4.2D**), suggesting B cell maturation state and/or disease localization can also alter Sig15 isoform expression.

Having observed this difference in Sig15 isoform expression between early pre-B leukemia and mature B cell lymphoma, we next sought to better understand the mechanisms by which these isoforms are differentially expressed. Stimulation with PMA for 24 hours strongly upregulated expression of all Sig15 isoforms in both a human B-ALL cell line and a healthy PBMC sample, where the latter consistently demonstrated higher baseline expression levels of alternative Sig15 isoforms (**Fig. 4.3A**). As PMA has pleiotropic stimulatory effects across PBMC populations, we further stimulated healthy PBMCs from two donors with antibodies against CD3 and CD28 to induce activation and proliferation of T cells for 24 hours (**Fig. 4.3B**). Stimulation of T cells induced a strikingly significant decrease in expression of all Sig15 isoforms, which can likely be attributed to either a downregulation of Sig15 expression across all or select PBMC populations, or a decrease in the proportion of Sig15-expressing PBMCs upon

expansion of stimulated T cells. To better understand this effect, we isolated T cells from 3 healthy PBMC samples and assessed Sig15 isoform expression. Sig15-201 and Sig15-203 were only present at background levels, but considerable expression of Sig15-204 was found in the T cells of all three donors (**Fig. 4.3C**). This demonstrates the decreased expression of Sig15 isoforms following T cell stimulation cannot solely be attributed to increased T cell proportions in the PBMCs, as the relative levels of Sig15-204 (which T cells appear to express) also decreases upon stimulation. This likely suggests a greater cell-cell interactive change is occurring upon T cell stimulation which changes Sig15 levels across Sig15-expressing populations. Though T cells have not been demonstrated to express detectable levels of canonical Sig15 protein (118), our preliminary studies concur with the GTEx database that Sig15-204 may be highly expressed across PBMC populations, including T cells.

Due to its lack of a putative ORF and its enhanced expression across tissues, Sig15-204 could likely operate as a non-coding RNA (ncRNA) in leukocytes and leukocyte-derived cancers. Non-coding RNAs have well-characterized roles in B cell malignancies (190), where expression of ncRNAs has been demonstrated to be both enriched and highly specific across malignant B cell subsets, including in B-ALL and DLBCL (191, 192). Sig15 expression has been demonstrated in some cancers to be regulated by ncRNAs encoded from different parts of the genome (142, 143), yet the possible existence of a Sig15 alternative ncRNA and its function in pathogenesis is undefined. While some Siglec family proteins, including Siglec-1 and Siglec-7 (193), have demonstrated non-coding alternative isoforms, the pathological (or, further, physiological) contributions of any of these Siglec family alternative isoforms remains to be discovered. Nevertheless, the enhanced expression of Sig15-204 on normal PBMCs and T cells as compared to human B-ALL and DLBCL cell lines would suggest that this isoform is likely suppressed in B cell malignancies, perhaps suggesting it may have tumor suppressive function.

4.2 Siglec-15 expression changes through the cell cycle and is highest in mitosis in leukocytes

NF-κB activation in both B-ALL and healthy PBMCs can induce downstream pro-growth pathways, modulating expression of cell-cycle regulated proteins. In order to resolve whether active cell cycling, independent of NF-κB activation, could regulate Sig15 expression, we began experiments in a

murine model of B-ALL. Though Sig15 knockout in this model did not alter proliferation rates of these murine B-ALL cells (**Fig. 3SA**), *Siglec15* expression was demonstrated to be highly sensitive to population growth phase and confluency. Cells which were seeded from confluence and harvested in lag phase of growth displayed a remarkable 70% decrease in *Siglec15* expression, while those cells which were seeded from logarithmic growth and harvested at the height of late logarithmic phase had the highest Sig15 expression (**Fig. 4.4A**). Culturing of healthy human PBMCs following cryopreservation revealed a similar sensitivity to active cell cycling, wherein PBMCs cultured for 24 hours following thaw had significantly higher amounts of detectable *SIGLEC15* as compared to PBMCs cultured for only 4 hours post-thaw (**Fig. 4.4B**). While RNA synthesis of most genes will naturally accumulate through the cell cycle, with peak at S phase, Sig15 expression in both murine and human models appeared to have enhanced sensitivity to cell cycling compared to reference genes.

With these data suggesting a role for active cell cycling in regulation of Sig15 expression, we performed cell cycle arrest and synchronization experiments using serum starvation conditions and the mitosis-arresting agent nocodazole. The entry of cells into G1 using serum synchronization induced a marked increase in SIGLEC15 expression, while release of mitotically-arrested cells from M phase with nocodazole synchronization slightly decreased SIGLEC15 (**Fig. 4.4C**). This data would suggest that Sig15 is in fact increased during active cell cycling. We consequently performed flow cytometry on REH cells to characterize the total SIGLEC15 expression of B-ALL cells through the phases of the cell cycle and observed that B-ALL cells in G2/M phase had the highest levels of detectable Sig15, which increased gradually through the cell cycle (**Fig. 4.4D-F**). Sig15 has been demonstrated to regulate actin filament organization and the formation of the actin ring in osteoclasts (123), which could suggest a critical role for it in mitosis. Though this mechanism has been established through Sig15 interaction with DAP12, which does not occur in B-ALL, the role of Sig15 in mitotic structural organization and its consequent regulation by the cell cycle could have interesting implications for a multifaceted function in leukemia progression, perhaps by stabilizing the actin filament network in rapidly proliferating leukemia cells during mitosis.

4.3 The extracellular domain of Sig15 has the capacity to localize to the nucleus

Though we have established the trafficking of Sig15 in human B-ALL cell lines from retention in the Golgi apparatus to and from the membrane and lysosome, we have observed an interesting phenomenon of Sig15 localization utilizing antibodies targeted towards different epitopes of the protein sequence. While the 1F7 clone antibody specific for the intracellular domain (ICD) of Sig15 detects the protein as previously established in perinuclear aggregates and cytoplasmic puncta, the A9E8 clone antibody raised against the Sig15 extracellular domain (ECD) demonstrates limited surface localization as well as a striking aggregate pattern within the nucleus (**Fig. 4.5A**). Nuclear Sig15 is observed consistently across B-ALL and osteosarcoma cell lines (**Fig. 4.5B**), with osteosarcoma cells displaying a more nuclear-diffuse distribution while nuclear Sig15 in B-ALL cells tended to concentrate in perinucleolar aggregates. To validate our findings, we performed a nuclear extraction of unstimulated REH cells and were successfully able to demonstrate strong SIGLEC15 signal in the nuclear compartment with an extracellularly-targeted antibody for Sig15 (**Fig. 4.5C**). The ICD-targeted antibody, however, did not demonstrate any Sig15-specific signal, further supporting that nuclear Sig15 does not possess the intracellular domain.

As the nuclear Sig15 signal in both B-ALL and osteosarcoma cells appears to be distanced from the nuclear envelope, it is also likely that this nuclear Sig15 is deficient in both its intracellular and transmembrane domains. Separation of the Sig15 extracellular domain from the latter two domains is possible through two primary means: cleavage of the protein in a similar manner to the suspected mechanism of generation of sSig15, or expression of an alternative isoform which lacks these domains. In the case of the latter, it should be noted that there are currently no predicted or validated isoforms of Sig15 which include the mRNA sequence for the extracellular domains (Exons 1, 3-5) and not those of the transmembrane and intracellular domains. Further isolation and mass spectrometry analysis is required to better understand the composition and generation of this nuclear-localized form of Sig15, but this is, to our knowledge, the first demonstration of a Siglec family member which may translocate to the nucleus, and the mechanism by which it does so is in ongoing investigation.

As the majority of proteins which translocate to the nucleus contain a classical importin α nuclear localization signal (NLS) (194), we analyzed the protein sequence of Sig15 but did not detect any canonical NLS motifs. Further investigation revealed the presence of a suspected PY-NLS in the V-set domain of Sig15 (**Fig. 4.6A**), an NLS motif that allows for recognition and direct binding of cargo to the transportin family proteins for nuclear translocation (195). Typically characterized by the proline-tyrosine motif, this possible PY-NLS is located on a short loop connecting two β strands in the V-set domain and is easily accessible for binding on the Sig15 protein (**Fig. 4.6B**). A positively-charged arginine residue is located three amino acids to the N-terminal side and, further beyond that, a short series of five basic amino acids is present which would classify this predicted motif as the basic subtype of PY-NLS. It should be noted, however, that PY-NLS motifs have been characterized to primarily be expressed on long, disordered protein regions free of secondary structure, which is not seen with this predicted motif. Thus, binding of the transportins to this motif on Sig15 remains to be experimentally verified.

Though no Siglec family members have demonstrated capacity to localize to the nucleus, the role of nuclear-localized immune checkpoint molecules, including PD-L1, has recently emerged. PD-L1 has been demonstrated to localize to the nucleus through acetylation-dependent binding to importin α to regulate transcription of interferon-related genes through direct DNA binding (196). Nuclear PD-L1 has been demonstrated to have several other functions, such as regulating genomic instability and pyroptosis, and it negatively correlates with patient outcomes across solid tumors (197), which suggests the utility of nuclear-localized immune checkpoints can be highly pleiotropic and impactful. The localization of Sig15 to the perinucleolar region in B-ALL cells could implicate a role for the protein in the perinucleolar compartment (PNC), a compartment found primarily in cancer cells which maintains the intersection of RNA binding proteins, RNA polymerases, and newly synthesized RNA messages (198). Though the role of the PNC in cancer is still under investigation, it has been proposed to regulate RNA metabolism to meet the increased need for biosynthesis in cancer cells, perhaps suggesting a role for nuclear Sig15 in involvement of RNA processing and metabolism.

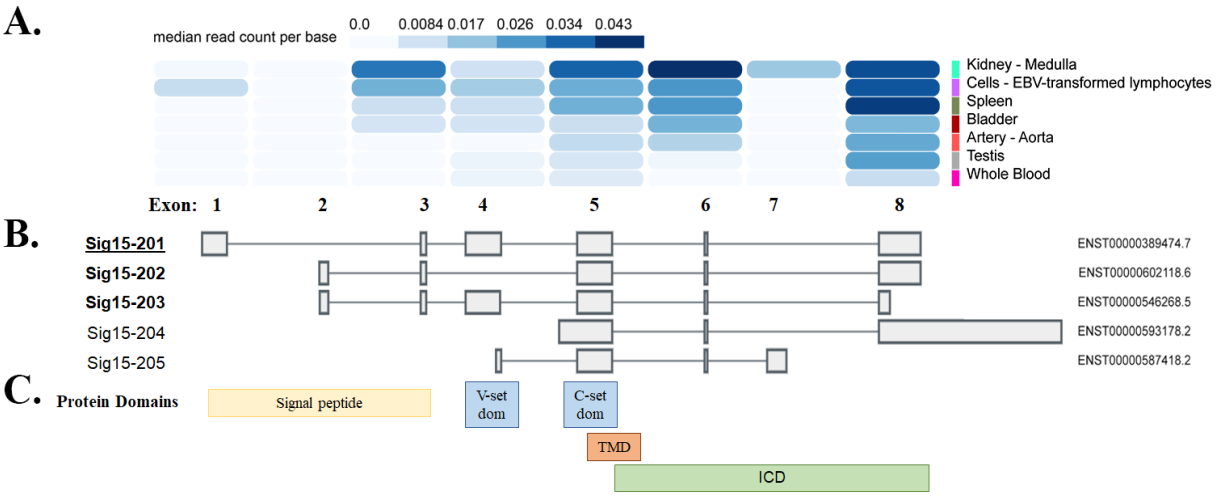

Figure 4.1 Predicted alternative splicing isoforms of human Siglec-15, adapted from GTEx (dbGaP Accession phs000424.v8.p2). (**A)** Relative exon read counts from RNA-sequencing data, with median read count displayed by increasing blue intensity and corresponding exon numbers below. Graphic displays highest and broadest detection of Exons 5-6 and 8 across all tissue types and minimal detection of Exon 1 aside from in EBV-transformed lymphocytes. (**B)** Alternative splicing isoforms of human Sig15, with common names listed to the left (**canonical isoform** in bold and underlined, **protein-coding isoforms** in bold) and Ensembl stable ID numbers listed to the right. Exons are depicted as large grey boxes while introns are displayed as the thin grey lines between. Non-coding Sig15-204 has the highest and most widely distributed expression across tissues. (**C)** Protein domain coding of Sig15 as distributed across the Sig15 exonic sequence. The first three exons of the canonical sequence (Exons 1, 3-4) code only for the signal peptide which is cleaved upon protein maturation, while the V-set domain is coded in Exon 4, the C2-set domain ("C-set domain"), transmembrane domain ("TMD"), and the beginning of the intracellular domain ("ICD") are all coded for in Exon 5, extending on through to Exon 8.

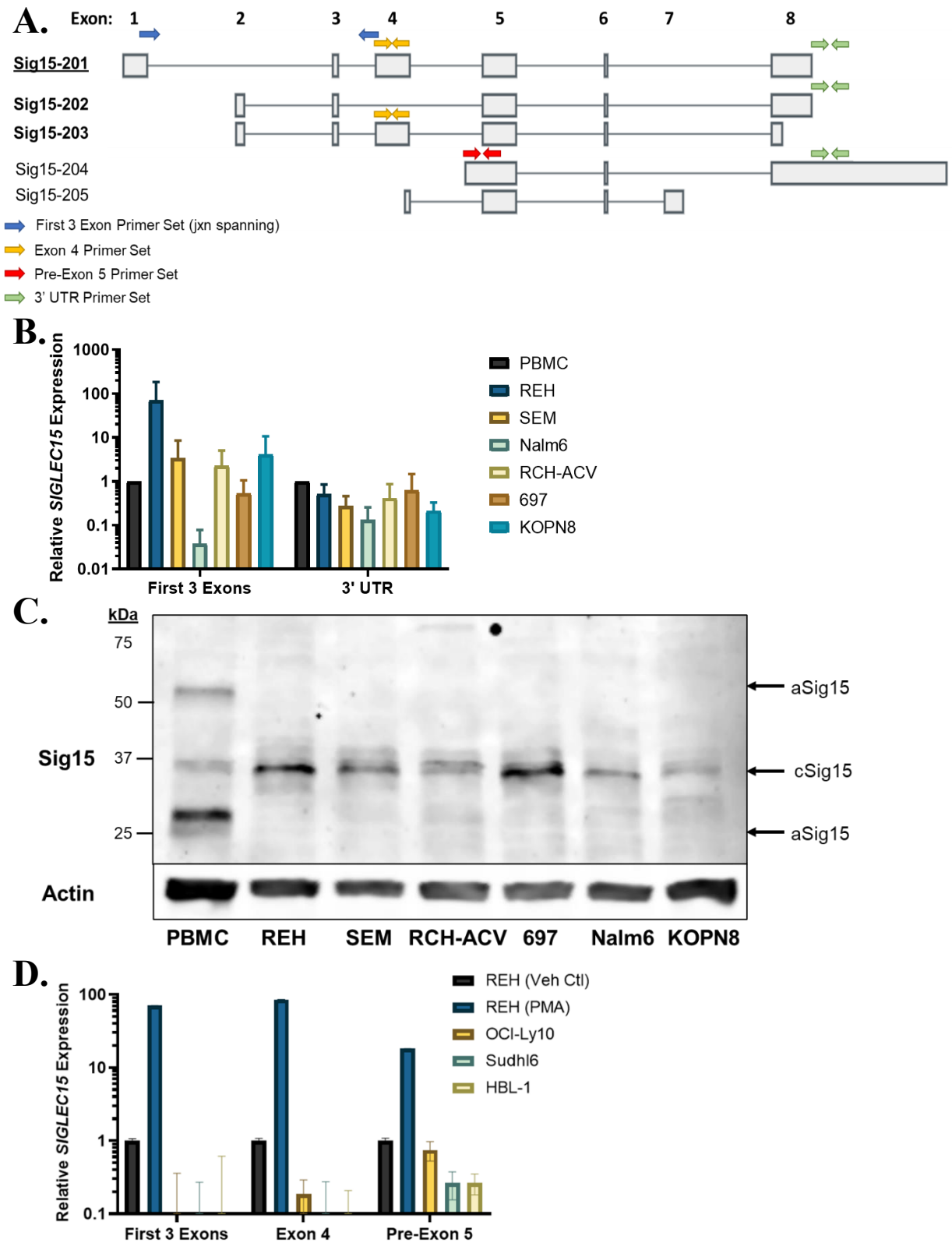

Figure 4.2 Normal leukocytes have differential Sig15 isoform expression from leukemia cells. (**A)**

Diagram showing the four generated sets of Sig15 primers designed to amplify specific Sig15 isoforms.

The alternative splicing isoforms of human Sig15, adapted from GTEx (dbGaP Accession phs000424.v8.p2), with common names listed to the left (**canonical isoform** in bold and underlined, **protein-coding isoforms** in bold). Primer sets are matched to left-facing and right-facing arrows which represent forward and reverse primers targeted to that part of the sequence, respectively. Primer sets included the First 3 Exons (which crossed the junctions between Exon 1 and 3 and Exon 3 and 4) which detects only the canonical Sig15 isoform, the E4 primers (mid-Exon 4) which detect Sig15-201 and Sig15-203, the Pre-Exon 5 primers (with a forward in the retained intronic region upstream of the start of Exon 5 and a reverse mid-Exon 5) which detects only Sig15-204, and the 3' UTR primers (mid-3' UTR) which detects Sig15-201, Sig15-202, and Sig15-204. (**B)** RT-qPCR of *SIGLEC15* expression in a panel of human B-ALL cell lines compared to a healthy PBMC control. Canonical Sig15 expression is equal to or greater than healthy controls across B-ALL but all B-ALL cell lines possessed comparatively lower expression of the 3' UTR amplified isoforms, suggesting these are more highly expressed in normal leukocytes. (**C)** Western blotting for SIGLEC15 in a panel of human B-ALL cell lines as compared to a healthy PBMC control. The canonical Sig15 signal (cSig15) appears around the expected 36 kDa, where as healthy PBMCs also show strong signal at 25 and 55 kDa, bands which can be attributed to yet-unidentified alternative Sig15 (aSig15). (**D)** RT-qPCR of *SIGLEC15* expression in a panel of human B-ALL and DLBCL cell lines compared. REH cells were also stimulated for 24 hours with 81 nM PMA ("PMA") or DMSO (Veh Ctl") prior to harvest. DLBCL cell lines do not express canonical Sig15 nor the alternative Sig15-203, but they do appear to have modest expression of Sig15-204 at levels slightly lower than control REH cells. These results suggest a reduction in expression of Sig15-204 non-coding isoform and an upregulation in canonical Sig15-201 expression in the context of hematological malignancies as compared to healthy leukocyte controls.

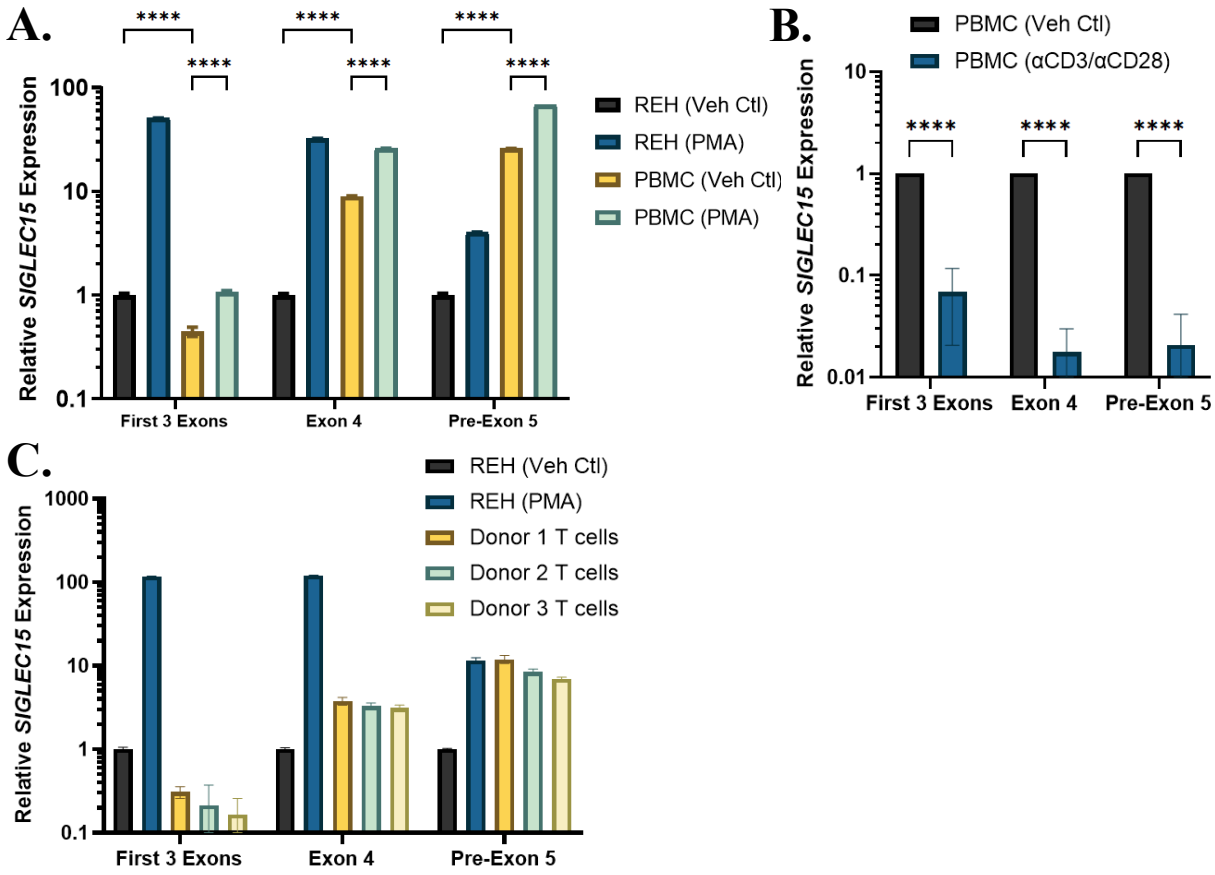

Figure 4.3 Alternative Sig15 isoform expression is present in healthy PBMCs and inducible through PMA stimulation. (**A)** RT-qPCR of *SIGLEC15* expression in REH cells and a healthy donor PBMC sample, which were stimulated for 24 hours with 81 nM PMA ("PMA") or DMSO (Veh Ctl") prior to harvest. Healthy PBMCs express minimal canonical Sig15 as observed prior, which is inducible following 24 hour stimulation with PMA. PBMCs also express significantly higher levels of Sig15 alternative isoforms Sig15-203 and Sig15-204 relative to REH controls (****P<0.0001). (**B)** RT-qPCR of *SIGLEC15* expression in two healthy donor PBMC samples which were treated with either PBS ("Veh Ctl") or stimulated with 10 ug/mL plate-bound anti-CD3 and 1 ug/mL soluble anti-CD28 ("aCD3/aCD28") to promote T cell activation for 24 hours prior to harvest. Stimulation of T cells caused significantly decreased expression of all Sig15 isoforms (****P<0.0001). (**C)** RT-qPCR of *SIGLEC15* expression in T cells isolated from 3 healthy donor PBMC samples. T cells expressed low-to-background levels of canonical Sig15-201 but significant amounts of Sig15-204 relative to REH cells. Despite the

detectable signal observed in T cells using the Exon 4 primers, the melting curves of these reactions suggests a non-specific amplification of these primers occurred in T cell samples and cannot be fully interpreted. These data together suggest PMA may increase Sig15 expression in healthy PBMCs while T cell activation significantly decreases it, which is independent of Sig15 expression on T cells.

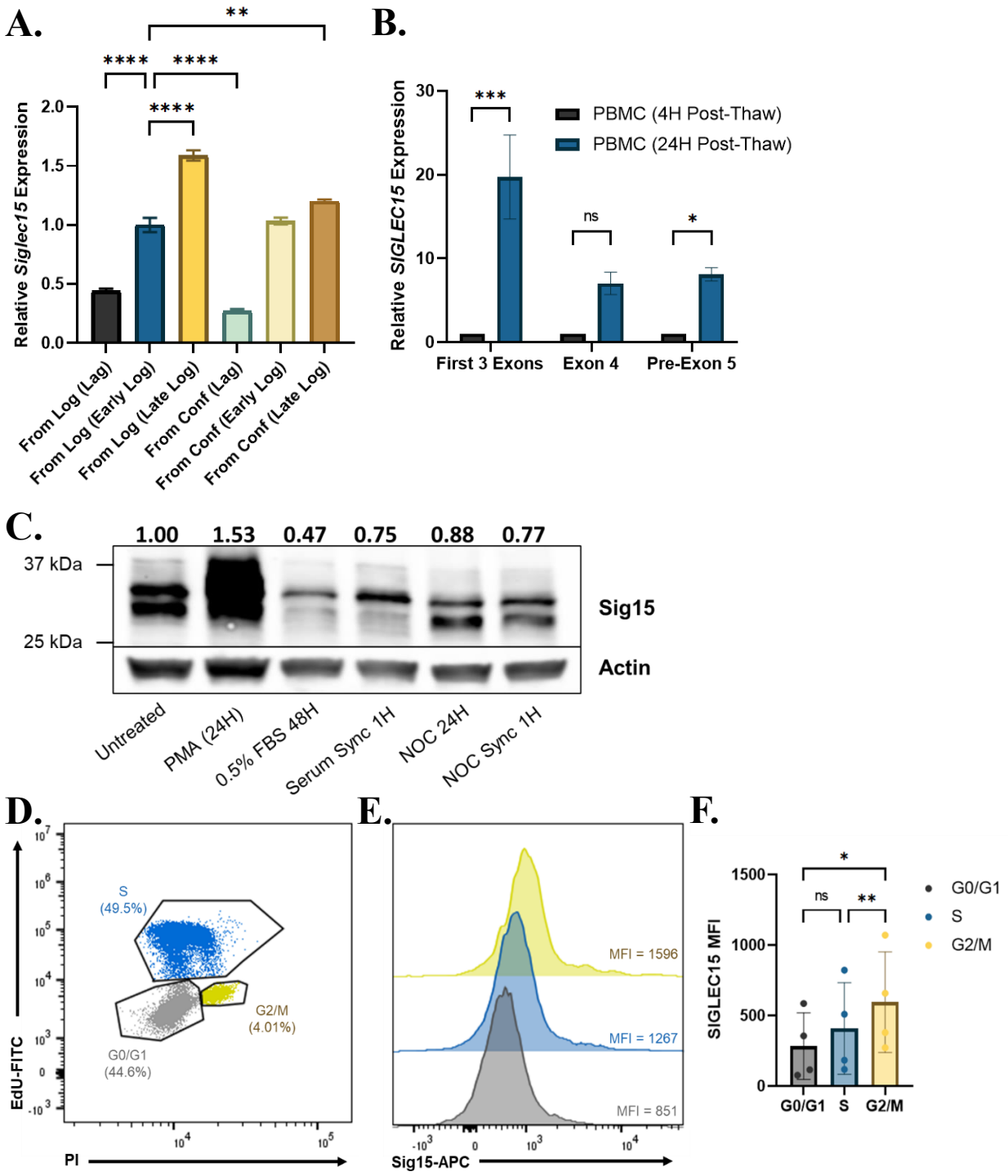

Figure 4.4 Sig15 expression is regulated by active cell cycling in human B-ALL cells. **(A)** RT-qPCR of *Siglec15* expression in murine B-ALL cells which were cultured at logarithmic growth (approx. $8.0x10^5$ cells/mL; "From Log") or confluence (approx. $3x10^6$ cells/mL; "From Conf") prior to reseeding, at which point cells were seeded to concentrations consistent with lag phase growth ($2.0x10^5$ cells/mL;

"Lag"), early logarithmic growth ($4.0x10^5$ cells/mL; "Early Log"), or late logarithmic growth ($8.0x10^5$ cells/mL; "Late Log") and cultured for another 24 hours prior to harvest. Under or overconfluent cells demonstrated significant reductions in Sig15 expression (**P<0.01; ****P<0.0001). (**B)** RT-qPCR of *SIGLEC15* expression in two healthy donor PBMC samples which were cryopreserved, thawed, and cultured for either 4 hours ("4H Post-Thaw") or 24 hours ("24H Post-Thaw") prior to harvest. All detectable isoforms of Sig15 are significantly upregulated in PBMCs which have been cultured for longer periods post-thaw (*P<0.05; ***P<0.001). (**C)** Western blotting for SIGLEC15 in REH cells which were stimulated with 81 nM PMA for 24 hours ("PMA (24H)"), cultured in 0.5% FBS serum starvation conditions for 48 hours ("0.5% FBS 48H"), serum synchronized 1 hour prior to harvest ("Serum Sync 1H"), treated with 1.66 uM nocodazole for 24 hours ("NOC 24H"), and nocodazole synchronized 1 hour prior to harvest ("NOC Sync 1H"). Densitometric analysis of relative fold change is given by the bold numbers above the blot. Sig15 expression increased when REH cells began synchronized cycling as mediated by serum but decreased when mitosis-arrested nocodazole cells were released and synchronized, suggesting Sig15 expression increases in active cell cycling with highest expression in M phase. **D-F.** Cell cycle analysis of REH cells stained with EdU and PI to discriminate G0/G1, S, and G2/M phase populations and Sig15 to assess alterations in SIGLEC15 expression through the cell cycle. (**D)** Dot plot showing the gating for cell cycle phases. Percentages per phase of one representative sample are shown. (**E)** Demonstrated by representative Sig15 histogram plots, Sig15 expression was found to increase gradually through the cell cycle, with highest expression being observed in G2/M phase. (**F)** Quantification of changes in Sig15 MFI across different phases of the cell cycle in REH cells. Sig15 MFI was significantly higher in G2/M phase REH cells compared to G0/G1 and S phase cells, suggesting Sig15 expression is highest in mitosis in B-ALL cells.

A.

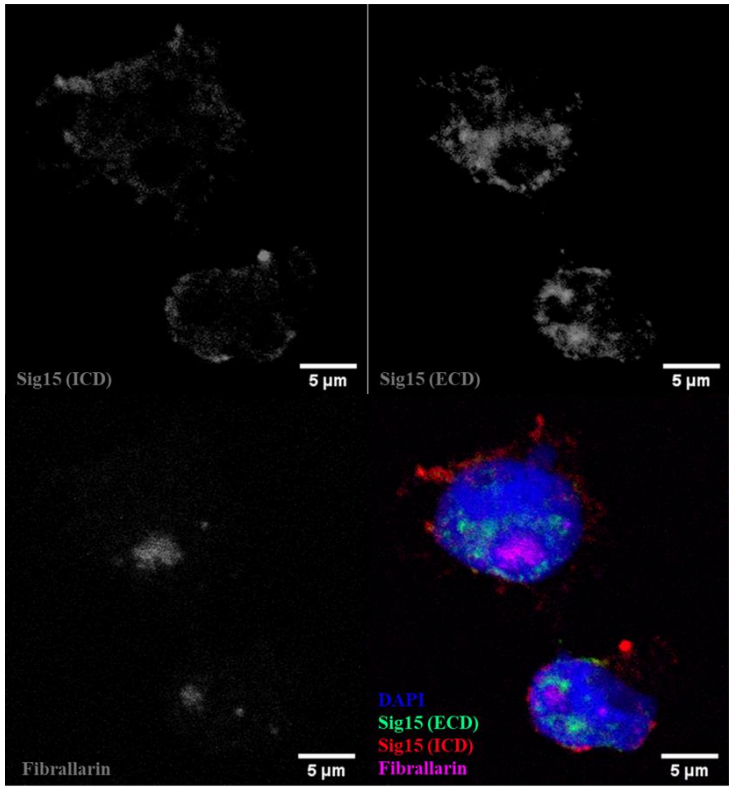
Sig15 (ICD)
5 µm
Sig15 (ECD)
5 µm
DAPI
Sig15 (ECD)
Sig15 (ICD)
Fibrallarin
Fibrallarin
5 µm
5 µm

B.

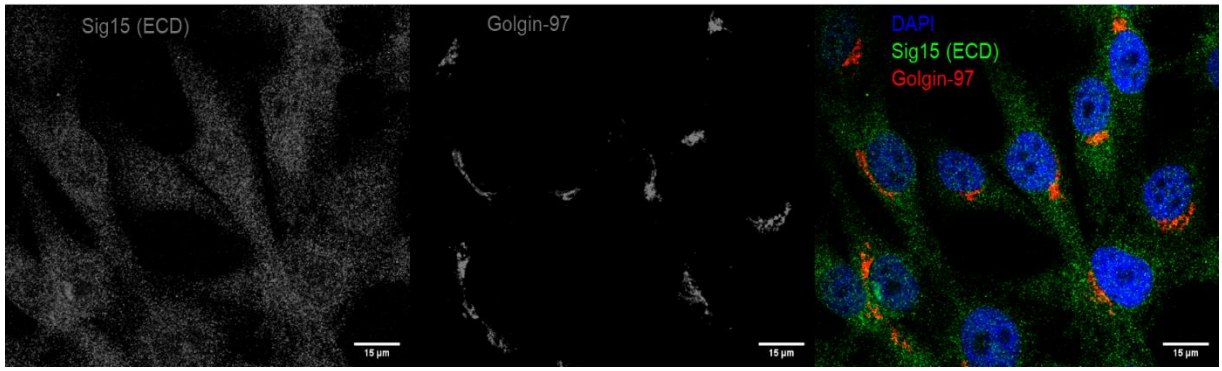
Sig15 (ECD)
Golgin-97
DAPI
Sig15 (ECD)
Golgin-97
15 µm
15 µm
15 µm

C.

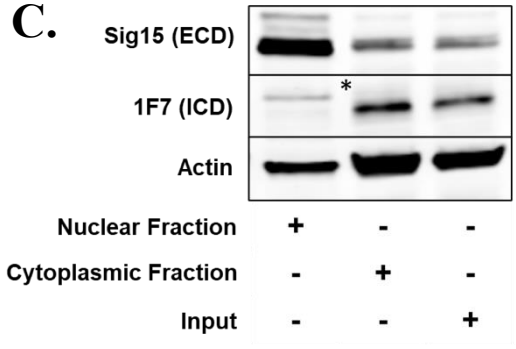
Sig15 (ECD)
1F7 (ICD)
*
Actin
Nuclear Fraction + - -
Cytoplasmic Fraction - + -
Input - - +

Figure 4.5 Sig15 extracellular and intracellular domains localize to different compartments of B-ALL and osteosarcoma cells. (**A)** Immunofluorescence imaging of REH cells stained for DAPI nuclear signal (**blue**), nucleoli (fibrallarin; **magenta**), and two different Sig15 antibodies: the 1F7 antibody specific for the intracellular domain of Sig15 ("Sig15 ICD"; **red**) and the A9E8 antibody specific for the V-set domain in the extracellular region of Sig15 ("Sig15 ECD"; **green**). The intracelluarly-targeted antibody depicts Sig15 in the perinuclear space and trafficking to and from the surface as previously described, while the extracellularly-targeted antibody depicts both surface-localized and strong perinucleolar aggregates of Sig15, suggesting differential compartmentalization of these protein domains in B-ALL. (**B)** Immunofluorescence imaging of MG-63 osteosarcoma cells stained for DAPI nuclear signal (**blue**), a polyclonal extracellularly-targeted Sig15 antibody (**green**), and the Golgi-localized marker Golgin-97. Strong colocalization of Sig15 with Golgin-97 was not observed as previously seen in B-ALL cells. Sig15 instead appeared to be widely distributed across the cellular compartments, including small puncta through the cytoplasm and nucleus. Osteosarcoma lines thus also demonstrate detection of the Sig15 extracellular domain within the nucleus. Data were generated in collaboration with Maggie Phillips. (**C)** Nuclear and cytoplasmic extraction of Sig15 from REH cells, blotted alongside whole cell lysate ("Input"). An extracellularly-targeted Sig15 antibody detects enriched signal in the nuclear compartment compared to cytoplasmic or whole cell, while an intracellularly-targeted antibody only detects Sig15 in the cytoplasmic and whole cell samples (*indicates a non-specific band from actin staining). It should be noted that the cytoplasmic compartment control, Actin, stained modestly positive in the nuclear compartment which could suggest slight cytoplasmic contamination, though this remains to be verified. These results suggest the nuclear translocation of the extracellular (but not the intracellular) domain of Sig15 in human B-ALL and osteosarcoma cell line models.

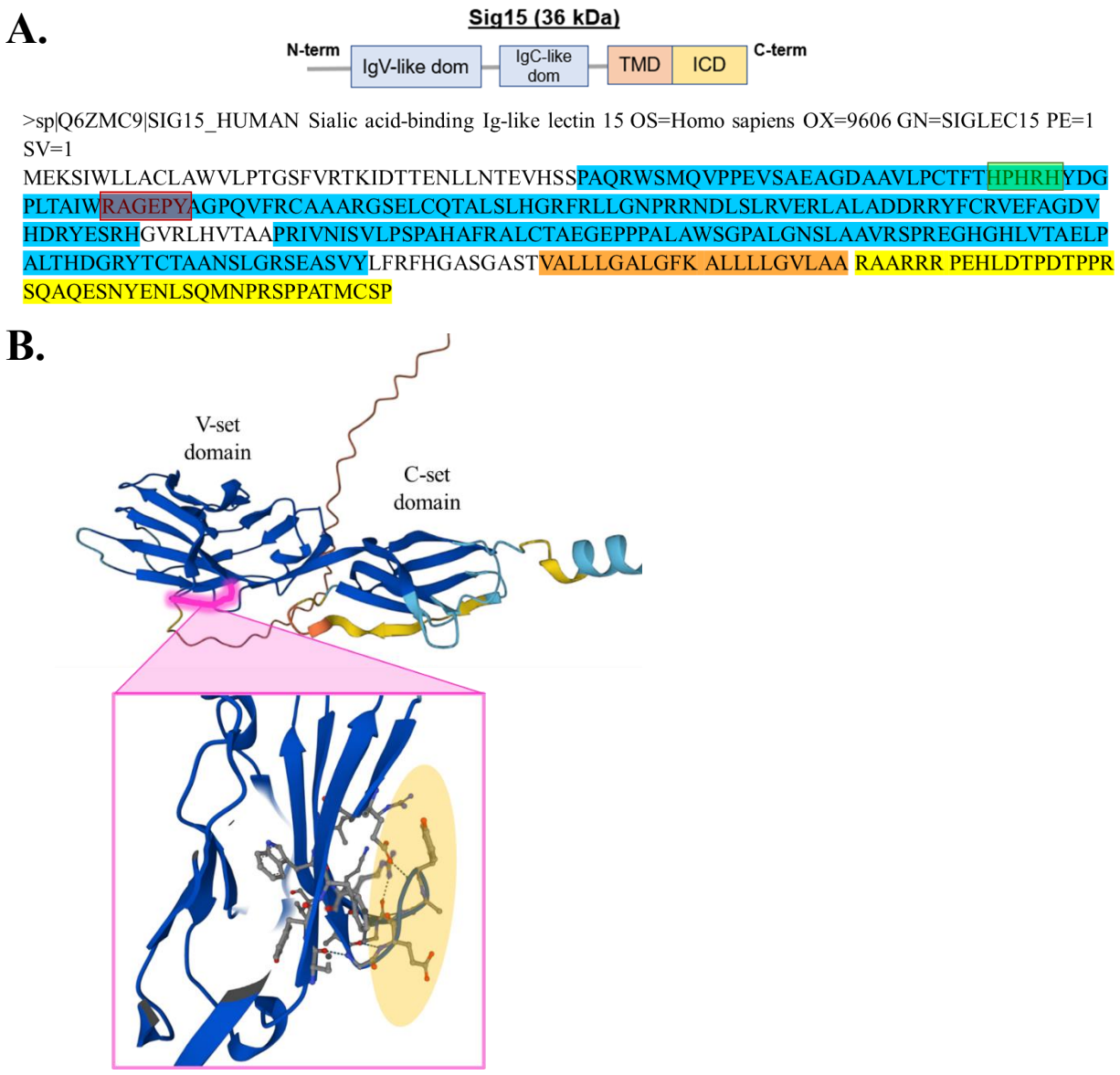

Figure 4.6 A short amino acid sequence within the Sig15 V-set domain resembles the established model for a PY-NLS motif. (**A)** Within the protein sequence of Sig15, there exists two extracellular domains (an N-terminal V-set domain and C2-set domain further C-terminal, **in blue**), a transmembrane domain (**in orange**), and an intracellular domain (**in yellow**). The "RAGE-PY" motif highlighted **in red** within the V-set domain closely resembles that of other putative PY-NLS sequences, with a region of five basic amino acids further N-terminal (highlighted **in green**) would further subclassify this motif as a basic PY-NLS. The extracellular domain of Sig15 thus may have the capacity to translocate to the nucleus through binding of this motif to the transportin proteins in B-ALL and osteosarcoma. (**B)** The region for this

suspected PY-NLS motif is easily accessible in the protein structure of Sig15, being on a short loop (highlighted **in pink**) between β strands in the folded V-set domain structure which is easily accessible (highlighted region, **in orange**) and contains several hydrophobic amino acids that could facilitate interface with the hydrophobic interface domain of importin β (195). Adapted from the AlphaFold Protein Structure Database (199). Nuclear Sig15 thus may be able to traffic into the nucleus through utilization of this NLS motif, though this still requires experimental demonstration.

Chapter 5: General Discussion and Closing Remarks

5.1 Sig15 is pathologically expressed in blood cancers

We have demonstrated aberrant expression of Sig15 in human blood cancers, including B-ALL, T-ALL, AML, and DLBCL, as compared to healthy PBMCs. In the case of B-ALL, this upregulated expression of Sig15 was demonstrated *in silico*, in cell line models, and in primary patient samples. In the case of the latter, surface-detectable Sig15 was found on B-ALL cells from 3 of 7 bone marrow aspirate samples and 1 of 8 peripheral blood samples as compared to non-leukemia bone marrow hematogones and circulating mature B cells, indicating both pathological expression of Sig15 and its enhanced expression or surface localization in the bone marrow context. Pathological overexpression of Sig15 in cancer is a phenomenon that has emerged in the literature through the last five years, being widely expressed across such cancers as NSCLC, bladder, colon, endometrial, kidney, liver, thyroid, clear cell renal cell carcinoma, osteosarcoma, and AML (118, 141, 143, 158). While some of this pathological expression can be attributed to tumor-infiltrating macrophages (118), there are nevertheless some cancer types which have been demonstrated to directly upregulate Sig15 expression, including B-ALL.

Interestingly, the canonical Sig15 sequence (Sig15-201) was found to be most highly expressed in B-ALL compared to normal PBMCs, T cells, and even lymphoma cells, while the non-coding alternative isoform Sig15-204 was much more highly expressed across healthy leukocytes and other tissue types. This could suggest differential roles for canonical Sig15 and this ncRNA in physiological leukocytes as compared to B-ALL cells. Most literature to-date on alternative isoforms in Siglec family members characterizes protein-coding isoforms with alternative numbers of intracellular signaling domains (187, 188) or generation of soluble isoforms which lack hydrophobic transmembrane domains (164, 165, 189). While Sig15 does possess a secreted/soluble form in B-ALL which could be generated through alternative splicing of a yet-undiscovered isoform, immunoprecipitation mass spectrometry studies by collaborators (data not shown) have demonstrated that sSig15 consists solely of the V-set and C2-set extracellular domains and truncates just above the transmembrane domain, suggesting sSig15 is likely cleaved at the membrane and shed from the cell instead. It is currently unknown how these Sig15 isoforms are

differentially regulated across normal and malignant lymphocytes, though our data suggest all isoforms are downregulated following T cell stimulation in healthy PBMCs and upregulated following PMA stimulation in B-ALL and PBMCs.

PMA-mediated NF-κB activation was found to be a powerful regulator of Sig15 expression in B-ALL cells and PBMCs. As an activation pathway important to lymphocyte biology, NF-κB hyperactivation is commonly observed in subsets of lymphocytic cancers (161, 176, 200). SIGLEC15 expression correlates with upstream markers of NF-κB activation in the pediatric TARGET database, and experimental inhibition of PMA-induced NF-κB activation significantly abrogates Sig15 upregulation at both the RNA and protein levels. CD40L, an upstream activator of NF-κB, was able to increase Sig15 protein in B-ALL cells but notably did not cause change in expression at the RNA level, suggesting a stabilization effect that is still currently under investigation.

5.2 NF-κB and calcineurin activation drives Sig15 pathology in B-ALL

While NF-κB activation was found to regulate Sig15 expression in B-ALL, it was also demonstrated to regulate Sig15 localization to the cellular membrane. B-ALL cells lack expression of all characterized adaptor protein binding partners, including DAP12, DAP10, and FcRγ, and lack of expression of these binding partners is not altered following PMA stimulation in REH cells. Thus it appears that Sig15 in NF-κB-activated B-ALL cells is stabilized at the membrane through a DAP12-independent process which is yet to be elucidated.

One hypothesis is that upregulation of Sig15 increases the total amount of Sig15 protein at the membrane, which in turn could increase the odds for Sig15 dimerization and stabilization at the membrane. Roughly half of the Siglec family members have been previously demonstrated to form dimers or multimers at the cellular membrane, such as CD22 (201), Siglec-5 (202), and the murine homolog of Siglec-9 (203), where disulfide-linked dimerization has been shown to stabilize this rapidly internalized Siglec at the membrane. SIGLEC15 does possess approximately 6 extracellular cysteine amino acid residues in its fully processed form which could potentially mediate disulfide linkages, though each of these residues is predicted to be involved with maintaining β strand folding of the V-set and C2-

set domain and thus may not be “available” for disulfide linking. Whether or not Sig15 has the capacity to dimerize remains unanswered, though future experiments such as native gel electrophoresis on Sig15 from B-ALL cells could elucidate this possibility.

Yet another hypothesis is that NF-κB activation alters expression of other Sig15 binding partners aside from the adaptor proteins. As the V-set domain of Sig15 has the capacity to bind sialylated proteins, it is possible that upregulation of sialoglycans could increase Sig15 binding and stabilization at the membrane. NF-κB activation has been shown in some non-cancer diseases to promote expression of sialyltransferases (204, 205), leading to increased global sialylation of surface membrane proteins. Due to the short length of the Sig15 extracellular domain, it is likely that the majority of its sialoglycan binding capacity is in *cis*- rather than *trans*- interactions. If NF-κB activation can be demonstrated to increase sialyltransferase expression and global sialylation levels in B-ALL, it is possible that this is the mechanism by which Sig15 is stabilized at the membrane, though investigation is required.

5.3 Sig15 mediates immunosuppression in B-ALL

Our studies demonstrated a critical role for Sig15 in regulating B-ALL-mediated immunosuppression in both *in vivo* and *ex vivo* model systems. Ablation of Sig15 in a murine B-ALL model significantly increased survival in immunocompetent but not immunodeficient recipients, indicating B-ALL-expressed Sig15 mediates immune evasion in this disease. The leukemia bone marrow microenvironment at Day 7 post-engraftment was dramatically altered in Sig15 knockout recipients, where $CD8^+$ T cell were demonstrated to be more expanded, activated, and differentiated into a variety of different anti-leukemia effector populations. Other populations, such as NK cells, neutrophils, and classical dendritic cells, were also shown to be more reactive to Sig15 leukemia, suggesting an overall more robust immune response to B-ALL. These changes also corresponded with changes to the leukemia bone marrow cytokine milieu, where Sig15-knockout marrow had baseline levels of IL-6, LIF, and IL-5, all of which have implicated roles in immunosuppression and leukemia (169-171).

These studies corroborate those which have recently been published characterizing Sig15 as a new immune checkpoint molecule in solid tumors (118), where it has been shown to play a role in

suppressing antigen-specific T cell cancer immunity. Stimulation of human T cells (118) or CAR-expressing Jurkat models (**Fig. 4E**) followed by exposure to recombinant Sig15 promotes decreased activation and proliferation, which demonstrates a role for Sig15 to act directly on T cells in suppressing immune response. The receptor for Sig15, however, has yet to be identified. Early studies into Sig15 ligation in artificial model systems have proposed a number of probable, heavily-glycosylated binding partners, including CD44 (174), yet demonstrations of Sig15 binding endogenous protein on T cell populations or indeed any others remain elusive. Possible reasons for this obscurity could include the reduced sialic acid binding capacity of human vs. murine Sig15 (113), the modest length of the Sig15 extracellular domain which may limit interactions to only *cis*- configurations, and the possibility of a context-dependent expression of the purported Sig15 "receptor" on T cells.

Though the sialic acid binding of Sig15 has been suggested to be weaker and perhaps more promiscuous than the CD33-related Siglecs, this raises an interesting possibility that Sig15 may instead have an elevated capacity for binding non-sialylated proteins. Tumor-expressed CD24 has been demonstrated to bind Siglec-10 on TAMS even when completely removed of all sialic acid modifications (92), suggesting some Siglecs do have the capacity for non-sialylated binding. Regarding preferential *cis*-interactions, recombinant Sig15 has shown efficacy in binding and suppressing T cell activation in co-culture models, and the existence of sSig15 might render this caveat of less concern. Yet it nevertheless remains poorly understood how capable surface-bound Sig15 is of interacting with T cells. It is possible that the receptor for Sig15 expressed on T cells has an especially long, protruding extracellular domain which allows for *trans*- interactions. Perhaps more likely, though Sig15 protein has not been shown to be expressed by human T cells, they may nevertheless acquire Sig15 protein at their cellular membrane through interaction with cancer cells and the process of trogocytosis. Trogocytosis is the pinching off and endocytosis of parts of the membrane from neighboring cells, which occurs often during immune response in a variety of lymphocytes and myeloid cells, including T cells (206). Through trogocytosis, Sig15 could be obtained by T cells from cancer cells or TAMS and undergo *cis*- binding of its receptor along the T cell membrane. While we are currently in ongoing investigation of the receptor of Sig15 on T

cells, the possibility of context-dependent expression of this receptor remains a consideration which may require more complex *ex vivo* assays to properly observe.

5.4 Secreted/soluble and nuclear Sig15 may demonstrate unique roles in Sig15 pathology

While calcineurin activity was found to have no effect on Sig15 expression, it was demonstrated to regulate the release of sSig15 from REH cells. Being another activation pathway critical to normal and malignant lymphocyte function, calcineurin/NFAT activation is often enhanced in blood cancers and is in fact critical for both lymphocytic leukemias and normal lymphocyte survival (49, 207). sSig15 contains the extracellular domain of Sig15 and is likely cleaved at the membrane through extracellular proteinases which may be regulated by calcineurin activity, such as the cathepsins (183). High levels of sSig15 were found to circulate in the plasma of pediatric B-ALL patients as compared to healthy, T-ALL, or AML patients. sSig15 also correlated with pro-leukemia immunosuppressive factors MCP-1/CCL2 and IL-6 while negatively correlating with immunostimulatory IL-12, suggesting sSig15 is a part of a systemically immunosuppressed cytokine profile. The functionality of sSig15 is still under investigation, though, being that sSig15 contains the full extracellular domain of Sig15, it is likely to maintain the same binding capacity as surface-bound Sig15 for receptors on populations such as T cells.

Nuclear Sig15 was yet another novel discovery, being detected in both B-ALL and osteosarcoma cells. The method by which Sig15 enters the nucleus is yet to be putatively demonstrated, but the implications for its presence in the nucleus of these cancer cells are fascinating. As previously discussed, other immune checkpoint molecules such as PD-L1 (196) have been shown to translocate to the nucleus in cancer cells, where they play diverse roles in transcriptional regulation, promotion of anti-apoptosis pathways, and cellular proliferation, acting as a prognostic indicator for tumor invasion and overall reduced patient survival. While the function of nuclear Sig15 is currently unknown, its structure (similar to that of its secreted/soluble form) appears to lack its intracellular domain, suggesting its mediated effects are performed exclusively through interaction with its extracellular domain. Considering nuclear Sig15 appears to localize to the PNC in B-ALL cells, nuclear Sig15 may have the capacity to regulate RNA metabolism and broader gene expression profiles, though this remains to be explored.

5.5 Future Directions

We have thus characterized a complex, unique regulatory and localization profile of Sig15 as an immunomodulator in the context of B-ALL (**Fig. 5**). As concluded in the previous sections, there remain several questions at large about the biology and function of Sig15 in both physiological and pathological contexts. Regarding differentially spliced Sig15 isoforms, the functionality and regulation of the non-coding Sig15-204 remains unknown despite its enriched expression and distribution across a wide variety of tissues. RNAi can be employed to induce trapping and degradation of the Sig15-204 RNA sequence through targeting of its intronic region upstream of Exon 5, allowing for specific targeting of Sig15-204 as compared to the other fully spliced and matured isoforms. Though B-ALL and lymphoma cells express detectable levels of this isoform, the largest expression is in normal leukocytes, which suggests the possibility of knocking down Sig15-204 in normal PBMCs alongside leukemia cells and performing unbiased proteomics to assess which proteins are affected by the ablation of this isoform. Expression levels of the other Sig15 isoforms may also be assessed in this context to observe any regulation Sig15-204 may have on the expression of other Sig15 isoforms.

More broadly, though T cells have demonstrated expression of this Sig15-204, it remains unclear which PBMC populations express Sig15-204, which could also provide suggestion to its function. Flow-based sorting or MACS column selection of the major PBMC populations, including T cells, B cells, monocytes, NK cells, and others, can be performed to isolate these populations, at which point qPCR analysis can be used to assess the expression of all Sig15 isoforms in these different populations. If samples can be obtained from both healthy donor and leukemia peripheral blood, this analysis could also extend to circulating leukemia cells, which could be used to correlate the different Sig15 isoforms with leukemia pathology in the primary setting by comparing expression to circulating normal B cells. This would be particularly useful across different leukemia genetic subtypes, which may hint at the differential regulation of these isoforms depending on the driving oncogenic pathway in these cells.

There are many interesting directions to proceed with investigation of the role of Sig15 in immunity. While we and our collaborators have previously attempted to use antibody inhibition of Sig15

in syngeneic murine and humanized mouse B-ALL models (data not shown), results have been inconsistent, suggesting the targeting of Sig15 in these diseases requires further investigation. This may in part be due to the tightly regulated surface localization of Sig15 in B-ALL, in which case understanding the dimerization capacity of Sig15 and how it may be enhanced using extracellular targeting constructs would be critical in therapeutic development. We are also in the process of developing a co-culture-based screening assay, using CRISPR knockout libraries on CAR-expressing Jurkats with NF-κB/NFAT GFP reporters and co-culturing with Sig15-expressing or deficient B-ALL cells to identify a putative T cell receptor for Sig15.

Aside from our demonstrations of broad immune profile changes within the bone marrow, another important investigation which remains is the study of how B-ALL-expressed Sig15 changes the interaction and activity of osteoblasts and osteoclasts in the bone marrow. IL-6, LIF, and IL-5 all have implicated roles in immunosuppression and leukemia, they are also very important factors in the interactions and function of osteoblasts and osteoclasts in the bone (208, 209). The contributions of these populations to the formation of the leukemia bone marrow niche are still emerging in the literature, but wide data support shows that they are capable of interacting with leukemia cells directly and through cytokine-mediated crosstalk which can promote B-ALL progression (133). Due to the importance of Sig15 in physiological osteoclast development and function, it is possible leukemia-expressed Sig15 may affect these populations and thus should be further explored.

The presence of sSig15 and nuclear Sig15 appear thus far to be unique to the pathological context, which could support a role for them as prognostic biomarkers alongside functional molecules. We are currently in the process of working with the Children's Oncology Group (COG) to begin correlating sSig15 levels with patient outcomes in pediatric B-ALL. As experiments inhibiting sSig15 from B-ALL cell line supernatant are inconsistent, we plan to perform these experiments using plasma from pediatric B-ALL patients instead, characterizing the effects of sSig15 inhibition on stimulated T cell activation in B-ALL plasma.

For nuclear Sig15, flow imaging could be used to efficiently characterize nuclear localization of Sig15 in B-ALL cell line models and primary patient samples. Better understanding of the nuclear Sig15 structure can also be performed using a nuclear extraction followed by an immunoprecipitation (with an antibody targeted to the extracellular domain of Sig15) to isolate nuclear Sig15 and send for mass spectrometry analysis. As a suspected NLS has been identified in our studies, site-directed mutagenesis of that motif in B-ALL and osteosarcoma cell lines is the next logical step. Pending confirmation of Sig15 exclusion from the nucleus, we will characterize any changes in cell proliferation, basal apoptosis, and lysis in co-culture assays with healthy PBMCs. We would also send these samples for RNA-seq analysis to assess in nuclear Sig15 directly affects gene expression in these diseases.

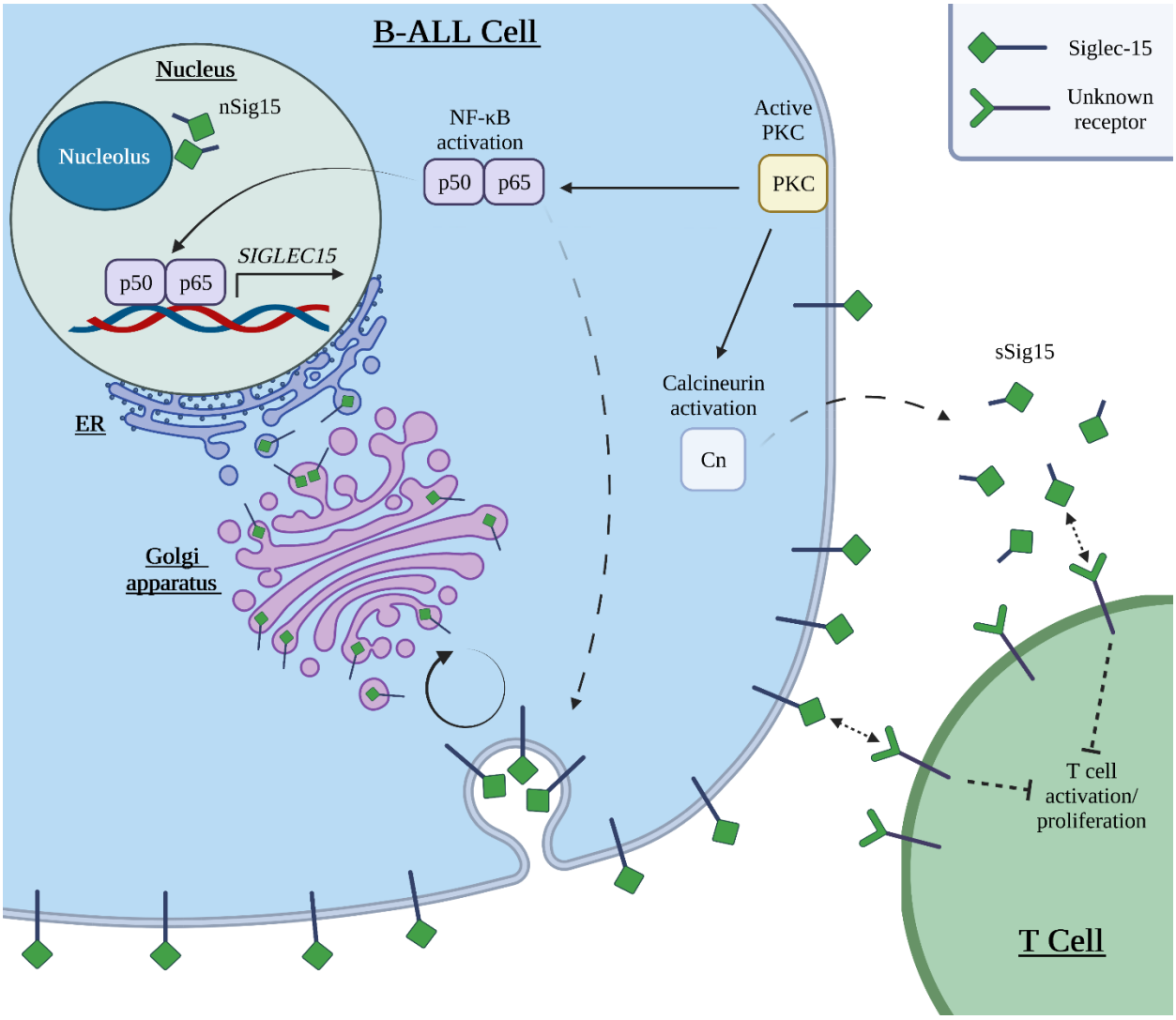

Figure 5. Model figure depicting the role of Sig15 in B-ALL-mediated immunosuppression. NF-κB activation downstream of PKC activation in B-ALL induces expression of Sig15, which is retained primarily in the Golgi apparatus and cycles rapidly to and from the membrane through the endosomal compartment unless otherwise stabilized at the membrane through NF-κB activation. Calcineurin activation regulates the release of a secreted/soluble form of Sig15 (sSig15) into the extracellular space, which, alongside surface-bound Sig15, is proposed to bind a yet-undiscovered receptor on T cells to attenuate T cell activation and proliferation during immune response. The extracellular domain of Sig15 is also demonstrated to localize to the nucleus in the perinucleolar compartment, where it may have function interacting with RNA-binding proteins.

References

1. Sung H, Ferlay J, Siegel RL, Laversanne M, Soerjomataram I, Jemal A, Bray F. Global Cancer Statistics 2020: GLOBOCAN Estimates of Incidence and Mortality Worldwide for 36 Cancers in 185 Countries. CA: a cancer journal for clinicians. 2021;71(3):209-49. doi: https://doi.org/10.3322/caac.21660.
2. SEER 22 2015–2019, All Races, Both Sexes: Surveillance Research Program, National Cancer Institute; [cited 2023]. Available from: https://seer.cancer.gov/statistics-network/explorer/.
3. Ferlay J LM, Ervik M, Lam F, Colombet M, Mery L, Piñeros M, Znaor A, Soerjomataram I, Bray F. Global Cancer Observatory: Cancer Tomorrow. Lyon, France: International Agency for Research on Cancer.; 2020 [cited 2023]. Available from: https://gco.iarc.fr/tomorrow.
4. Siegel RL, Miller KD, Wagle NS, Jemal A. Cancer statistics, 2023. CA: a cancer journal for clinicians. 2023;73(1):17-48. doi: https://doi.org/10.3322/caac.21763.
5. Key Statistics for Childhood Cancers: American Cancer Society; [cited 2023]. Available from: http://cancerstatisticscenter.cancer.org.
6. What Is Acute Lymphocytic Leukemia (ALL)? : American Cancer Society; [cited 2023]. Available from: https://www.cancer.org/cancer/acute-lymphocytic-leukemia/about/what-is-all.html.
7. Treating Acute Lymphocytic Leukemia (ALL): American Cancer Society; [cited 2023]. Available from: https://www.cancer.org/cancer/acute-lymphocytic-leukemia/treating.html.
8. Pui CH, Mullighan CG, Evans WE, Relling MV. Pediatric acute lymphoblastic leukemia: where are we going and how do we get there? Blood. 2012;120(6):1165-74. Epub 20120622. doi: 10.1182/blood-2012-05-378943. PubMed PMID: 22730540; PMCID: PMC3418713.
9. Borowitz MJ, Wood BL, Devidas M, Loh ML, Raetz EA, Salzer WL, Nachman JB, Carroll AJ, Heerema NA, Gastier-Foster JM, Willman CL, Dai Y, Winick NJ, Hunger SP, Carroll WL, Larsen E. Prognostic significance of minimal residual disease in high risk B-ALL: a report from Children's Oncology Group study AALL0232. Blood. 2015;126(8):964-71. doi: 10.1182/blood-2015-03-633685.
10. Key Statistics for Acute Lymphocytic Leukemia (ALL): American Cancer Society; [cited 2023]. Available from: https://www.cancer.org/cancer/acute-lymphocytic-leukemia/about/key-statistics.html.
11. National Vital Statistics System, Mortality 2018-2021. In: Prevention CfDCa, editor. CDC WONDER Online Database: National Center for Health Statistics; 2021.
12. Acute Lymphoblastic Leukemia (ALL): Leukemia & Lymphoma Society; [cited 2023]. Available from: https://www.lls.org/research/acute-lymphoblastic-leukemia-all.
13. Roberts KG, Mullighan CG. The Biology of B-Progenitor Acute Lymphoblastic Leukemia. Cold Spring Harb Perspect Med. 2020;10(7). Epub 20200701. doi: 10.1101/cshperspect.a034835. PubMed PMID: 31653664; PMCID: PMC7328455.
14. Schultz KR, Bowman WP, Slayton W, Aledo A, Devidas M, Sather H, Borowitz MJ, Davies SM, Trigg M, Pasut B, Jorstad D, Eslinger T, Burden LE, Wang C, Rutledge R, Gaynon PS, Carroll AJ, Heerema NA, Winick N, Hunger S, Carroll WL, Camitta B. Improved Early Event Free Survival (EFS) in Children with Philadelphia Chromosome-Positive (Ph+) Acute Lymphoblastic Leukemia (ALL) with Intensive Imatinib in Combination with High Dose Chemotherapy: Children's Oncology Group (COG) Study AALL0031. Blood. 2007;110(11):4. doi: https://doi.org/10.1182/blood.V110.11.4.4.
15. Terwilliger T, Abdul-Hay M. Acute lymphoblastic leukemia: a comprehensive review and 2017 update. Blood Cancer Journal. 2017;7(6):e577-e. doi: 10.1038/bcj.2017.53.
16. Chessells JM, Veys P, Kempski H, Henley P, Leiper A, Webb D, Hann IM. Long-term follow-up of relapsed childhood acute lymphoblastic leukaemia. British Journal of Haematology. 2003;123(3):396-405. doi: 10.1046/j.1365-2141.2003.04584.x.
17. Hunger SP, Raetz E. How I Treat Relapsed Acute Lymphoblastic Leukemia in the Pediatric Population. Blood. 2020. Epub 2020/06/27. doi: 10.1182/blood.2019004043. PubMed PMID: 32589723.
18. Grupp SA, Maude SL, Shaw PA, Aplenc R, Barrett DM, Callahan C, Lacey SF, Levine BL, Melenhorst JJ, Motley L. Durable remissions in children with relapsed/refractory ALL treated with T cells engineered with a CD19-targeted chimeric antigen receptor (CTL019). Am Soc Hematology; 2015.

19. Locatelli F, Zugmaier G, Mergen N, Bader P, Jeha S, Schlegel PG, Bourquin JP, Handgretinger R, Brethon B, Rössig C, Kormany WN, Viswagnachar P, Chen-Santel C. Blinatumomab in pediatric relapsed/refractory B-cell acute lymphoblastic leukemia: RIALTO expanded access study final analysis. Blood Adv. 2022;6(3):1004-14. doi: 10.1182/bloodadvances.2021005579. PubMed PMID: 34979020; PMCID: PMC8945309.
20. O'Brien MM, Ji L, Shah NN, Rheingold SR, Bhojwani D, Yuan CM, Xu X, Yi JS, Harris AC, Brown PA, Borowitz MJ, Militano O, Kairalla J, Devidas M, Raetz EA, Gore L, Loh ML. Phase II Trial of Inotuzumab Ozogamicin in Children and Adolescents With Relapsed or Refractory B-Cell Acute Lymphoblastic Leukemia: Children's Oncology Group Protocol AALL1621. Journal of Clinical Oncology. 2022;40(9):956-67. doi: 10.1200/jco.21.01693. PubMed PMID: 35007127.
21. Kim SK, Cho SW. The Evasion Mechanisms of Cancer Immunity and Drug Intervention in the Tumor Microenvironment. Front Pharmacol. 2022;13:868695. Epub 20220524. doi: 10.3389/fphar.2022.868695. PubMed PMID: 35685630; PMCID: PMC9171538.
22. Coulie PG, Van den Eynde BJ, van der Bruggen P, Boon T. Tumour antigens recognized by T lymphocytes: at the core of cancer immunotherapy. Nat Rev Cancer. 2014;14(2):135-46. doi: 10.1038/nrc3670. PubMed PMID: 24457417.
23. Taylor BC, Balko JM. Mechanisms of MHC-I Downregulation and Role in Immunotherapy Response. Front Immunol. 2022;13:844866. Epub 20220228. doi: 10.3389/fimmu.2022.844866. PubMed PMID: 35296095; PMCID: PMC8920040.
24. Garris CS, Arlauckas SP, Kohler RH, Trefny MP, Garren S, Piot C, Engblom C, Pfirschke C, Siwicki M, Gungabeesoon J, Freeman GJ, Warren SE, Ong S, Browning E, Twitty CG, Pierce RH, Le MH, Algazi AP, Daud AI, Pai SI, Zippelius A, Weissleder R, Pittet MJ. Successful Anti-PD-1 Cancer Immunotherapy Requires T Cell-Dendritic Cell Crosstalk Involving the Cytokines IFN-γ and IL-12. Immunity. 2018;49(6):1148-61.e7. doi: 10.1016/j.immuni.2018.09.024.
25. Herbst RS, Giaccone G, de Marinis F, Reinmuth N, Vergnenegre A, Barrios CH, Morise M, Felip E, Andric Z, Geater S, Özgüroğlu M, Zou W, Sandler A, Enquist I, Komatsubara K, Deng Y, Kuriki H, Wen X, McCleland M, Mocci S, Jassem J, Spigel DR. Atezolizumab for First-Line Treatment of PD-L1–Selected Patients with NSCLC. New England Journal of Medicine. 2020;383(14):1328-39. doi: 10.1056/NEJMoa1917346. PubMed PMID: 32997907.
26. Schmid P, Cortes J, Dent R, Pusztai L, McArthur H, Kümmel S, Bergh J, Denkert C, Park YH, Hui R, Harbeck N, Takahashi M, Untch M, Fasching PA, Cardoso F, Andersen J, Patt D, Danso M, Ferreira M, Mouret-Reynier M-A, Im S-A, Ahn J-H, Gion M, Baron-Hay S, Boileau J-F, Ding Y, Tryfonidis K, Aktan G, Karantza V, O'Shaughnessy J. Event-free Survival with Pembrolizumab in Early Triple-Negative Breast Cancer. New England Journal of Medicine. 2022;386(6):556-67. doi: 10.1056/NEJMoa2112651. PubMed PMID: 35139274.
27. Fishman M, Dutcher JP, Clark JI, Alva A, Miletello GP, Curti B, Agarwal N, Hauke R, Mahoney KM, Moon H, Treisman J, Tykodi SS, Daniels G, Morse MA, Wong MKK, Kaufman H, Gregory N, McDermott DF. Overall survival by clinical risk category for high dose interleukin-2 (HD IL-2) treated patients with metastatic renal cell cancer (mRCC): data from the PROCLAIM^{SM} registry. Journal for ImmunoTherapy of Cancer. 2019;7(1):84. doi: 10.1186/s40425-019-0567-3.
28. Brouwer RE, van der Heiden P, Schreuder GM, Mulder A, Datema G, Anholts JD, Willemze R, Claas FH, Falkenburg JH. Loss or downregulation of HLA class I expression at the allelic level in acute leukemia is infrequent but functionally relevant, and can be restored by interferon. Hum Immunol. 2002;63(3):200-10. doi: 10.1016/s0198-8859(01)00381-0. PubMed PMID: 11872238.
29. Romanski A, Bug G, Becker S, Kampfmann M, Seifried E, Hoelzer D, Ottmann OG, Tonn T. Mechanisms of resistance to natural killer cell-mediated cytotoxicity in acute lymphoblastic leukemia. Exp Hematol. 2005;33(3):344-52. doi: 10.1016/j.exphem.2004.11.006. PubMed PMID: 15730858.
30. Rouce RH, Shaim H, Sekine T, Weber G, Ballard B, Ku S, Barese C, Murali V, Wu MF, Liu H, Shpall EJ, Bollard CM, Rabin KR, Rezvani K. The TGF-β/SMAD pathway is an important mechanism for NK cell immune evasion in childhood B-acute lymphoblastic leukemia. Leukemia. 2016;30(4):800-11. Epub 20151201. doi: 10.1038/leu.2015.327. PubMed PMID: 26621337; PMCID: PMC4823160.

31. Biernacki MA, Bleakley M. Neoantigens in Hematologic Malignancies. Front Immunol. 2020;11:121. Epub 20200214. doi: 10.3389/fimmu.2020.00121. PubMed PMID: 32117272; PMCID: PMC7033457.
32. Chao MP, Alizadeh AA, Tang C, Jan M, Weissman-Tsukamoto R, Zhao F, Park CY, Weissman IL, Majeti R. Therapeutic Antibody Targeting of CD47 Eliminates Human Acute Lymphoblastic Leukemia. Cancer Research. 2011;71(4):1374-84. doi: 10.1158/0008-5472.Can-10-2238.
33. Köhnke T, Krupka C, Tischer J, Knösel T, Subklewe M. Increase of PD-L1 expressing B-precursor ALL cells in a patient resistant to the CD19/CD3-bispecific T cell engager antibody blinatumomab. J Hematol Oncol. 2015;8:111. Epub 20151008. doi: 10.1186/s13045-015-0213-6. PubMed PMID: 26449653; PMCID: PMC4599591.
34. Lee M, Hamilton JAG, Talekar GR, Ross AJ, Michael L, Rupji M, Dwivedi B, Raikar SS, Boss J, Scharer CD, Graham DK, DeRyckere D, Porter CC, Henry CJ. Obesity-induced galectin-9 is a therapeutic target in B-cell acute lymphoblastic leukemia. Nat Commun. 2022;13(1):1157. Epub 20220303. doi: 10.1038/s41467-022-28839-y. PubMed PMID: 35241678; PMCID: PMC8894417.
35. Valencia J, L MF-S, Fraile-Ramos A, Sacedón R, Jiménez E, Vicente A, Varas A. Acute Lymphoblastic Leukaemia Cells Impair Dendritic Cell and Macrophage Differentiation: Role of BMP4. Cells. 2019;8(7). Epub 20190714. doi: 10.3390/cells8070722. PubMed PMID: 31337120; PMCID: PMC6679123.
36. Witkowski MT, Dolgalev I, Evensen NA, Ma C, Chambers T, Roberts KG, Sreeram S, Dai Y, Tikhonova AN, Lasry A, Qu C, Pei D, Cheng C, Robbins GA, Pierro J, Selvaraj S, Mezzano V, Daves M, Lupo PJ, Scheurer ME, Loomis CA, Mullighan CG, Chen W, Rabin KR, Tsirigos A, Carroll WL, Aifantis I. Extensive Remodeling of the Immune Microenvironment in B Cell Acute Lymphoblastic Leukemia. Cancer cell. 2020;37(6):867-82.e12. doi: 10.1016/j.ccell.2020.04.015.
37. Escobar G, Barbarossa L, Barbiera G, Norelli M, Genua M, Ranghetti A, Plati T, Camisa B, Brombin C, Cittaro D, Annoni A, Bondanza A, Ostuni R, Gentner B, Naldini L. Interferon gene therapy reprograms the leukemia microenvironment inducing protective immunity to multiple tumor antigens. Nat Commun. 2018;9(1):2896. Epub 20180724. doi: 10.1038/s41467-018-05315-0. PubMed PMID: 30042420; PMCID: PMC6057972.
38. Niedźwiecki M, Budziło O, Adamkiewicz-Drożyńska E, Pawlik-Gwozdecka D, Zieliński M, Maciejka-Kembłowska L, Szczepański T, Trzonkowski P. CD4(+)CD25(high)CD127(low/-)FoxP(3) (+) Regulatory T-Cell Population in Acute Leukemias: A Review of the Literature. J Immunol Res. 2019;2019:2816498. Epub 20190303. doi: 10.1155/2019/2816498. PubMed PMID: 30944830; PMCID: PMC6421759.
39. An F, Wang H, Liu Z, Wu F, Zhang J, Tao Q, Li Y, Shen Y, Ruan Y, Zhang Q, Pan Y, Zhu W, Qin H, Wang Y, Fu Y, Feng Z, Zhai Z. Influence of patient characteristics on chimeric antigen receptor T cell therapy in B-cell acute lymphoblastic leukemia. Nat Commun. 2020;11(1):5928. Epub 20201123. doi: 10.1038/s41467-020-19774-x. PubMed PMID: 33230103; PMCID: PMC7683530.
40. Duell J, Dittrich M, Bedke T, Mueller T, Eisele F, Rosenwald A, Rasche L, Hartmann E, Dandekar T, Einsele H, Topp MS. Frequency of regulatory T cells determines the outcome of the T-cell-engaging antibody blinatumomab in patients with B-precursor ALL. Leukemia. 2017;31(10):2181-90. Epub 20170125. doi: 10.1038/leu.2017.41. PubMed PMID: 28119525; PMCID: PMC5629361.
41. Blaeschke F, Willier S, Stenger D, Lepenies M, Horstmann MA, Escherich G, Zimmermann M, Rojas Ringeling F, Canzar S, Kaeuferle T, Rohlfs M, Binder V, Klein C, Feuchtinger T. Leukemia-induced dysfunctional TIM-3(+)CD4(+) bone marrow T cells increase risk of relapse in pediatric B-precursor ALL patients. Leukemia. 2020;34(10):2607-20. Epub 20200313. doi: 10.1038/s41375-020-0793-1. PubMed PMID: 32203137.
42. Qin H, Ishii K, Nguyen S, Su PP, Burk CR, Kim BH, Duncan BB, Tarun S, Shah NN, Kohler ME, Fry TJ. Murine pre-B-cell ALL induces T-cell dysfunction not fully reversed by introduction of a chimeric antigen receptor. Blood. 2018;132(18):1899-910. Epub 20180912. doi: 10.1182/blood-2017-12-815548. PubMed PMID: 30209120; PMCID: PMC6213322.

43. Zhang X, Zhang H, Chen L, Feng Z, Gao L, Li Q. TIGIT expression is upregulated in T cells and causes T cell dysfunction independent of PD-1 and Tim-3 in adult B lineage acute lymphoblastic leukemia. Cell Immunol. 2019;344:103958. Epub 20190724. doi: 10.1016/j.cellimm.2019.103958. PubMed PMID: 31376919.
44. Cassaday RD, Garcia KA, Fromm JR, Percival MM, Turtle CJ, Nghiem PT, Stevenson PA, Estey EH. Phase 2 study of pembrolizumab for measurable residual disease in adults with acute lymphoblastic leukemia. Blood Adv. 2020;4(14):3239-45. doi: 10.1182/bloodadvances.2020002403. PubMed PMID: 32692850; PMCID: PMC7391137.
45. Wang X, Chen Y, Li Z, Huang B, Xu L, Lai J, Lu Y, Zha X, Liu B, Lan Y, Li Y. Single-Cell RNA-Seq of T Cells in B-ALL Patients Reveals an Exhausted Subset with Remarkable Heterogeneity. Advanced Science. 2021;8(19):2101447. doi: https://doi.org/10.1002/advs.202101447.
46. Rabe JL, Gardner L, Hunter R, Fonseca JA, Dougan J, Gearheart CM, Leibowitz MS, Lee-Miller C, Baturin D, Fosmire SP, Zelasko SE, Jones CL, Slansky JE, Rupji M, Dwivedi B, Henry CJ, Porter CC. IL-12 abrogates calcineurin-dependent immune evasion during leukemia progression. Cancer Research. 2019:canres.3800.2018. doi: 10.1158/0008-5472.CAN-18-3800.
47. Hunter R, Imbach KJ, Zhou C, Dougan J, Hamilton JAG, Chen KZ, Do P, Townsel A, Gibson G, Dreaden EC, Waller EK, Haynes KA, Henry CJ, Porter CC. B-cell acute lymphoblastic leukemia promotes an immune suppressive microenvironment that can be overcome by IL-12. Sci Rep. 2022;12(1):11870. Epub 2022/07/14. doi: 10.1038/s41598-022-16152-z. PubMed PMID: 35831470; PMCID: PMC9279427.
48. Medyouf H, Alcalde H, Berthier C, Guillemin MC, dos Santos NR, Janin A, Decaudin D, de Thé H, Ghysdael J. Targeting calcineurin activation as a therapeutic strategy for T-cell acute lymphoblastic leukemia. Nature Medicine. 2007;13:736. doi: 10.1038/nm1588

https://www.nature.com/articles/nm1588#supplementary-information.
49. Gachet S, Genescà E, Passaro D, Irigoyen M, Alcalde H, Clémenson C, Poglio S, Pflumio F, Janin A, Lasgi C, Dodier S, Soyer M, Duménil G, Ghysdael J. Leukemia-initiating cell activity requires calcineurin in T-cell acute lymphoblastic leukemia. Leukemia. 2013;27:2289. doi: 10.1038/leu.2013.156

https://www.nature.com/articles/leu2013156#supplementary-information.
50. Musson REA, Cobbaert CM, Smit NPM. Molecular Diagnostics of Calcineurin-Related Pathologies. Clinical Chemistry. 2012;58(3):511. doi: 10.1373/clinchem.2011.167296.
51. Rabe J, Gardner LA, Hunter R, Fonseca JA, Dougan J, Gearheart CM, Fonseca J, Liebowitz MS, Lee-Miller CA, Baturin D, Fosmire SP, Zelasko S, Jones CL, Slansky JE, Rupji M, Dwivedi B, Henry CJ, CC. P. IL-12 abrogates calcineurin-dependent immune evasion during leukemia progression. Cancer Research. 2019.
52. Angata T, Brinkman-Van der Linden ECM. I-type lectins. Biochimica et Biophysica Acta (BBA) - General Subjects. 2002;1572(2):294-316. doi: https://doi.org/10.1016/S0304-4165(02)00316-1.
53. Crocker PR, Paulson JC, Varki A. Siglecs and their roles in the immune system. Nat Rev Immunol. 2007;7(4):255-66. doi: 10.1038/nri2056. PubMed PMID: 17380156.
54. Cummings RD, Chiffoleau E, van Kyook Y, McEver RP. C-Type Lectins. In: Varki A, Cummings RD, Esko JD, Stanley P, Hart GW, Aebi M, Mohnen D, Kinoshita T, Packer NH, Prestegard JH, Schnaar RL, Seeberger PH, editors. Essentials of Glycobiology. Cold Spring Harbor (NY): Cold Spring Harbor Laboratory Press

55. Pearce OMT, Läubli H. Sialic acids in cancer biology and immunity. Glycobiology. 2015;26(2):111-28. doi: 10.1093/glycob/cwv097.
56. Varki A. Since there are PAMPs and DAMPs, there must be SAMPs? Glycan “self-associated molecular patterns” dampen innate immunity, but pathogens can mimic them. Glycobiology. 2011;21(9):1121-4. doi: 10.1093/glycob/cwr087. PubMed PMID: 21932452; PMCID: PMC3150115.

57. Vimr ER, Kalivoda KA, Deszo EL, Steenbergen SM. Diversity of microbial sialic acid metabolism. Microbiol Mol Biol Rev. 2004;68(1):132-53. doi: 10.1128/mmbr.68.1.132-153.2004. PubMed PMID: 15007099; PMCID: PMC362108.
58. Lewis AL, Chen X, Schnaar RL, Varki A. Sialic Acids and Other Nonulosonic Acids. In: Varki A, Cummings RD, Esko JD, Stanley P, Hart GW, Aebi M, Mohnen D, Kinoshita T, Packer NH, Prestegard JH, Schnaar RL, Seeberger PH, editors. Essentials of Glycobiology. Cold Spring Harbor (NY): Cold Spring Harbor Laboratory Press

59. Rodrigues E, Macauley MS. Hypersialylation in Cancer: Modulation of Inflammation and Therapeutic Opportunities. Cancers (Basel). 2018;10(6). Epub 20180618. doi: 10.3390/cancers10060207. PubMed PMID: 29912148; PMCID: PMC6025361.
60. Li F, Ding J. Sialylation is involved in cell fate decision during development, reprogramming and cancer progression. Protein Cell. 2019;10(8):550-65. Epub 20181126. doi: 10.1007/s13238-018-0597-5. PubMed PMID: 30478534; PMCID: PMC6626595.
61. Durocher JR, Payne RC, Conrad ME. Role of sialic acid in erythrocyte survival. Blood. 1975;45(1):11-20. PubMed PMID: 803103.
62. Lizcano A, Secundino I, Döhrmann S, Corriden R, Rohena C, Diaz S, Ghosh P, Deng L, Nizet V, Varki A. Erythrocyte sialoglycoproteins engage Siglec-9 on neutrophils to suppress activation. Blood. 2017;129(23):3100-10. Epub 20170417. doi: 10.1182/blood-2016-11-751636. PubMed PMID: 28416510; PMCID: PMC5465837.
63. Hadengue AL, Del-Pino M, Simon A, Levenson J. Erythrocyte Disaggregation Shear Stress, Sialic Acid, and Cell Aging in Humans. Hypertension. 1998;32(2):324-30. doi: doi:10.1161/01.HYP.32.2.324.
64. Munkley J, Scott E. Targeting Aberrant Sialylation to Treat Cancer. Medicines (Basel). 2019;6(4). Epub 20191013. doi: 10.3390/medicines6040102. PubMed PMID: 31614918; PMCID: PMC6963943.
65. Angata T. Molecular diversity and evolution of the Siglec family of cell-surface lectins. Molecular Diversity. 2006;10(4):555-66. doi: 10.1007/s11030-006-9029-1.
66. Varki A, Angata T. Siglecs—the major subfamily of I-type lectins. Glycobiology. 2005;16(1):1R-27R. doi: 10.1093/glycob/cwj008.
67. Altheide TK, Hayakawa T, Mikkelsen TS, Diaz S, Varki N, Varki A. System-wide genomic and biochemical comparisons of sialic acid biology among primates and rodents: Evidence for two modes of rapid evolution. J Biol Chem. 2006;281(35):25689-702. Epub 20060612. doi: 10.1074/jbc.M604221200. PubMed PMID: 16769723.
68. Taylor VC, Buckley CD, Douglas M, Cody AJ, Simmons DL, Freeman SD. The myeloid-specific sialic acid-binding receptor, CD33, associates with the protein-tyrosine phosphatases, SHP-1 and SHP-2. J Biol Chem. 1999;274(17):11505-12. doi: 10.1074/jbc.274.17.11505. PubMed PMID: 10206955.
69. Bornhöfft KF, Goldammer T, Rebl A, Galuska SP. Siglecs: A journey through the evolution of sialic acid-binding immunoglobulin-type lectins. Developmental & Comparative Immunology. 2018;86:219-31. doi: https://doi.org/10.1016/j.dci.2018.05.008.
70. Angata T, Hayakawa T, Yamanaka M, Varki A, Nakamura M. Discovery of Siglec-14, a novel sialic acid receptor undergoing concerted evolution with Siglec-5 in primates. Faseb j. 2006;20(12):1964-73. doi: 10.1096/fj.06-5800com. PubMed PMID: 17012248.
71. Cao H, Lakner U, de Bono B, Traherne JA, Trowsdale J, Barrow AD. SIGLEC16 encodes a DAP12-associated receptor expressed in macrophages that evolved from its inhibitory counterpart SIGLEC11 and has functional and non-functional alleles in humans. Eur J Immunol. 2008;38(8):2303-15. doi: 10.1002/eji.200738078. PubMed PMID: 18629938.
72. Veninga H, Borg EGF, Vreeman K, Taylor PR, Kalay H, van Kooyk Y, Kraal G, Martinez-Pomares L, den Haan JMM. Antigen targeting reveals splenic CD169+ macrophages as promoters of

germinal center B-cell responses. European Journal of Immunology. 2015;45(3):747-57. doi: https://doi.org/10.1002/eji.201444983.
73. Ohnishi K, Komohara Y, Saito Y, Miyamoto Y, Watanabe M, Baba H, Takeya M. CD169-positive macrophages in regional lymph nodes are associated with a favorable prognosis in patients with colorectal carcinoma. Cancer Sci. 2013;104(9):1237-44. Epub 20130709. doi: 10.1111/cas.12212. PubMed PMID: 23734742; PMCID: PMC7657174.
74. Kumamoto K, Tasaki T, Ohnishi K, Shibata M, Shimajiri S, Harada M, Komohara Y, Nakayama T. CD169 Expression on Lymph Node Macrophages Predicts in Patients With Gastric Cancer. Front Oncol. 2021;11:636751. Epub 20210319. doi: 10.3389/fonc.2021.636751. PubMed PMID: 33816277; PMCID: PMC8017296.
75. Saito Y, Ohnishi K, Miyashita A, Nakahara S, Fujiwara Y, Horlad H, Motoshima T, Fukushima S, Jinnin M, Ihn H, Takeya M, Komohara Y. Prognostic Significance of CD169+ Lymph Node Sinus Macrophages in Patients with Malignant Melanoma. Cancer Immunol Res. 2015;3(12):1356-63. Epub 20150821. doi: 10.1158/2326-6066.Cir-14-0180. PubMed PMID: 26297710.
76. van Dinther D, Veninga H, Iborra S, Borg EG, Hoogterp L, Olesek K, Beijer MR, Schetters ST, Kalay H, Garcia-Vallejo JJ. Functional CD169 on macrophages mediates interaction with dendritic cells for CD8+ T cell cross-priming. Cell reports. 2018;22(6):1484-95.
77. Swanson BJ, McDermott KM, Singh PK, Eggers JP, Crocker PR, Hollingsworth MA. MUC1 is a counter-receptor for myelin-associated glycoprotein (Siglec-4a) and their interaction contributes to adhesion in pancreatic cancer perineural invasion. Cancer Res. 2007;67(21):10222-9. doi: 10.1158/0008-5472.Can-06-2483. PubMed PMID: 17974963.
78. Stanczak MA, Siddiqui SS, Trefny MP, Thommen DS, Boligan KF, von Gunten S, Tzankov A, Tietze L, Lardinois D, Heinzelmann-Schwarz V, von Bergwelt-Baildon M, Zhang W, Lenz HJ, Han Y, Amos CI, Syedbasha M, Egli A, Stenner F, Speiser DE, Varki A, Zippelius A, Läubli H. Self-associated molecular patterns mediate cancer immune evasion by engaging Siglecs on T cells. The Journal of clinical investigation. 2018;128(11):4912-23. Epub 20180924. doi: 10.1172/jci120612. PubMed PMID: 30130255; PMCID: PMC6205408.
79. Vuchkovska A, Glanville DG, Scurti GM, Nishimura MI, White P, Ulijasz AT, Iwashima M. Siglec-5 is an inhibitory immune checkpoint molecule for human T cells. Immunology. 2022;166(2):238-48. Epub 20220401. doi: 10.1111/imm.13470. PubMed PMID: 35290663.
80. Pepin M, Mezouar S, Pegon J, Muczynski V, Adam F, Bianchini EP, Bazaa A, Proulle V, Rupin A, Paysant J, Panicot-Dubois L, Christophe OD, Dubois C, Lenting PJ, Denis CV. Soluble Siglec-5 associates to PSGL-1 and displays anti-inflammatory activity. Sci Rep. 2016;6:37953. Epub 20161128. doi: 10.1038/srep37953. PubMed PMID: 27892504; PMCID: PMC5125011.
81. Zhang JQ, Nicoll G, Jones C, Crocker PR. Siglec-9, a Novel Sialic Acid Binding Member of the Immunoglobulin Superfamily Expressed Broadly on Human Blood Leukocytes *. Journal of Biological Chemistry. 2000;275(29):22121-6. doi: 10.1074/jbc.M002788200.
82. Jandus C, Boligan KF, Chijioke O, Liu H, Dahlhaus M, Démoulins T, Schneider C, Wehrli M, Hunger RE, Baerlocher GM, Simon H-U, Romero P, Münz C, von Gunten S. Interactions between Siglec-7/9 receptors and ligands influence NK cell–dependent tumor immunosurveillance. The Journal of clinical investigation. 2014;124(4):1810-20. doi: 10.1172/JCI65899.
83. Tao L, Wang S, Yang L, Jiang L, Li J, Wang X. Reduced Siglec-7 expression on NK cells predicts NK cell dysfunction in primary hepatocellular carcinoma. Clin Exp Immunol. 2020;201(2):161-70. Epub 20200517. doi: 10.1111/cei.13444. PubMed PMID: 32319079; PMCID: PMC7366747.
84. Brunetta E, Fogli M, Varchetta S, Bozzo L, Hudspeth KL, Marcenaro E, Moretta A, Mavilio D. The decreased expression of Siglec-7 represents an early marker of dysfunctional natural killer–cell subsets associated with high levels of HIV-1 viremia. Blood. 2009;114(18):3822-30. doi: 10.1182/blood-2009-06-226332.
85. Läubli H, Pearce OM, Schwarz F, Siddiqui SS, Deng L, Stanczak MA, Deng L, Verhagen A, Secrest P, Lusk C, Schwartz AG, Varki NM, Bui JD, Varki A. Engagement of myelomonocytic Siglecs by tumor-associated ligands modulates the innate immune response to cancer. Proc Natl Acad Sci U S A.

2014;111(39):14211-6. Epub 20140915. doi: 10.1073/pnas.1409580111. PubMed PMID: 25225409; PMCID: PMC4191788.
86. Rodriguez E, Boelaars K, Brown K, Eveline Li RJ, Kruijssen L, Bruijns SCM, van Ee T, Schetters STT, Crommentuijn MHW, van der Horst JC, van Grieken NCT, van Vliet SJ, Kazemier G, Giovannetti E, Garcia-Vallejo JJ, van Kooyk Y. Sialic acids in pancreatic cancer cells drive tumour-associated macrophage differentiation via the Siglec receptors Siglec-7 and Siglec-9. Nat Commun. 2021;12(1):1270. Epub 20210224. doi: 10.1038/s41467-021-21550-4. PubMed PMID: 33627655; PMCID: PMC7904912.
87. Haas Q, Boligan KF, Jandus C, Schneider C, Simillion C, Stanczak MA, Haubitz M, Seyed Jafari SM, Zippelius A, Baerlocher GM, Läubli H, Hunger RE, Romero P, Simon HU, von Gunten S. Siglec-9 Regulates an Effector Memory CD8(+) T-cell Subset That Congregates in the Melanoma Tumor Microenvironment. Cancer Immunol Res. 2019;7(5):707-18. Epub 20190415. doi: 10.1158/2326-6066.Cir-18-0505. PubMed PMID: 30988027.
88. Ibarlucea-Benitez I, Weitzenfeld P, Smith P, Ravetch JV. Siglecs-7/9 function as inhibitory immune checkpoints in vivo and can be targeted to enhance therapeutic antitumor immunity. Proceedings of the National Academy of Sciences. 2021;118(26):e2107424118. doi: doi:10.1073/pnas.2107424118.
89. Wu Y, Huang W, Xie Y, Wang C, Luo N, Chen Y, Wang L, Cheng Z, Gao Z, Liu S. Siglec-9, a Putative Immune Checkpoint Marker for Cancer Progression Across Multiple Cancer Types. Front Mol Biosci. 2022;9:743515. Epub 20220317. doi: 10.3389/fmolb.2022.743515. PubMed PMID: 35372497; PMCID: PMC8968865.
90. Li N, Zhang W, Wan T, Zhang J, Chen T, Yu Y, Wang J, Cao X. Cloning and Characterization of Siglec-10, a Novel Sialic Acid Binding Member of the Ig Superfamily, from Human Dendritic Cells *. Journal of Biological Chemistry. 2001;276(30):28106-12. doi: 10.1074/jbc.M100467200.
91. Chen G-Y, Tang J, Zheng P, Liu Y. CD24 and Siglec-10 Selectively Repress Tissue Damage–Induced Immune Responses. Science. 2009;323(5922):1722-5. doi: doi:10.1126/science.1168988.
92. Barkal AA, Brewer RE, Markovic M, Kowarsky M, Barkal SA, Zaro BW, Krishnan V, Hatakeyama J, Dorigo O, Barkal LJ, Weissman IL. CD24 signalling through macrophage Siglec-10 is a target for cancer immunotherapy. Nature. 2019;572(7769):392-6. Epub 20190731. doi: 10.1038/s41586-019-1456-0. PubMed PMID: 31367043; PMCID: PMC6697206.
93. Bandala-Sanchez E, N GB, Goddard-Borger ED, Ngui K, Naselli G, Stone NL, Neale AM, Pearce LA, Wardak A, Czabotar P, Haselhorst T, Maggioni A, Hartley-Tassell LA, Adams TE, Harrison LC. CD52 glycan binds the proinflammatory B box of HMGB1 to engage the Siglec-10 receptor and suppress human T cell function. Proc Natl Acad Sci U S A. 2018;115(30):7783-8. Epub 20180711. doi: 10.1073/pnas.1722056115. PubMed PMID: 29997173; PMCID: PMC6065011.
94. Rashidi M, Bandala-Sanchez E, Lawlor KE, Zhang Y, Neale AM, Vijayaraj SL, O'Donoghue R, Wentworth JM, Adams TE, Vince JE, Harrison LC. CD52 inhibits Toll-like receptor activation of NF-κB and triggers apoptosis to suppress inflammation. Cell Death Differ. 2018;25(2):392-405. Epub 20171215. doi: 10.1038/cdd.2017.173. PubMed PMID: 29244050; PMCID: PMC5762852.
95. Thiesler H, Gretenkort L, Hoffmeister L, Albers I, Ohlmeier L, Röckle I, Verhagen A, Banan R, Köpcke N, Krönke N, Feuerhake F, Behling F, Barrantes-Freer A, Mielke D, Rohde V, Hong B, Varki A, Schwabe K, Krauss JK, Stadelmann C, Hartmann C, Hildebrandt H. Proinflammatory macrophage activation by the polysialic acid-Siglec-16 axis is linked to increased survival of glioblastoma patients. Clinical Cancer Research. 2023. doi: 10.1158/1078-0432.Ccr-22-1488.
96. Jellusova J, Nitschke L. Regulation of B cell functions by the sialic acid-binding receptors siglec-G and CD22. Front Immunol. 2011;2:96. Epub 20120111. doi: 10.3389/fimmu.2011.00096. PubMed PMID: 22566885; PMCID: PMC3342095.
97. Poe JC, Fujimoto Y, Hasegawa M, Haas KM, Miller AS, Sanford IG, Bock CB, Fujimoto M, Tedder TF. CD22 regulates B lymphocyte function in vivo through both ligand-dependent and ligand-independent mechanisms. Nat Immunol. 2004;5(10):1078-87. Epub 20040919. doi: 10.1038/ni1121. PubMed PMID: 15378059.

98. Lanza F, Maffini E, Rondoni M, Massari E, Faini AC, Malavasi F. CD22 Expression in B-Cell Acute Lymphoblastic Leukemia: Biological Significance and Implications for Inotuzumab Therapy in Adults. Cancers (Basel). 2020;12(2). Epub 20200128. doi: 10.3390/cancers12020303. PubMed PMID: 32012891; PMCID: PMC7072635.
99. Micallef IN, Maurer MJ, Wiseman GA, Nikcevich DA, Kurtin PJ, Cannon MW, Perez DG, Soori GS, Link BK, Habermann TM, Witzig TE. Epratuzumab with rituximab, cyclophosphamide, doxorubicin, vincristine, and prednisone chemotherapy in patients with previously untreated diffuse large B-cell lymphoma. Blood. 2011;118(15):4053-61. Epub 20110614. doi: 10.1182/blood-2011-02-336990. PubMed PMID: 21673350; PMCID: PMC3204728.
100. Leonard JP, Schuster SJ, Emmanouilides C, Couture F, Teoh N, Wegener WA, Coleman M, Goldenberg DM. Durable complete responses from therapy with combined epratuzumab and rituximab: final results from an international multicenter, phase 2 study in recurrent, indolent, non-Hodgkin lymphoma. Cancer. 2008;113(10):2714-23. doi: 10.1002/cncr.23890. PubMed PMID: 18853418.
101. Shor B, Gerber HP, Sapra P. Preclinical and clinical development of inotuzumab-ozogamicin in hematological malignancies. Mol Immunol. 2015;67(2 Pt A):107-16. Epub 20141007. doi: 10.1016/j.molimm.2014.09.014. PubMed PMID: 25304309.
102. Sterner RC, Sterner RM. CAR-T cell therapy: current limitations and potential strategies. Blood Cancer Journal. 2021;11(4):69. doi: 10.1038/s41408-021-00459-7.
103. Shah NN, Stevenson MS, Yuan CM, Richards K, Delbrook C, Kreitman RJ, Pastan I, Wayne AS. Characterization of CD22 expression in acute lymphoblastic leukemia. Pediatr Blood Cancer. 2015;62(6):964-9. Epub 20150301. doi: 10.1002/pbc.25410. PubMed PMID: 25728039; PMCID: PMC4405453.
104. Fry TJ, Shah NN, Orentas RJ, Stetler-Stevenson M, Yuan CM, Ramakrishna S, Wolters P, Martin S, Delbrook C, Yates B, Shalabi H, Fountaine TJ, Shern JF, Majzner RG, Stroncek DF, Sabatino M, Feng Y, Dimitrov DS, Zhang L, Nguyen S, Qin H, Dropulic B, Lee DW, Mackall CL. CD22-targeted CAR T cells induce remission in B-ALL that is naive or resistant to CD19-targeted CAR immunotherapy. Nature Medicine. 2018;24(1):20-8. doi: 10.1038/nm.4441.
105. Spiegel JY, Patel S, Muffly L, Hossain NM, Oak J, Baird JH, Frank MJ, Shiraz P, Sahaf B, Craig J, Iglesias M, Younes S, Natkunam Y, Ozawa MG, Yang E, Tamaresis J, Chinnasamy H, Ehlinger Z, Reynolds W, Lynn R, Rotiroti MC, Gkitsas N, Arai S, Johnston L, Lowsky R, Majzner RG, Meyer E, Negrin RS, Rezvani AR, Sidana S, Shizuru J, Weng W-K, Mullins C, Jacob A, Kirsch I, Bazzano M, Zhou J, Mackay S, Bornheimer SJ, Schultz L, Ramakrishna S, Davis KL, Kong KA, Shah NN, Qin H, Fry T, Feldman S, Mackall CL, Miklos DB. CAR T cells with dual targeting of CD19 and CD22 in adult patients with recurrent or refractory B cell malignancies: a phase 1 trial. Nature Medicine. 2021;27(8):1419-31. doi: 10.1038/s41591-021-01436-0.
106. Balaian L, Zhong RK, Ball ED. The inhibitory effect of anti-CD33 monoclonal antibodies on AML cell growth correlates with Syk and/or ZAP-70 expression. Exp Hematol. 2003;31(5):363-71. doi: 10.1016/s0301-472x(03)00044-4. PubMed PMID: 12763134.
107. Guglielmi C, Martelli MP, Diverio D, Fenu S, Vegna ML, Cantù-Rajnoldi A, Biondi A, Cocito MG, Del Vecchio L, Tabilio A, Avvisati G, Basso G, Lo Coco F. Immunophenotype of adult and childhood acute promyelocytic leukaemia: correlation with morphology, type of PML gene breakpoint and clinical outcome. A cooperative Italian study on 196 cases. Br J Haematol. 1998;102(4):1035-41. doi: 10.1046/j.1365-2141.1998.00871.x. PubMed PMID: 9734655.
108. Molica M, Perrone S, Mazzone C, Niscola P, Cesini L, Abruzzese E, de Fabritiis P. CD33 Expression and Gentuzumab Ozogamicin in Acute Myeloid Leukemia: Two Sides of the Same Coin. Cancers (Basel). 2021;13(13). Epub 20210628. doi: 10.3390/cancers13133214. PubMed PMID: 34203180; PMCID: PMC8268215.
109. Tambaro FP, Singh H, Jones E, Rytting M, Mahadeo KM, Thompson P, Daver N, DiNardo C, Kadia T, Garcia-Manero G, Chan T, Shah RR, Wierda WG. Autologous CD33-CAR-T cells for treatment of relapsed/refractory acute myelogenous leukemia. Leukemia. 2021;35(11):3282-6. doi: 10.1038/s41375-021-01232-2.

110. Ravandi F, Stein AS, Kantarjian HM, Walter RB, Paschka P, Jongen-Lavrencic M, Ossenkoppele GJ, Yang Z, Mehta B, Subklewe M. A Phase 1 First-in-Human Study of AMG 330, an Anti-CD33 Bispecific T-Cell Engager (BiTE®) Antibody Construct, in Relapsed/Refractory Acute Myeloid Leukemia (R/R AML). Blood. 2018;132(Supplement 1):25-. doi: 10.1182/blood-2018-99-109762.
111. Kovalovsky D, Yoon JH, Cyr MG, Simon S, Voynova E, Rader C, Wiestner A, Alejo J, Pittaluga S, Gress RE. Siglec-6 is a target for chimeric antigen receptor T-cell treatment of chronic lymphocytic leukemia. Leukemia. 2021;35(9):2581-91. doi: 10.1038/s41375-021-01188-3.
112. Wang X, Mitra N, Secundino I, Banda K, Cruz P, Padler-Karavani V, Verhagen A, Reid C, Lari M, Rizzi E, Balsamo C, Corti G, De Bellis G, Longo L, Program NCS, Beggs W, Caramelli D, Tishkoff SA, Hayakawa T, Green ED, Mullikin JC, Nizet V, Bui J, Varki A. Specific inactivation of two immunomodulatory SIGLEC genes during human evolution. Proceedings of the National Academy of Sciences of the United States of America. 2012;109(25):9935-40. Epub 2012/06/04. doi: 10.1073/pnas.1119459109. PubMed PMID: 22665810.
113. Angata T, Tabuchi Y, Nakamura K, Nakamura M. Siglec-15: an immune system Siglec conserved throughout vertebrate evolution. Glycobiology. 2007;17(8):838-46. doi: 10.1093/glycob/cwm049. PubMed PMID: 17483134.
114. Philippe D, Paula AV, Sylvain J. Sialyl-Tn in Cancer: (How) Did We Miss the Target?2012.
115. Munkley J. The Role of Sialyl-Tn in Cancer. Int J Mol Sci. 2016;17(3):275. Epub 20160224. doi: 10.3390/ijms17030275. PubMed PMID: 26927062; PMCID: PMC4813139.
116. Takamiya R, Ohtsubo K, Takamatsu S, Taniguchi N, Angata T. The interaction between Siglec-15 and tumor-associated sialyl-Tn antigen enhances TGF-beta secretion from monocytes/macrophages through the DAP12-Syk pathway. Glycobiology. 2013;23(2):178-87. doi: 10.1093/glycob/cws139. PubMed PMID: 23035012.
117. Murugesan G, Correia VG, Palma AS, Chai W, Li C, Feizi T, Martin E, Laux B, Franz A, Fuchs K, Weigle B, Crocker PR. Siglec-15 recognition of sialoglycans on tumor cell lines can occur independently of sialyl Tn antigen expression. Glycobiology. 2020;31(1):44-54. doi: 10.1093/glycob/cwaa048.
118. Wang J, Sun J, Liu LN, Flies DB, Nie X, Toki M, Zhang J, Song C, Zarr M, Zhou X, Han X, Archer KA, O'Neill T, Herbst RS, Boto AN, Sanmamed MF, Langermann S, Rimm DL, Chen L. Siglec-15 as an immune suppressor and potential target for normalization cancer immunotherapy. Nature Medicine. 2019. doi: 10.1038/s41591-019-0374-x.
119. Ishida-Kitagawa N, Tanaka K, Bao X, Kimura T, Miura T, Kitaoka Y, Hayashi K, Sato M, Maruoka M, Ogawa T, Miyoshi J, Takeya T. Siglec-15 protein regulates formation of functional osteoclasts in concert with DNAX-activating protein of 12 kDa (DAP12). J Biol Chem. 2012;287(21):17493-502. doi: 10.1074/jbc.M111.324194. PubMed PMID: 22451653; PMCID: PMC3366812.
120. Bonifacino JS, Dell'Angelica EC. Molecular bases for the recognition of tyrosine-based sorting signals. The Journal of cell biology. 1999;145(5):923-6. doi: 10.1083/jcb.145.5.923. PubMed PMID: 10352010; PMCID: PMC2133128.
121. Bhattacherjee A, Rodrigues E, Jung J, Luzentales-Simpson M, Enterina JR, Galleguillos D, St. Laurent CD, Nakhaei-Nejad M, Fuchsberger FF, Streith L, Wang Q, Kawasaki N, Duan S, Bains A, Paulson JC, Rademacher C, Giuliani F, Sipione S, Macauley MS. Repression of phagocytosis by human CD33 is not conserved with mouse CD33. Communications Biology. 2019;2(1):450. doi: 10.1038/s42003-019-0698-6.
122. Matsuo K, Irie N. Osteoclast-osteoblast communication. Arch Biochem Biophys. 2008;473(2):201-9. Epub 20080329. doi: 10.1016/j.abb.2008.03.027. PubMed PMID: 18406338.
123. Kameda Y, Takahata M, Komatsu M, Mikuni S, Hatakeyama S, Shimizu T, Angata T, Kinjo M, Minami A, Iwasaki N. Siglec-15 regulates osteoclast differentiation by modulating RANKL-induced phosphatidylinositol 3-kinase/Akt and Erk pathways in association with signaling Adaptor DAP12. J Bone Miner Res. 2013;28(12):2463-75. doi: 10.1002/jbmr.1989. PubMed PMID: 23677868.

124. Hiruma Y, Tsuda E, Maeda N, Okada A, Kabasawa N, Miyamoto M, Hattori H, Fukuda C. Impaired osteoclast differentiation and function and mild osteopetrosis development in Siglec-15-deficient mice. Bone. 2013;53(1):87-93. doi: 10.1016/j.bone.2012.11.036. PubMed PMID: 23238125.
125. Korn MA, Schmitt H, Angermüller S, Chambers D, Seeling M, Lux UT, Brey S, Royzman D, Brückner C, Popp V, Percivalle E, Bäuerle T, Zinser E, Winkler TH, Steinkasserer A, Nimmerjahn F, Nitschke L. Siglec-15 on Osteoclasts Is Crucial for Bone Erosion in Serum-Transfer Arthritis. J Immunol. 2020;205(10):2595-605. Epub 20201005. doi: 10.4049/jimmunol.2000472. PubMed PMID: 33020147.
126. Hiruma Y, Hirai T, Tsuda E. Siglec-15, a member of the sialic acid-binding lectin, is a novel regulator for osteoclast differentiation. Biochem Biophys Res Commun. 2011;409(3):424-9. doi: 10.1016/j.bbrc.2011.05.015. PubMed PMID: 21586272.
127. Zhen G, Dan Y, Wang R, Dou C, Guo Q, Zarr M, Liu LN, Chen L, Deng R, Li Y, Shao Z, Cao X. An antibody against Siglec-15 promotes bone formation and fracture healing by increasing TRAP(+) mononuclear cells and PDGF-BB secretion. Bone Res. 2021;9(1):47. Epub 20211101. doi: 10.1038/s41413-021-00161-1. PubMed PMID: 34719673; PMCID: PMC8558327.
128. Akkawi I, Zmerly H. Osteoporosis: Current Concepts. Joints. 2018;6(2):122-7. Epub 20180614. doi: 10.1055/s-0038-1660790. PubMed PMID: 30051110; PMCID: PMC6059859.
129. Kameda Y, Takahata M, Mikuni S, Shimizu T, Hamano H, Angata T, Hatakeyama S, Kinjo M, Iwasaki N. Siglec-15 is a potential therapeutic target for postmenopausal osteoporosis. Bone. 2015;71:217-26. doi: 10.1016/j.bone.2014.10.027. PubMed PMID: 25460183.
130. Tsukazaki H, Kikuta J, Ao T, Morimoto A, Fukuda C, Tsuda E, Minoshima M, Kikuchi K, Kaito T, Ishii M. Anti-Siglec-15 antibody suppresses bone resorption by inhibiting osteoclast multinucleation without attenuating bone formation. Bone. 2021;152:116095. doi: https://doi.org/10.1016/j.bone.2021.116095.
131. Orgel E, Mueske NM, Wren TAL, Gilsanz V, Butturini AM, Freyer DR, Mittelman SD. Early injury to cortical and cancellous bone from induction chemotherapy for adolescents and young adults treated for acute lymphoblastic leukemia. Bone. 2016;85:131-7. doi: https://doi.org/10.1016/j.bone.2016.01.027.
132. Sato D, Takahata M, Ota M, Fukuda C, Hasegawa T, Yamamoto T, Amizuka N, Tsuda E, Okada A, Hiruma Y, Fujita R, Iwasaki N. Siglec-15-targeting therapy protects against glucocorticoid-induced osteoporosis of growing skeleton in juvenile rats. Bone. 2020;135:115331. doi: https://doi.org/10.1016/j.bone.2020.115331.
133. Rajakumar SA, Danska JS. Bad to the bone: B cell acute lymphoblastic leukemia cells mediate bone destruction. Mol Cell Oncol. 2020;8(1):1835423. Epub 20201106. doi: 10.1080/23723556.2020.1835423. PubMed PMID: 33553597; PMCID: PMC7849691.
134. Kiesel JR, Buchwald ZS, Aurora R. Cross-Presentation by Osteoclasts Induces FoxP3 in CD8+ T Cells. The Journal of Immunology. 2009;182(9):5477-87. doi: 10.4049/jimmunol.0803897.
135. Li H, Lu Y, Qian J, Zheng Y, Zhang M, Bi E, He J, Liu Z, Xu J, Gao JY, Yi Q. Human Osteoclasts Are Inducible Immunosuppressive Cells in Response to T cell–Derived IFN-γ and CD40 Ligand In Vitro. Journal of Bone and Mineral Research. 2014;29(12):2666-75. doi: https://doi.org/10.1002/jbmr.2294.
136. An G, Acharya C, Feng X, Wen K, Zhong M, Zhang L, Munshi NC, Qiu L, Tai Y-T, Anderson KC. Osteoclasts promote immune suppressive microenvironment in multiple myeloma: therapeutic implication. Blood, The Journal of the American Society of Hematology. 2016;128(12):1590-603.
137. Soares RMA, de A. Soares RM, Alviano DS, Angluster J, Alviano CS, Travassos LR. Identification of sialic acids on the cell surface of Candida albicans. Biochimica et Biophysica Acta (BBA) - General Subjects. 2000;1474(2):262-8. doi: https://doi.org/10.1016/S0304-4165(00)00003-9.
138. Jaeger M, Pinelli M, Borghi M, Constantini C, Dindo M, van Emst L, Puccetti M, Pariano M, Ricaño-Ponce I, Büll C, Gresnigt MS, Wang X, Gutierrez Achury J, Jacobs CWM, Xu N, Oosting M, Arts P, Joosten LAB, van de Veerdonk FL, Veltman JA, Ten Oever J, Kullberg BJ, Feng M, Adema GJ, Wijmenga C, Kumar V, Sobel J, Gilissen C, Romani L, Netea MG. A systems genomics approach

identifies SIGLEC15 as a susceptibility factor in recurrent vulvovaginal candidiasis. Sci Transl Med. 2019;11(496). doi: 10.1126/scitranslmed.aar3558. PubMed PMID: 31189718.
139. Dewi IMW, Cunha C, Jaeger M, Gresnigt MS, Gkountzinopoulou ME, Garishah FM, Duarte-Oliveira C, Campos CF, Vanderbeke L, Sharpe AR, Brüggemann RJ, Verweij PE, Lagrou K, Vande Velde G, de Mast Q, Joosten LAB, Netea MG, van der Ven AJAM, Wauters J, Carvalho A, van de Veerdonk FL. Neuraminidase and SIGLEC15 modulate the host defense against pulmonary aspergillosis. Cell Reports Medicine. 2021;2(5). doi: 10.1016/j.xcrm.2021.100289.
140. Xiao X, Peng Y, Wang Z, Zhang L, Yang T, Sun Y, Chen Y, Zhang W, Chang X, Huang W, Tian S, Feng Z, Xinhua N, Tang Q, Mao Y. A novel immune checkpoint siglec-15 antibody inhibits LUAD by modulating mφ polarization in TME. Pharmacological Research. 2022;181:106269. doi: https://doi.org/10.1016/j.phrs.2022.106269.
141. Fan M-K, Zhang G-C, Chen W, Qi L-L, Xie M-F, Zhang Y-Y, Wang L, Zhang Q. Siglec-15 Promotes Tumor Progression in Osteosarcoma via DUSP1/MAPK Pathway. Front Oncol. 2021;11:710689-. doi: 10.3389/fonc.2021.710689. PubMed PMID: 34336699.
142. Ren Y, Lyu J, Guo Y, Yao Y, Hu L. Long Noncoding RNA TUG1 Inhibits Tumor Progression through Regulating Siglec-15-Related Anti-Immune Activity in Hepatocellular Carcinoma. Journal of Immunology Research. 2022;2022:9557859. doi: 10.1155/2022/9557859.
143. Liu Y, Li X, Zhang C, Zhang H, Huang Y. LINC00973 is involved in cancer immune suppression through positive regulation of Siglec-15 in clear-cell renal cell carcinoma. Cancer Sci. 2020;111(10):3693-704. Epub 2020/08/31. doi: 10.1111/cas.14611. PubMed PMID: 32780490.
144. Hou X, Chen C, Lan X, He X. Unveiling the molecular features, relevant immune and clinical characteristics of SIGLEC15 in thyroid cancer. Front Immunol. 2022;13:975787. Epub 20220909. doi: 10.3389/fimmu.2022.975787. PubMed PMID: 36159823; PMCID: PMC9500188.
145. Cao HA-O, Neerincx A, de Bono B, Lakner U, Huntington C, Elvin J, Gudgin E, Pridans C, Vickers MA, Huntly B, Trowsdale J, Barrow AD. Sialic acid-binding immunoglobulin-like lectin (Sigelac)-15 is a rapidly internalised cell-surface antigen expressed by acute myeloid leukaemia cells(1365-2141 (Electronic)).
146. Fudaba H, Momii Y, Hirakawa T, Onishi K, Asou D, Matsushita W, Kawasaki Y, Sugita K, Fujiki M. Sialic acid-binding immunoglobulin-like lectin-15 expression on peritumoral macrophages is a favorable prognostic factor for primary central nervous system lymphoma patients. Sci Rep. 2021;11(1):1206. Epub 20210113. doi: 10.1038/s41598-020-79742-9. PubMed PMID: 33441719; PMCID: PMC7806611.
147. Mitra N, Banda K, Altheide TK, Schaffer L, Johnson-Pais TL, Beuten J, Leach RJ, Angata T, Varki N, Varki A. SIGLEC12, a human-specific segregating (pseudo)gene, encodes a signaling molecule expressed in prostate carcinomas. J Biol Chem. 2011;286(26):23003-11. Epub 20110509. doi: 10.1074/jbc.M111.244152. PubMed PMID: 21555517; PMCID: PMC3123068.
148. MacDougall A, Volynkin V, Saidi R, Poggioli D, Zellner H, Hatton-Ellis E, Joshi V, O'Donovan C, Orchard S, Auchincloss AH, Baratin D, Bolleman J, Coudert E, de Castro E, Hulo C, Masson P, Pedruzzi I, Rivoire C, Arighi C, Wang Q, Chen C, Huang H, Garavelli J, Vinayaka CR, Yeh L-S, Natale DA, Laiho K, Martin M-J, Renaux A, Pichler K, Consortium TU. UniRule: a unified rule resource for automatic annotation in the UniProt Knowledgebase. Bioinformatics. 2020;36(17):4643-8. doi: 10.1093/bioinformatics/btaa485.
149. Howlader N, Noone A-M, Krapcho M, Garshell J, Miller D, Altekruse S, Kosary C, Yu M, Ruhl J, Tatalovich Z. SEER cancer statistics review, 1975–2011. Bethesda, MD: National Cancer Institute. 2014;19.
150. Board PPTE. Childhood Acute Lymphoblastic Leukemia Treatment (PDQ®): Health Professional Version. PDQ Cancer Information Summaries. 2021.
151. Li Y, Gupta G, Molofsky A, Xie Y, Shihabi N, McCormick J, Jaffe ES. B Lymphoblastic Leukemia/Lymphoma With Burkitt-like Morphology and IGH/MYC Rearrangement: Report of 3 Cases in Adult Patients. The American journal of surgical pathology. 2018;42(2):269-76. Epub 2017/11/08. doi: 10.1097/pas.0000000000000982. PubMed PMID: 29112016; PMCID: PMC5762415.

152. Gore L, Locatelli F, Zugmaier G, Handgretinger R, O'Brien MM, Bader P, Bhojwani D, Schlegel P-G, Tuglus CA, von Stackelberg A. Survival after blinatumomab treatment in pediatric patients with relapsed/refractory B-cell precursor acute lymphoblastic leukemia. Blood cancer journal. 2018;8(9):80-. doi: 10.1038/s41408-018-0117-0. PubMed PMID: 30190453.
153. Williams RT, Roussel MF, Sherr CJ. Arf gene loss enhances oncogenicity and limits imatinib response in mouse models of Bcr-Abl-induced acute lymphoblastic leukemia. Proc Natl Acad Sci U S A. 2006;103(17):6688-93. Epub 2006/04/19. doi: 10.1073/pnas.0602030103. PubMed PMID: 16618932; PMCID: PMC1440588.
154. Williams RT, den Besten W, Sherr CJ. Cytokine-dependent imatinib resistance in mouse BCR-ABL+, Arf-null lymphoblastic leukemia. Genes Dev. 2007;21(18):2283-7. Epub 2007/09/01. doi: 10.1101/gad.1588607. PubMed PMID: 17761812; PMCID: PMC1973142.
155. Boulos N, Mulder HL, Calabrese CR, Morrison JB, Rehg JE, Relling MV, Sherr CJ, Williams RT. Chemotherapeutic agents circumvent emergence of dasatinib-resistant BCR-ABL kinase mutations in a precise mouse model of Philadelphia chromosome-positive acute lymphoblastic leukemia. Blood. 2011;117(13):3585-95. Epub 2011/01/26. doi: 10.1182/blood-2010-08-301267. PubMed PMID: 21263154; PMCID: PMC3072880.
156. Rafiq S, Yeku OO, Jackson HJ, Purdon TJ, van Leeuwen DG, Drakes DJ, Song M, Miele MM, Li Z, Wang P, Yan S, Xiang J, Ma X, Seshan VE, Hendrickson RC, Liu C, Brentjens RJ. Targeted delivery of a PD-1-blocking scFv by CAR-T cells enhances anti-tumor efficacy in vivo. Nat Biotechnol. 2018;36(9):847-56. Epub 2018/08/14. doi: 10.1038/nbt.4195. PubMed PMID: 30102295; PMCID: PMC6126939.
157. Schindelin J, Arganda-Carreras I, Frise E, Kaynig V, Longair M, Pietzsch T, Preibisch S, Rueden C, Saalfeld S, Schmid B, Tinevez J-Y, White DJ, Hartenstein V, Eliceiri K, Tomancak P, Cardona A. Fiji: an open-source platform for biological-image analysis. Nature Methods. 2012;9(7):676-82. doi: 10.1038/nmeth.2019.
158. Cao H, Neerincx A, de Bono B, Lakner U, Huntington C, Elvin J, Gudgin E, Pridans C, Vickers MA, Huntly B, Trowsdale J, Barrow AD. Sialic acid-binding immunoglobulin-like lectin (Sigelac)-15 is a rapidly internalised cell-surface antigen expressed by acute myeloid leukaemia cells. Br J Haematol. 2021;193(5):946-50. Epub 20210505. doi: 10.1111/bjh.17496. PubMed PMID: 33951750.
159. Elvin J, Huntington C, Trowsdale J, Barrow A, Cao H, inventors; Cambridge Enterprise Limited, MedImmune Limited, assignee. Anti-Siglec15 antibodies and uses thereof. 2015/0037356 A1. 2015.
160. Montaño A, Ordoñez JL, Alonso-Pérez V, Hernández-Sánchez J, Santos S, González T, Benito R, García-Tuñón I, Hernández-Rivas JM. ETV6/RUNX1 Fusion Gene Abrogation Decreases the Oncogenicity of Tumour Cells in a Preclinical Model of Acute Lymphoblastic Leukaemia. Cells. 2020;9(1). Epub 2020/01/19. doi: 10.3390/cells9010215. PubMed PMID: 31952221; PMCID: PMC7017301.
161. Hsieh M-Y, Van Etten RA. IKK-dependent activation of NF-κB contributes to myeloid and lymphoid leukemogenesis by BCR-ABL1. Blood. 2014;123(15):2401-11. Epub 2014/01/24. doi: 10.1182/blood-2014-01-547943. PubMed PMID: 24464015.
162. Chang Y-C, Nizet V. The interplay between Siglecs and sialylated pathogens. Glycobiology. 2014;24(9):818-25. Epub 2014/07/04. doi: 10.1093/glycob/cwu067. PubMed PMID: 24996821.
163. Derby MC, van Vliet C, Brown D, Luke MR, Lu L, Hong W, Stow JL, Gleeson PA. Mammalian GRIP domain proteins differ in their membrane binding properties and are recruited to distinct domains of the TGN. Journal of Cell Science. 2004;117(24):5865-74. doi: 10.1242/jcs.01497.
164. Legrand F, Cao Y, Bochner BS, Klion AD. Serum soluble Siglec-8 in hypereosinophilic syndromes. The Journal of Immunology. 2017;198(1 Supplement):55.34.
165. Huang P-CJ, Low P-Y, Wang I, Hsu S-TD, Angata T. Soluble Siglec-14 glycan-recognition protein is generated by alternative splicing and suppresses myeloid inflammatory responses. Journal of Biological Chemistry. 2018;293(51):19645-58. doi: 10.1074/jbc.RA118.005676.
166. Isidro-Hernández M, Mayado A, Casado-García A, Martínez-Cano J, Palmi C, Fazio G, Orfao A, Ribera J, Ribera JM, Zamora L, Raboso-Gallego J, Blanco O, Alonso-López D, De Las Rivas J, Jiménez

R, García Criado FJ, García Cenador MB, Ramírez-Orellana M, Cazzaniga G, Cobaleda C, Vicente-Dueñas C, Sánchez-García I. Inhibition of inflammatory signaling in Pax5 mutant cells mitigates B-cell leukemogenesis. Sci Rep. 2020;10(1):19189-. doi: 10.1038/s41598-020-76206-y. PubMed PMID: 33154497.
167. de Vasconcellos JF, Laranjeira AB, Zanchin NI, Otubo R, Vaz TH, Cardoso AA, Brandalise SR, Yunes JA. Increased CCL2 and IL-8 in the bone marrow microenvironment in acute lymphoblastic leukemia. Pediatr Blood Cancer. 2011;56(4):568-77. Epub 20101222. doi: 10.1002/pbc.22941. PubMed PMID: 21298741.
168. Akondy RS, Fitch M, Edupuganti S, Yang S, Kissick HT, Li KW, Youngblood BA, Abdelsamed HA, McGuire DJ, Cohen KW, Alexe G, Nagar S, McCausland MM, Gupta S, Tata P, Haining WN, McElrath MJ, Zhang D, Hu B, Greenleaf WJ, Goronzy JJ, Mulligan MJ, Hellerstein M, Ahmed R. Origin and differentiation of human memory CD8 T cells after vaccination. Nature. 2017;552(7685):362-7. Epub 2017/12/14. doi: 10.1038/nature24633. PubMed PMID: 29236685; PMCID: PMC6037316.
169. Nasef A, Mazurier C, Bouchet S, François S, Chapel A, Thierry D, Gorin NC, Fouillard L. Leukemia inhibitory factor: Role in human mesenchymal stem cells mediated immunosuppression. Cell Immunol. 2008;253(1-2):16-22. Epub 2008/07/22. doi: 10.1016/j.cellimm.2008.06.002. PubMed PMID: 18639869.
170. Tran GT, Hodgkinson SJ, Carter NM, Verma ND, Plain KM, Boyd R, Robinson CM, Nomura M, Killingsworth M, Hall BM. IL-5 promotes induction of antigen-specific CD4+CD25+ T regulatory cells that suppress autoimmunity. Blood. 2012;119(19):4441-50. doi: 10.1182/blood-2011-12-396101.
171. Bent EH, Millán-Barea LR, Zhuang I, Goulet DR, Fröse J, Hemann MT. Microenvironmental IL-6 inhibits anti-cancer immune responses generated by cytotoxic chemotherapy. Nature Communications. 2021;12(1):6218. doi: 10.1038/s41467-021-26407-4.
172. Xiao Y, Zijl S, Wang L, de Groot DC, van Tol MJ, Lankester AC, Borst J. Identification of the Common Origins of Osteoclasts, Macrophages, and Dendritic Cells in Human Hematopoiesis. Stem Cell Reports. 2015;4(6):984-94. Epub 2015/05/21. doi: 10.1016/j.stemcr.2015.04.012. PubMed PMID: 26004632.
173. Lanier LL. DAP10- and DAP12-associated receptors in innate immunity. Immunol Rev. 2009;227(1):150-60. doi: 10.1111/j.1600-065X.2008.00720.x. PubMed PMID: 19120482.
174. Chang L, Chen YJ, Fan CY, Tang CJ, Chen YH, Low PY, Ventura A, Lin CC, Chen YJ, Angata T. Identification of Siglec Ligands Using a Proximity Labeling Method. J Proteome Res. 2017;16(10):3929-41. Epub 20170922. doi: 10.1021/acs.jproteome.7b00625. PubMed PMID: 28899088.
175. Stuible M, Moraitis A, Fortin A, Saragosa S, Kalbakji A, Filion M, Tremblay GB. Mechanism and function of monoclonal antibodies targeting siglec-15 for therapeutic inhibition of osteoclastic bone resorption. J Biol Chem. 2014;289(10):6498-512. doi: 10.1074/jbc.M113.494542. PubMed PMID: 24446437; PMCID: PMC3945315.
176. Sommermann TG, O'Neill K, Plas DR, Cahir-McFarland E. IKKβ and NF-κB transcription govern lymphoma cell survival through AKT-induced plasma membrane trafficking of GLUT1. Cancer research. 2011;71(23):7291-300. Epub 2011/10/10. doi: 10.1158/0008-5472.CAN-11-1715. PubMed PMID: 21987722.
177. Liu J, Xiang J, Li X, Blankson S, Zhao S, Cai J, Jiang Y, Redmond HP, Wang JH. NF-κB activation is critical for bacterial lipoprotein tolerance-enhanced bactericidal activity in macrophages during microbial infection. Sci Rep. 2017;7(1):40418. doi: 10.1038/srep40418.
178. Balandrán JC, Purizaca J, Enciso J, Dozal D, Sandoval A, Jiménez-Hernández E, Alemán-Lazarini L, Perez-Koldenkova V, Quintela-Núñez del Prado H, Rios de los Ríos J, Mayani H, Ortiz-Navarrete V, Guzman ML, Pelayo R. Pro-inflammatory-Related Loss of CXCL12 Niche Promotes Acute Lymphoblastic Leukemic Progression at the Expense of Normal Lymphopoiesis. Frontiers in Immunology. 2017;7. doi: 10.3389/fimmu.2016.00666.
179. Zippelius A, Schreiner J, Herzig P, Müller P. Induced PD-L1 Expression Mediates Acquired Resistance to Agonistic Anti-CD40 Treatment. Cancer Immunology Research. 2015;3(3):236-44. doi: 10.1158/2326-6066.CIR-14-0226.

180. Blobel G, Dobberstein B. Transfer of proteins across membranes. I. Presence of proteolytically processed and unprocessed nascent immunoglobulin light chains on membrane-bound ribosomes of murine myeloma. The Journal of cell biology. 1975;67(3):835-51. Epub 1975/12/01. doi: 10.1083/jcb.67.3.835. PubMed PMID: 811671; PMCID: PMC2111658.
181. Ito T, Ishigami M, Matsushita Y, Hirata M, Matsubara K, Ishikawa T, Hibi H, Ueda M, Hirooka Y, Goto H, Yamamoto A. Secreted Ectodomain of SIGLEC-9 and MCP-1 Synergistically Improve Acute Liver Failure in Rats by Altering Macrophage Polarity. Sci Rep. 2017;7:44043. Epub 20170308. doi: 10.1038/srep44043. PubMed PMID: 28272428; PMCID: PMC5358744.
182. Ye L, Gratton A, Hannan NJ, Cannon P, Deo M, Palmer KR, Tong S, Kaitu'u-Lino TJ, Brownfoot FC. Nuclear factor of activated T-cells (NFAT) regulates soluble fms-like tyrosine kinase-1 secretion (sFlt-1) from human placenta(1532-3102 (Electronic)).
183. Balkan W, Martinez AF, Fernandez I, Rodriguez MA, Pang M, Troen BR. Identification of NFAT binding sites that mediate stimulation of cathepsin K promoter activity by RANK ligand. Gene. 2009;446(2):90-8. Epub 20090627. doi: 10.1016/j.gene.2009.06.013. PubMed PMID: 19563866.
184. Sarkar S, Kalia V, Haining WN, Konieczny BT, Subramaniam S, Ahmed R. Functional and genomic profiling of effector CD8 T cell subsets with distinct memory fates. The Journal of experimental medicine. 2008;205(3):625-40. Epub 2008/03/05. doi: 10.1084/jem.20071641. PubMed PMID: 18316415; PMCID: PMC2275385.
185. Haferlach T, Kohlmann A, Wieczorek L, Basso G, Kronnie GT, Bene MC, De Vos J, Hernandez JM, Hofmann WK, Mills KI, Gilkes A, Chiaretti S, Shurtleff SA, Kipps TJ, Rassenti LZ, Yeoh AE, Papenhausen PR, Liu WM, Williams PM, Foa R. Clinical utility of microarray-based gene expression profiling in the diagnosis and subclassification of leukemia: report from the International Microarray Innovations in Leukemia Study Group. Journal of clinical oncology : official journal of the American Society of Clinical Oncology. 2010;28(15):2529-37. Epub 2010/04/22. doi: 10.1200/jco.2009.23.4732. PubMed PMID: 20406941; PMCID: PMC5569671.
186. Clancy S. RNA splicing: introns, exons and spliceosome. In: Moss B, editor. Nucleic Acid Structure and Function. Scitable: Nature Education; 2008.
187. Connolly NP, Jones M, Watt SM. Human Siglec-5: tissue distribution, novel isoforms and domain specificities for sialic acid-dependent ligand interactions. Br J Haematol. 2002;119(1):221-38. doi: 10.1046/j.1365-2141.2002.03808.x. PubMed PMID: 12358929.
188. Nutku E, Aizawa H, Hudson SA, Bochner BS. Ligation of Siglec-8: a selective mechanism for induction of human eosinophil apoptosis. Blood. 2003;101(12):5014-20. doi: 10.1182/blood-2002-10-3058.
189. Oliveira JJ, Karrar S, Rainbow DB, Pinder CL, Clarke P, Rubio García A, Al-Assar O, Burling K, Morris S, Stratton R, Vyse TJ, Wicker LS, Todd JA, Ferreira RC. The plasma biomarker soluble SIGLEC-1 is associated with the type I interferon transcriptional signature, ethnic background and renal disease in systemic lupus erythematosus. Arthritis Research & Therapy. 2018;20(1):152. doi: 10.1186/s13075-018-1649-1.
190. Ghafouri-Fard S, Khoshbakht T, Hussen BM, Taheri M, Jamali E. The emerging role non-coding RNAs in B cell-related disorders. Cancer Cell International. 2022;22(1):91. doi: 10.1186/s12935-022-02521-1.
191. Cuadros M, García DJ, Andrades A, Arenas AM, Coira IF, Baliñas-Gavira C, Peinado P, Rodríguez MI, Álvarez-Pérez JC, Ruiz-Cabello F, Camós M, Jiménez-Velasco A, Medina PP. LncRNA-mRNA Co-Expression Analysis Identifies AL133346.1/CCN2 as Biomarkers in Pediatric B-Cell Acute Lymphoblastic Leukemia. Cancers. 2020;12(12):3803. PubMed PMID: doi:10.3390/cancers12123803.
192. Qian C-S, Li L-J, Huang H-W, Yang H-F, Wu D-P. MYC-regulated lncRNA NEAT1 promotes B cell proliferation and lymphomagenesis via the miR-34b-5p-GLI1 pathway in diffuse large B-cell lymphoma. Cancer Cell International. 2020;20(1):87. doi: 10.1186/s12935-020-1158-6.
193. O'Leary NA, Wright MW, Brister JR, Ciufo S, Haddad D, McVeigh R, Rajput B, Robbertse B, Smith-White B, Ako-Adjei D, Astashyn A, Badretdin A, Bao Y, Blinkova O, Brover V, Chetvernin V, Choi J, Cox E, Ermolaeva O, Farrell CM, Goldfarb T, Gupta T, Haft D, Hatcher E, Hlavina W, Joardar

VS, Kodali VK, Li W, Maglott D, Masterson P, McGarvey KM, Murphy MR, O'Neill K, Pujar S, Rangwala SH, Rausch D, Riddick LD, Schoch C, Shkeda A, Storz SS, Sun H, Thibaud-Nissen F, Tolstoy I, Tully RE, Vatsan AR, Wallin C, Webb D, Wu W, Landrum MJ, Kimchi A, Tatusova T, DiCuccio M, Kitts P, Murphy TD, Pruitt KD. Reference sequence (RefSeq) database at NCBI: current status, taxonomic expansion, and functional annotation. Nucleic Acids Res. 2016;44(D1):D733-45. Epub 20151108. doi: 10.1093/nar/gkv1189. PubMed PMID: 26553804; PMCID: PMC4702849.
194. Conti E, Izaurralde E. Nucleocytoplasmic transport enters the atomic age. Curr Opin Cell Biol. 2001;13(3):310-9. doi: 10.1016/s0955-0674(00)00213-1. PubMed PMID: 11343901.
195. Lee BJ, Cansizoglu AE, Süel KE, Louis TH, Zhang Z, Chook YM. Rules for nuclear localization sequence recognition by karyopherin beta 2. Cell. 2006;126(3):543-58. doi: 10.1016/j.cell.2006.05.049. PubMed PMID: 16901787; PMCID: PMC3442361.
196. Gao Y, Nihira NT, Bu X, Chu C, Zhang J, Kolodziejczyk A, Fan Y, Chan NT, Ma L, Liu J, Wang D, Dai X, Liu H, Ono M, Nakanishi A, Inuzuka H, North BJ, Huang Y-H, Sharma S, Geng Y, Xu W, Liu XS, Li L, Miki Y, Sicinski P, Freeman GJ, Wei W. Acetylation-dependent regulation of PD-L1 nuclear translocation dictates the efficacy of anti-PD-1 immunotherapy. Nature Cell Biology. 2020;22(9):1064-75. doi: 10.1038/s41556-020-0562-4.
197. Xiong W, Gao Y, Wei W, Zhang J. Extracellular and nuclear PD-L1 in modulating cancer immunotherapy. Trends in Cancer. 2021;7(9):837-46. doi: https://doi.org/10.1016/j.trecan.2021.03.003.
198. Norton JT, Huang S. The perinucleolar compartment: RNA metabolism and cancer. Cancer Treat Res. 2013;158:139-52. doi: 10.1007/978-3-642-31659-3_6. PubMed PMID: 24222357; PMCID: PMC4374481.
199. Jumper J, Evans R, Pritzel A, Green T, Figurnov M, Ronneberger O, Tunyasuvunakool K, Bates R, Žídek A, Potapenko A, Bridgland A, Meyer C, Kohl SAA, Ballard AJ, Cowie A, Romera-Paredes B, Nikolov S, Jain R, Adler J, Back T, Petersen S, Reiman D, Clancy E, Zielinski M, Steinegger M, Pacholska M, Berghammer T, Bodenstein S, Silver D, Vinyals O, Senior AW, Kavukcuoglu K, Kohli P, Hassabis D. Highly accurate protein structure prediction with AlphaFold. Nature. 2021;596(7873):583-9. doi: 10.1038/s41586-021-03819-2.
200. Carrà G, Torti D, Crivellaro S, Panuzzo C, Taulli R, Cilloni D, Guerrasio A, Saglio G, Morotti A. The BCR-ABL/NF-κB signal transduction network: a long lasting relationship in Philadelphia positive Leukemias. Oncotarget. 2016;7(40):66287-98. doi: 10.18632/oncotarget.11507. PubMed PMID: 27563822.
201. Han S, Collins BE, Bengtson P, Paulson JC. Homomultimeric complexes of CD22 in B cells revealed by protein-glycan cross-linking. Nat Chem Biol. 2005;1(2):93-7. Epub 20050612. doi: 10.1038/nchembio713. PubMed PMID: 16408005.
202. Cornish AL, Freeman S, Forbes G, Ni J, Zhang M, Cepeda M, Gentz R, Augustus M, Carter KC, Crocker PR. Characterization of siglec-5, a novel glycoprotein expressed on myeloid cells related to CD33. Blood. 1998;92(6):2123-32. PubMed PMID: 9731071.
203. Siddiqui S, Schwarz F, Springer S, Khedri Z, Yu H, Deng L, Verhagen A, Naito-Matsui Y, Jiang W, Kim D, Zhou J, Ding B, Chen X, Varki N, Varki A. Studies on the Detection, Expression, Glycosylation, Dimerization, and Ligand Binding Properties of Mouse Siglec-E. J Biol Chem. 2017;292(3):1029-37. Epub 20161205. doi: 10.1074/jbc.M116.738351. PubMed PMID: 27920204; PMCID: PMC5247637.
204. Hatano K, Miyamoto Y, Nonomura N, Kaneda Y. Expression of gangliosides, GD1a, and sialyl paragloboside is regulated by NF-κB-dependent transcriptional control of α2,3-sialyltransferase I, II, and VI in human castration-resistant prostate cancer cells. Int J Cancer. 2011;129(8):1838-47. Epub 20110413. doi: 10.1002/ijc.25860. PubMed PMID: 21165949.
205. Dewald JH, Colomb F, Bobowski-Gerard M, Groux-Degroote S, Delannoy P. Role of Cytokine-Induced Glycosylation Changes in Regulating Cell Interactions and Cell Signaling in Inflammatory Diseases and Cancer. Cells [Internet]. 2016; 5 4.

206. Zhao S, Zhang L, Xiang S, Hu Y, Wu Z, Shen J. Gnawing Between Cells and Cells in the Immune System: Friend or Foe? A Review of Trogocytosis. Frontiers in Immunology. 2022;13. doi: 10.3389/fimmu.2022.791006.
207. Gardner LA, Klawitter J, Gregory MA, Zaberezhnyy V, Baturin D, Pollyea DA, Takebe N, Christians U, Gore L, DeGregori J, Porter CC. Inhibition of calcineurin combined with dasatinib has direct and indirect anti-leukemia effects against BCR-ABL1(+) leukemia. American journal of hematology. 2014;89(9):896-903. doi: 10.1002/ajh.23776. PubMed PMID: 24891015; PMCID: 4134764.
208. Liu F, Aubin JE, Malaval L. Expression of leukemia inhibitory factor (LIF)/interleukin-6 family cytokines and receptors during in vitro osteogenesis: differential regulation by dexamethasone and LIF. Bone. 2002;31(1):212-9. doi: 10.1016/s8756-3282(02)00806-2. PubMed PMID: 12110437.
209. Macias MP, Fitzpatrick LA, Brenneise I, McGarry MP, Lee JJ, Lee NA. Expression of IL-5 alters bone metabolism and induces ossification of the spleen in transgenic mice. The Journal of clinical investigation. 2001;107(8):949-59. Epub 2001/04/18. doi: 10.1172/jci11232. PubMed PMID: 11306598; PMCID: PMC199553.